**Faculdade de Engenharia**
**Instituto de Ciências Biomédicas Abel Salazar**
**Universidade do Porto**



# The Role of $Y_1$ Receptor in Osteoclastogenesis and Bone Resorption

Francisco Pereira dos Santos Conceição

Msc Thesis Project
Integrated Masters in Bioengineering
Major Molecular Biotechnology

Project Supervisor: Prof. Dr. Meriem Lamghari
Project Co-supervisor: Dr. Daniela Sousa

September 2015

Faculdade de Engenharia
Instituto de Ciências Biomédicas Abel Salazar
Universidade do Porto



# The Role of $Y_1$ Receptor in Osteoclastogenesis and Bone Resorption

Francisco Pereira dos Santos Conceição

Msc Thesis Project
Integrated Masters in Bioengineering
Major Molecular Biotechnology

Project Supervisor: Prof. Dr. Meriem Lamghari
Project Co-supervisor: Dr. Daniela Sousa

September 2015

# Abstract

The role of the Peripheral Nervous System on the regulation of bone remodelling is widely accepted, mainly through $Y_1$ Receptor ($Y_1R$) signalling. $Y_1R$ knockout (KO) mice demonstrated an increase in Osteoblast (OB) driven bone formation and Osteoclast (OC) surface and therefore demonstrate a great therapeutic potential in the treatment of bone degenerative diseases. However, the effect of $Y_1R$ in osteoclastogenesis is unknown.

Therefore, the main objective of this work is to study the role of $Y_1R$ in OC differentiation and bone resorption. In order to achieve this goal, $Y_1R$ KO animal model was used to ascertain the influence of $Y_1R$ in OC behaviour. In addition, OC $Y_1R$ blockage with the specific antagonist BIBP3226 was used to determine if the $Y_1R$ pathway was responsible for the observed results in $Y_1R$ KO OCs. Furthermore, the involvement of $Y_1R$ in OB/OC crosstalk was studied using an OB/OC direct co-culture.

The absence of $Y_1R$ signalling led to increased osteoclastogenesis, with increased $TRAP^+$ Multinucleated Cells (MNC) formation and OC section area, together with an increase in Macrophage Chemotactic protein 1 (MCP1) expression. However, $Y_1R$ KO OC exhibited impaired resorption activity, with decreased TRAP and Cathepsin K (CATK) expression. In addition, BIBP3226 treatment of WT OCs led to increased osteoclastogenesis with higher number of $TRAP^+$ MNCs, but no significant differences in OC section area. However, similarly to $Y_1R$ KO cells, OC resorption capacity was impaired, with reduced resorption pit volume and area.

OB derived from $Y_1R$ KO mice revealed a significant increase of Receptor activator of nuclear factor-κβ ligand (RANKL) expression, which was associated with an increased expression of OC differentiation markers in a direct OB/OC co-culture. However, no differences were observed in $TRAP^+$ MNC numbers. Mineralization staining and quantification did not led to any definite conclusion, with no statistically significant differences being observed. BIBP3226 treatment of the OB/OC co-culture also revealed increased OC differentiation markers and no significant differences in osteoclastogenesis and calcium deposition.

Taken together, these results helped decipher the role of $Y_1R$ signalling in OC behaviour while studying the effect of BIBP3226 treatment. Furthermore, the influence of $Y_1R$ in OB/OC crosstalk was explored.

# Acknowledgements

I would like to acknowledge all of those who contributed to this project, providing me with the tools necessary to successfully develop my work. This achievement was greatly reliant on the guidance and cheering of many individuals:

- After many months of hard work, I could not thank Dr. Meriem Lamghari enough for the opportunity of working in her team, for her guidance and constant challenges that improved the quality of my work.
- Most of the tasks in this project were performed with the close supervision of Dr. Daniela Sousa, and therefore I am greatly thankful for her patience, availability and guidance through every step of the way. I can say surely say that was very lucky to have a supervisor like Daniela.
- Of course I must mention the great work environment at INEB and for that I must thank the rest of the NOG team (Inês, Juliana, Estrela, Luís and Joana) for their help in the daily routine of the lab and to put me to work with a smile on my face.
- The Masters student's room has been my workplace for the entirety of the project and I would like to thank all the members of this exquisite community for the "not so professional" moments during the project and for organizing the INEB football matches, allowing a much needed break once in a while.
- Every person needs friends and I am luckily blessed with excellent ones. I would like to thank my friends from High School for keeping in touch and for their support and fun moments we shared in all these years. Of course I also would like to thank my friends from FEUP and most of all the "010" generation for being there by my side in the 5 year voyage through university.
- In every moment I was with my family, they had only words of encouragement and kindness, so I want to thank them for being with me during all this time.
- Surely I cannot thank enough my parents for all their support during this stage of my life, for their understanding and help in the pursuit of my dreams and for providing my every need without compensation. I hope I can start giving back all that you gave me during these years with this graduation.
- And lastly, I do not need to put in words what I feel but I can at least thank Isa for being with me during these years and for being my personal Thesaurus and English dictionary during my endless writing sessions.

# Index

# List of Figures

# List of Tables

# Acronyms

| | |
|---|---|
| ADAM | A disintegrin and metalloprotease |
| ALP | Alkaline Phosphatase |
| Atp6v0d2 | d2 isoform of the Vacuolar ATPase v0 domain |
| BIBP3226 | *((R)-N*2-(diphenylacetyl)-N-[(4-hydroxyphenyl)methyl]-argininamide) |
| BMSC | Bone Marrow Stromal Cells |
| BMU | Basic Multicellular Unit |
| BMP | Bone Morphogenetic Protein |
| BSP | Bone Sialoprotein |
| CATK | Cathepsin K |
| CGRP | Calcitonin gene-related protein |
| CNS | Central Nervous System |
| CPC | Cetylpyridinium chloride |
| CTR | Calcitonin Receptor |
| DC-STAMP | Dendritic-cell specific transmembrane protein |
| ECM | Extracellular Matrix |
| ERK | MAPK extracellular signalling-regulated kinase |
| GADPH | Glyceraldehyde 3-phosphate dehydrogenase |
| GPCR | G-Protein Coupled Receptor |
| GSK-3β | Glycogen synthase kinase 3β |
| IGF-1 | Insulin Growth Factor 1 |
| IKK | Inhibitor of Nuclear Factor κβ kinase |
| IL | Interleukin |
| JAK | Janus Kinase |
| JNK | c-Jun N-Terminal Kinase |
| KO | Knockout |
| LRP5/6 | Low-density lipoprotein receptor-related protein 5/6 |
| MAPK | Mitogen-activated protein kinase |
| MCP1 | Monocyte Chemotactic Protein 1 |
| M-CSF | Macrophage-colony-stimulating factor |
| M-CSFR | Macrophage-colony-stimulating factor receptor |
| MEK | MAPK ERK kinase |
| MFR | Macrophage Fusion Receptor |

| | |
|---|---|
| MITF | Microphtalamia-associated transcription factor |
| MMP | Matrix Metalloproteinases |
| MSC | Mesenchymal Stem Cells |
| NF-κβ | Nuclear Factor κβ |
| NFAT | Nuclear Factor of Activated T cells |
| NPY | Neuropeptide Y |
| OB | Osteoblasts |
| OC | Osteoclasts |
| OPG | Osteoprotegerin |
| OSCAR | Osteoclast Associated Receptor |
| Osx | Osterix |
| PCR | Polymerase Chain Reaction |
| PDGF-BB | Platelet-Derived Growth Factor-BB |
| PGE2 | Prostaglandin E2 |
| PI3K | Phosphatidylinositol 3-kinase |
| PKA | Protein Kinase A |
| PKC | Protein Kinase C |
| PLC | Phospholipase C |
| PP | Pancreatic polypeptide |
| PPARγ | Peroxisome proliferator-activated receptor gamma |
| PTH | Parathyroid hormone |
| PYY | Peptide YY |
| RANK | Receptor activator of nuclear factor-κβ |
| RANKL | Receptor activator of nuclear factor-κβ ligand |
| RT-PCR | Reverse Transcriptase Polymerase Chain Reaction |
| RT-qPCR | Real-Time quantitative Polymerase Chain Reaction |
| Runx2 | Runt-related transcription factor 2 |
| S1P | Sphingosine-1-phosphate |
| SEM | Scanning Electron Microscope |
| SP | Substance P |
| STAT | Signal transducer and activator of transcription |
| TGF-β | Transforming growth factor β |
| TNF | Tumour Necrosis Factor |
| TNFR | Tumour Necrosis Factor Receptor |
| TRAF | TNFR-associated cytoplasmic factor |

| | |
|---|---|
| TRAP | Tartrate-Resistant Acid Phosphatase |
| $TRAP^+$ MNCs | TRAP positive Multinucleate Cells |
| TREM2 | Triggering receptor expressed on myeloid cells 2 |
| v-ATPase | Vacuolar ATPase |
| VIP | Vasoactive Intestinal Peptide |
| VitD3 | 1,25-dihydroxyvitamin-D3 |
| $Y_1R$ | $Y_1$ Receptor |
| $Y_2R$ | $Y_2$ Receptor |

# Chapter 1 – An Introduction to Bone Biology

## Bone Functions, structure and composition

Although usually regarded as a static and inert material, bone is a highly dynamic living tissue. It is constituted by inorganic and organic components which together with various types of cells carry out several important functions in the human body.

The Skeletal System is responsible as the support of body architecture, as the softer tissues and organs are attached to the skeleton. It ensures the protection of internal organs from external damage as well, protecting the heart, lungs and brain for instance. Other functions include locomotion, as the bones interact with skeletal muscles allowing movement, and also mineral homeostasis and energy storage. Finally, bone also provides a cavity for hematopoiesis, the production of blood cells and platelets[1].

There are two morphologically different forms of bone: cortical (compact) bone and cancellous (spongy) bone. Cortical bone is formed by densely packed collagen fibrils organized in concentric lamellae and they constitute around 80% of the skeleton, being found in the diaphysis of long bones (Figure 1)[2] and also in the outer surface of flat bones such as the skull. On the other hand, cancellous bone is composed of a loose and porous matrix established by

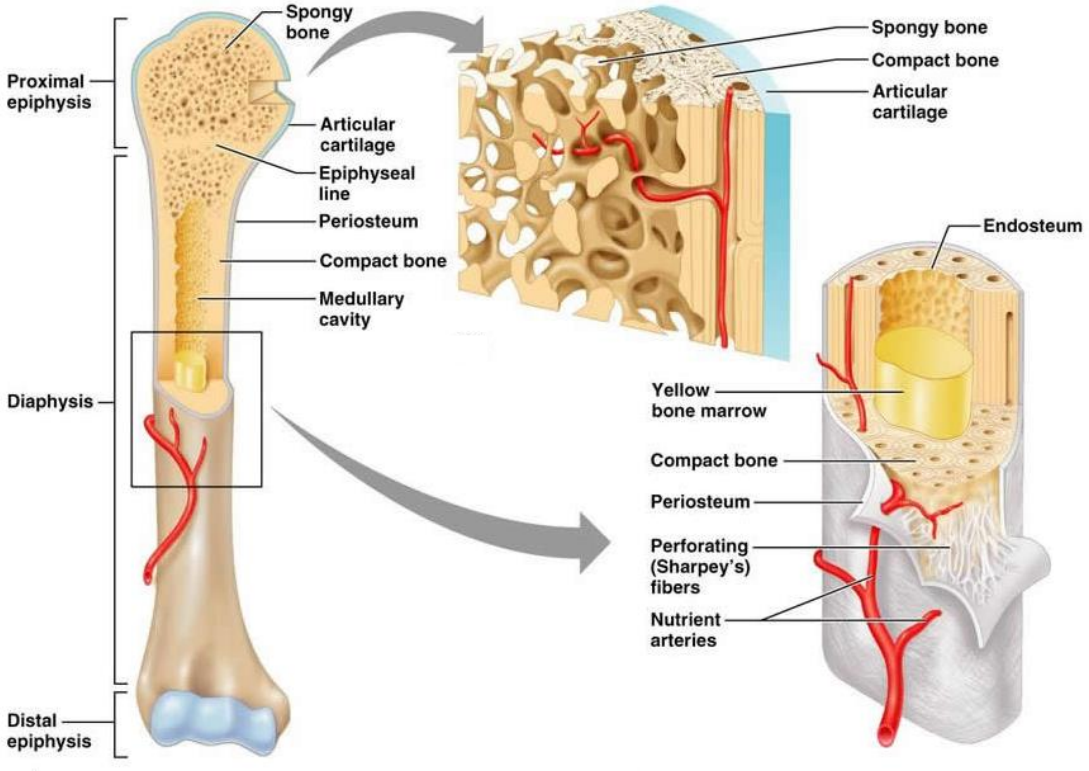


**Figure 1** – Long bone structure. Compact bone is formed by densely packed collagen fibrils organized in concentric lamellae, located mainly in the diaphysis of the long bone. Spongy bone is composed of a loose and porous matrix established by trabeculae and is found in the epiphysis. The bone is highly vascularized and enveloped by a fibrous structure in the outer surface, the periosteum, and a membrane in contact with the bone marrow, the endosteum. Adapted from [2].

of other proteins that promote the hydroxyapatite deposition. Besides collagen, other proteins such as proteoglycans, glycosylated proteins and serum-derived proteins play a fundamental role in the matrix organization and mineralization as well as in the modulation of bone cell attachment and activity. Finally, approximately 10% of the bone weight is attributed to water, which is important for cell nutrition, ion flux control and collagen structure maintenance[6].

## Bone Cells

OBs, OCs and Osteocytes are the main types of cells present in the bone and they are originated from different sources[7]. These cells communicate with each other in a tightly controlled manner either by direct contact or through signalling molecules in order to perform several key physiological processes such as bone growth and remodelling.

### Osteoblasts

OBs are the cells responsible for bone formation. They are derived from Mesenchymal Stem Cells (MSC) present in the bone marrow, which are also capable of differentiating into chondrocytes and adipocytes[8].

OB differentiation is highly regulated and can be divided in four stages: lineage commitment, proliferation, matrix maturation and mineralization stage[9]. This process is summarized in Figure 2. MSC commit to the OB lineage through the influence of Bone Morphogenetic Protein (BMP) and differentiate into Osteoprogenitor cells in the first stage.

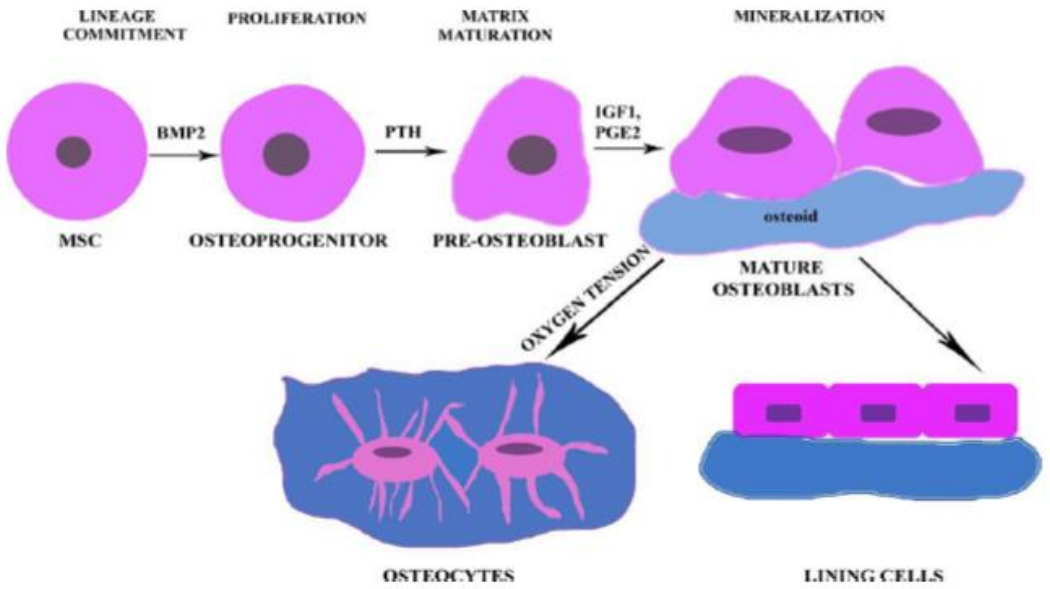


**Figure 2 -** Differentiation of MSC into mature OBs. MSC differentiate into osteoprogenitor cells by the influence of BMP2, which then differentiates into Pre-OBs through PTH signalling. Finally, IGF-1 and PGE2 cause the differentiation into mature OBs, which can then become into osteocytes or bone lining cells. Adapted from[11].

These cells have a high rate of proliferation and express Runt-related transcription factor 2 (Runx2), a transcription factor of great importance that suppresses MSC differentiation into chondrocytes and adipocytes. Runx2 regulatory element is present in the promoter of several OB genes controlling their expression, including type I collagen, alkaline phosphatase (ALP), bone sialoprotein (BSP) and osteocalcin leading to an OB phenotype[10]. Another important transcription factor is Osterix (Osx), a zinc-finger transcription factor that acts downstream of Runx2 and modulates OB differentiation, bone formation and mineralization[11].

Osteoprogenitor cells differentiate further into pre-OBs under the influence of the Parathyroid hormone (PTH). PTH induces the expression of ALP, collagen type I and BSP-II, involved in the production of bone matrix components[12]. In addition, PTH stimulates the receptor activator of nuclear factor(NF)-κβ (RANK) ligand (RANKL) mRNA expression, which performs a central role in OC maturation, as well as other matrix components and growth factors[13]. Parallel to PTH signalling, the Wnt/β-catenin signalling pathway also acts on the promotion of osteoblast differentiation, proliferation and matrix mineralization. Briefly, Wnt proteins, a group of secreted cysteine-rich glycoproteins, bind to a complex of receptors composed of Frizzled receptor and Low-density lipoprotein Receptor-related Protein 5 and 6 (LRP5/6) at the cell surface and inhibit glycogen synthase kinase 3β (GSK-3β) which was phosphorylating β-catenin for proteossomal degradation. Thus, β-catenin accumulates in the nucleus and causes target gene expression[14]. The importance of this pathway was demonstrated in gain-of-function studies where mice overexpressing LRP5 in OBs had increased bone volume and strength[15].

Subsequently, pre-OB differentiate into mature OBs through the combined action of Insulin growth factor 1 (IGF-1) and Prostaglandin E2 (PGE2) leading to the expression of specific markers such as osteocalcin, collagenases, BSPI, BSPII and ALP, characteristic of the matrix mineralization stage. Mature OBs are cuboidal cells which show typical secretory characteristics, with a well-developed rough endoplasmic reticulum and a large Golgi apparatus necessary to the production of bone matrix components[16].

Lastly, OBs may have three possible cellular fates: undergo apoptosis, become quiescent bone lining cells or become osteocytes. Osteocytes are OBs that became entrapped during bone deposition. They represent around 90% of the cells within the bone matrix and are characterized by a star-shape morphology with dendritic extensions that form a canalicular network, thus allowing the osteocyte network response to changes in mechanical and chemical stimulus from the bone microenvironment and systemic messages from the blood stream[17]. Aditionally, osteocytes are involved in the adaption of the bone to mechanical

forces and the regulation of OB and OC functions in the bone remodelling process. One of the most described proteins expressed by osteocytes is sclerostin, a protein that acts on OBs through LRP5 binding and interferes with the Wnt/β-catenin signalling cascade, leading to bone formation inhibition[18]. Bone lining cells, on the other hand, are important in bone remodelling regulation through the expression of several factors such as RANKL and for the formation of a closed canopy that keeps the cellular precursors localized and in contact with an adequate concentration of the factors released from the bone remodelling site[7].

Besides being responsible for bone formation, OBs have a preponderant role in OC regulation.

**Osteoclasts**

OCs are multinucleated cells responsible for bone resorption derived from cells of the hematopoietic myeloid lineage, as depicted in Figure 3. Myeloid progenitors differentiate into OC precursors (OCP) under the influence of factors such as PU.1 and microphtalamia - associated transcription factor (MITF), which induce the expression of Macrophage -colony stimulating factor (M-CSF) receptor (M-CSFR). M-CSF is secreted by OBs and upon priming with its receptor promotes the survival, proliferation and differentiation of OCPs by activation of extracellular signalling-regulated kinase (ERK) 1/2 and phosphatidylinositol 3-kinase (PI3K)/Akt signalling pathways[19]. Additionally, M-CSF leads to the expression of RANK, a Tumour Necrosis Factor (TNF) receptor (TNFR) related protein which is a key player in osteoclastogenesis and

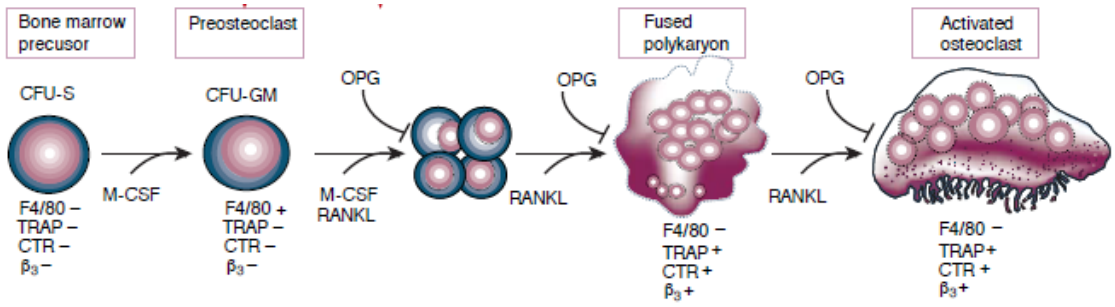


Figure 3 – Osteoclastogenesis. Bone marrow precursors differentiate into Pre-OC under the influence of M-CSF. Pre-OC express RANK which when bound to RANKL promotes proliferation, differentiation and Pre-OC fusion leading to the formation of multinucleated cells expressing characteristic OC markers such as TRAP and CTR. RANKL also modulates OC activity leading to active bone resorption. OPG acts as a soluble decoy of RANKL, inhibiting OC differentiation. Adapted from [20].

regulation of OC activity[20].

Activation of RANK by its ligand, RANKL, leads to the expression of OC specific genes during differentiation such as Cathepsin K (CATK), Tartrate -Resistant Acid Phosphatase (TRAP),

αvβ3 integrin and Calcitonin Receptor (CTR) and promotes further survival and activation of OC resorptive activity[21]. Trimerization of both RANK and RANKL is required for the activation of subsequent signalling cascades[7]. Considering that RANK lacks intrinsic enzymatic activity in its intracellular domain, signal transduction is accomplished by the recruitment of adaptor proteins such as the TNFR-associated cytoplasmic factor (TRAF) family of proteins. Specifically, TRAF6 is involved in the phosphorylation of the Inhibitor of NF-κβ kinase (IKK), c-Jun N-Terminal kinase (JNK) and Src, resulting in the activation of NF-κβ, Activator protein 1 (AP-1) and nuclear factor of activated T cells(NFAT)-2 which are then directed to the nucleus and promote the expression of OC specific genes and signalling for the survival, differentiation, motility and cytoskeleton rearrangement[20-22].

At this stage, proteins like Dendritic-cell specific transmembrane protein (DC-STAMP), CD9 and the d2 isoform of the vacuolar ATPase (v-ATPase) V0 domain (Atp6v0d2) begin to express and are crucial in Pre-OC cell fusion, the next step in Osteoclastogenesis[23]. CD9 is a membrane glycoprotein expressed under RANKL stimulation in lipid rafts that enhances Pre-OC fusion into multinucleated mature OC[24]. Similarly, DC-STAMP expression is stimulated by RANKL and its involvement in Pre-OC fusion was demonstrated through inhibition studies where DC-STAMP$^{-/-}$ mice showed a defect in Pre-OC fusion[25].Lastly, inactivation of Atp6v0d2 generates deficient osteoclasts without affecting the v-ATPase activity, being considered a regulator of Pre-OC fusion and bone formation[26].

OBs can further modulate OC activity through the secretion of Osteoprotegerin (OPG). OPG is a soluble TNFR-like protein that behaves as a soluble decoy of RANKL, thus inhibiting its activity and impairing OC differentiation [27, 28].

After Pre-OC fusion, mature OCs present a distinctive morphology, as represented in Figure 4. Its membrane forms an outer ring which isolates the bone surface to be resorbed, the "sealing zone", and the apical membrane presents irregularly shaped membrane extensions similar to microvilli, the "ruffled border"[29]. Mature OCs are responsible for actively resorbing bone surfaces and they do so by expressing several proteins important for the demineralization and degradation of the bone matrix: v-ATPase along with $2Cl^-/H^+$ antiporter are responsible for the acidification of the resorption area necessary for the demineralization

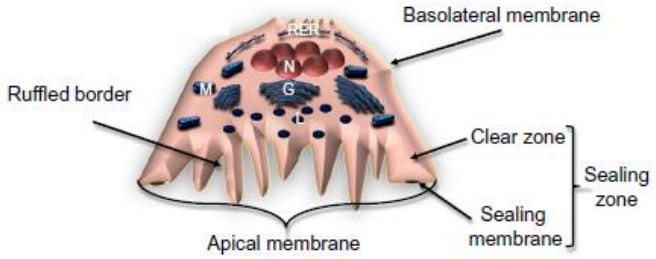


**Figure 4 –** Ilustration of OC Morphology. During maturation, OC membrane is restructured, forming a sealing zone to isolate the bone surface to be resorbed. In the apical membrane in contact with the bone, membrane extensions are projected forming a ruffled border which releases protons and enzymes causing the acidification and degradation of the bone surface. Organelles are situated in the basolateral side of the cell: RER-Rough Endoplasmatic Reticulum; N-Nuclei; G-Golgi Stack; M-Mitochondria; L-Lysosome. Adapted from [28].

of the bone surface; the acidic hydrolase CATK and also Matrix Metalloproteinases (MMP) such as MMP2 and MMP9 degrade the exposed Collagen type I network[29]; TRAP is a highly expressed acidic hydrolase that is crucial for bone resorption as demonstrated through experiments with $TRAP^{-/-}$ mice that showed an impairment in the bone resorption process[30], but the underlying molecular mechanisms are still poorly understood.

These key features in OC physiology and activity are tightly regulated by OBs and other cells and systemic factors, coupling bone formation and resorption during all stages of development, namely during bone growth and bone remodelling.

## Bone development, growth and remodelling

In the human foetus, bones are derived from three embryonic mesenchyme structures: the somites, which generate the axial skeleton; the lateral plate, which generates the limb skeleton; and the neural crests, which generate the skull and facial bones[31]. Bone formation occurs either by a direct conversion of the mesenchyme into bone tissue, the intramembranous ossification characteristic of the flat bones, or an indirect process where previously formed rudimental cartilage is replaced by bone tissue, the endochondral ossification, typical in the development of most of the bones including the long bones[3].

In both processes, the primary bone formed is a random arrangement of collagen type I fibers and no mechanical competence, also termed as osteoid, which is then replaced by a secondary bone with a highly organized collagen structure in concentric lamellae. Primary bone is produced rapidly and appears in the fourth month of foetal life, while the replacement with secondary bone starts before birth[31].

In intramembranous ossification, MSCs previously condensated in compact nodules expand outwards and differentiate into capillaries and cells from the OB lineage, defining the early shape of the developing bone. Following osteoid component secretion and early mineralization of bone spicules by OBs, these structures fuse together in a trabecular structure forming primary bone[32]. Contrarily, endochondral ossification involves the early formation of a cartilage model by chondroblasts derived from MSCs. A primary ossification center appears in the cartilage rudiments and starts forming the diaphysis of long bones, followed by the development of secondary ossification centers and cartilaginous growth plates in the epiphyseal ends. These are later replaced by primary bone and thus leading to bone growth[33].

Healthy skeletal growth is achieved through a bone modelling process characterized by a change in bone shape through an unbalanced mechanism favouring bone formation instead of

bone resorption leading to growth and mechanical adaptation. This starts in the late foetal stage of development and ends at about 18 to 25 years of age and its highly regulated through the effects of systemic factors, mainly PTH in childhood and sex hormones during puberty [31].

Once the human skeleton has matured, the maintenance of bone homeostasis is fundamental and it is mainly achieved through a Bone Remodelling process which main roles are the regulation of the mass, mechanical integrity and mineral composition of the bone[17]. In this process are involved various cell types such as OB, OC, Osteocytes and Bone Lining cells organized in basic multicellular units (BMU) throughout the bone's surface, as depicted in Figure 5. These BMU provide a sealed microenvironment where there can be a close interaction between the involved cells[7]. The BMU present in cortical and trabecular bone are distinct in their structures and bone remodelling mechanisms. In trabecular bone, BMUs are located on the surface of the bone and are covered by a canopy of lining cells with OB filling the previously OC resorbed space. On the other hand, BMU in the cortical bone are comprised of a cutting zone where OC proceed through the bone followed by bone forming OB. Bone remodelling takes place throughout the skeleton at BMUs in an independent and non-synchronous way[34].

Bone remodelling in each BMU is composed of four phases: activation of the target bone surface, recruitment of OC to perform bone resorption, transition from resorption to bone formation and finally recruitment of OB to form new bone[35]. The signal for the initiation of

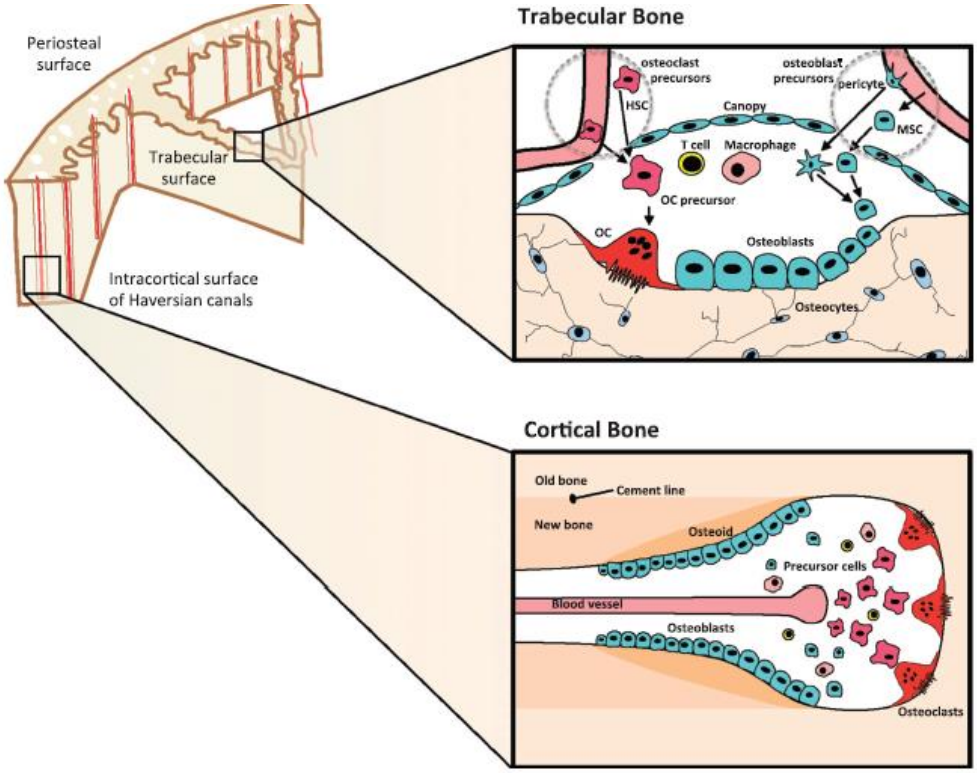


**Figure 5 -** The organization of a BMU. OBs and OCs are responsible for bone formation and resorption, respectively, and are formed from precursors supplied by the bone marrow or bloodstream. BMUs differ in their structure and organization depending on whether they are located on cortical or trabecular bone. Adapted from [30].

bone remodelling might be presented either by osteocyte secretion of sclerostin and other factors that stimulate osteoclastogenesis[17] or even by the apoptosis of some osteocytes and bone lining cells of the canopy in the BMU that release chemokines and paracrine factors, such as Sphingosine-1-phosphate (S1P) that recruit hematopoietic OCs precursors from the surrounding blood vessels and from the nearby bone marrow[36].

After Pre-OCs recruiting, M-CSF and RANKL secreted by cells from the OBs lineage come into play in the OC differentiation and multinucleated OCs start bone resorption. 1,25-dihydroxyvitamin-D3 (VitD3) is a hormone that stimulates osteoclastogenesis through its induction of RANKL secretion by OBs, being very important on bone remodelling induction, although there are reports of an administration of VitD3 being responsible for an increase in bone density in osteoporotic patients. This seemingly paradoxical interaction may be explained by different pharmacological and physiological effects of VitD3, which is involved also in intestinal absorption of calcium and thus explaining a decrease in osteoclastogenesis and increase in bone formation[37].

Soon after OC maturation, a combination of acid hydrolases like CATK and TRAP along with an acidification of the resorption site through the transport of H+ by v-ATPases and 2Cl-/1H+ antiporter causes the demineralization of the bone and the exposure and degradation of its organic components[29]. This process also causes the release of factors such as Transforming Growth Factor-β (TGF-β) and IGF-1 from the degraded matrix regulating OCs function, and these are linked to the coupling between bone resorption and bone formation by activating nearby OBs precursors. Other chemoattractant factors that recruit OBs precursors to the resorption site include Platelet-Derived Growth Factor-BB (PDGF-BB) and also S1P[35].

The transition between bone resorption and formation is very important and a balanced remodelling requires the formation of the same amount of resorbed bone. Calcitonin, a thyroidal hormone, inhibits OC activity by loss of the “ruffled border” and changes in the actin cytoskeleton and cell adhesion[38]. Similarly, OB produced OPG hinders osteoclastogenesis by sequestering RANKL and thus allowing the coupling from bone resorption to bone formation. At the same time, direct contact between OB and OC further stimulates OB differentiation and survival through the OC membrane protein EphrinB2 that binds to the membrane receptor with tyrosine kinase activity EphB4 present on the surface of OB precursors that activates ERK1/2 signalling pathways[34].

Finally, differentiated OBs adhere to bone surfaces and start to secrete an organic matrix composed of collagen type I, the osteoid, which is then mineralized through the deposition of hydroxyapatite crystals induced by alkaline phosphatase (ALP) expressed by OBs.

# Chapter 2 – Neuropeptide Y and Bone

It is evident that intercellular communication plays a fundamental role in bone remodelling. However, this is not exclusive for bone cell - bone cell signalling but instead the nervous system is also responsible for the regulation of bone remodelling. Sympathetic and sensory nerve fibres are present throughout the bone marrow, mineralised bone and periosteum and although there is no proof of the establishment of synapses between ne rve fibers and bone cells, the effect of several neuropeptides in close association with these cells is apparent[39].

Substance P (SP), Calcitonin gene-related protein (CGRP), Vasoactive Intestinal Peptide (VIP), Serotonin and Neuropeptide Y (NPY) are some of the neuropeptides studied that have a regulatory function in bone remodelling and homeostasis. SP is a well-known nociceptive molecule that is typically associated to sensory nerves and has been shown to promote BMU formation and OBs differentiation and cAMP production. At least one of its receptors, neurokinin-1, is also present in OCs and it drives OCs resorption activity[40]. CGRP has a similar effect on OBs, promoting the increase of intracellular cAMP and calcium which leads to changes in morphology and function. Thus, CGRP induces OBs proliferation, collagen synthesis and bone formation and besides being secreted by neuronal terminals it can also function as an autocrine mediator, because it can be also produced by OBs[41]. VIP is a neuropeptide associated to para-sympathetic nerves and it has an important role in controlling osteoclastogenesis by inhibiting RANK expression and increasing the expression of OPG in OBs, decreasing the resorption activity of OCs[40]. Serotonin is a peptide that modulates mood, emotion, sleep and appetite but it is also involved in bone regulation, namely on OBs and OCs differentiation and transduction of mechanical stimulus from osteocytes[41]. NPY function and importance are demonstrated below.

## NPY system

NPY is a 36 amino-acid peptide with a highly conserved primary structure that was isolated for the first time from porcine brain and since then has been found in all mammals and in a wide range of animal species[42]. NPY, in conjunction with the intestinal peptide YY

(PYY) and the pancreatic polypeptide (PP), form the NPY-family of proteins. In addition, these proteins are characterized by having a common tertiary structure, the PP-fold, with an N-terminal polyproline sequence and an amphiphilic α-helix joined together by type I β-turn creating a hairpin loop, having a critical importance in the interaction with its receptors[43].

NPY is highly abundant in the mammalian brain and is distributed throughout the central nervous system (CNS) particularly in the hypothalamus, cerebral cortex, brain stem, striatum and limbic structures. In the periphery, NPY is found in the sympathetic nervous system co-stored and released with noradrenaline during nerve stimulation[44]. Thus, due to this widespread expression, NPY plays an important role in a large range of biological processes such as feeding behaviour, learning and memory, body temperature regulation, emotional behaviour, circadian rythms, pain, sexual behaviour and hormone secretion. Furthermore, NPY seems to be implicated in several disorders such as obesity, epilepsy, depression and bone formation disorders[43]. Interestingly, NPY is being identified in peripheral tissues, where both OBs and adipocytes are able to produce NPY[44].

Overall, a pivotal role of a hypothalamic central pathway in bone homeostasis has been widely accepted due to *in vivo* evidence, especially from experiments where leptin deficient mice demonstrated an increased cancellous bone volume, and this effect is abrogated by the local administration of leptin in the hypothalamus[45, 46]. Leptin is a small polypeptide secreted by adipocytes that is primarily involved in the control of body weight and gonadal function and exerts its effects on the hypothalamus. The leptin-dependent bone formation inhibition seems to be independent from the NPY pathway, because the leptin-deficient stimulation of bone formation is maintained in the presence of high hypothalamic concentration of NPY[47].

The NPY system is the other major component of the neural output from the hypothalamus to bone. In humans, NPY can signal through four G-Protein Coupled Receptor (GPCR) subtypes, $Y_1$, $Y_2$, $Y_4$ and $Y_5$ expressed widely in central and peripheral tissues[48]. Their location and functions are explicit in Table I[49].

Particularly, $Y_1$ receptor ($Y_1R$) and $Y_2$ receptor ($Y_2R$) have been demonstrated to have an important role in bone growth and remodelling, which was further evidenced by the presence of NPY reactive nerve fibres on bone and surrounding tissues and by proof of expression of NPY by OBs[50]. These are activated by ligand binding and upon persistent agonist stimulation, the receptors are specifically phosphorylated at Ser/Thr residues which causes the uncoupling of the receptor from the G protein and consequent desensitization[49]. This is considered a crucial physiological process to avoid further G-protein signalling and maintain cellular homeostasis. The specific phosphorylation subsequently leads to arrestin protein binding and

clathrin-dependent internalization into endosomes. Once internalized, the receptor is dephosphorylated and can be recycled back to the cellular membrane or can be targeted for proteosomal degradation[51].

**Table I** – Y Receptor subtypes and their distribution and function

| Receptor | Location | Function |
|---|---|---|
| $Y_1$ | Brain<br>Vascular smooth muscle cells<br>Adipose tissue<br>Kidney<br>GI tract<br>Bone tissue | Energy homeostasis<br>Neuroendocrine regulation<br>Bone homeostasis<br>Ethanol consumption<br>Seizure regulation<br>Anxiety regulation<br>Angiogenesis |
| $Y_2$ | Neuronal tissue<br>Spleen<br>Liver<br>Blood vessels<br>Adipose tissue | Bone Homeostasis<br>Anxiety regulation<br>Cardiovascular regulation<br>Energy homeostasis |
| $Y_4$ | GI tract<br>Hippocampus | Cardiovascular regulation<br>Energy homeostasis |
| $Y_5$ | Hypothalamus<br>Thalamus<br>Amygdala<br>Cerebral cortex | Energy homeostasis<br>Seizure regulation<br>Angiogenesis |

Baldock and his team were the first to observe a two-fold increase in the trabecular bone density in $Y_2R$ germline knockout (KO) mice due to a higher OB activity without significant changes in OB and OC surface and have shown that a selective deletion of hypothalamic $Y_2R$ yielded a similar result, suggesting that $Y_2R$ signalling acts on bone homeostasis through a central pathway. The lack of changes in the levels of leptin and pituitary hormones in the plasma point to a $Y_2R$ modulation of bone formation by neural mechanisms and not by an indirect increase or decrease in blood circulating hormones[52]. Besides inherent changes in cellular metabolism, elevated bone mineralization and formation rate in $Y_2R$ KO mice might be due to an increased number of Osteoprogenitor cells in the bone , as Lundberg and co-workers demonstrated[53], although the colony-forming ability of these cells is unchanged when

compared to a wild-type phenotype. Furthermore, $Y_2R$ seems to be involved in the proliferation and differentiation of the OB lineage since treatment with NPY increased the expression of OB specific markers such as ALP and osteocalcin, a result that was maintained when the cells were treated with a $Y_2R$ agonist and abrogated upon treatment with a specific antagonist[54]. However, treatment with NPY decreased the mineral deposition in spite of the increase in OB markers expression, which is consistent with the increase in bone formation in $Y_2R$ KO mice but it is a process not yet fully understood[54].

Interestingly, $Y_1R$ expression was significantly down-regulated in $Y_2R$ KO mice probably due to the lack of feedback inhibition of NPY release leading to an over stimulation and consequent desensitization and down-regulation of $Y_1R$ in the bone cells, which may be involved in the increase in bone formation and mineralization phenotype observed in these mice[53].

## Role of the $Y_1R$ in the regulation of bone homeostasis

$Y_1R$ is a GPCR-like 384 amino acid protein with a seven-pass transmembrane domain and a C-terminal signal transduction tail. It exhibits a high affinity for NPY and PYY but a very low affinity for PP and it is one of the most extensively studied Y receptors, with a wide range of peptide and non-peptide agonists and antagonists available and described[43].

There is increasing evidence that NPY-induced proliferation *via* $Y_1R$ is a modulating process in the activity and growth of a wide range of cell types including among others vascular smooth muscle cells, neuronal precursor cells, pre-adipocytes and endothelial cells, mainly through the activation of ERK1/2 signalling cascade which eventually leads to proliferation and survival[43].

In bone tissue, $Y_1R$ is expressed in both OB and OC and evidences seem indicate that this receptor plays a crucial role in bone formation modulation[55]. Contrarily to the effect observed with $Y_2R$-driven stimulation of OB proliferation, $Y_1R$ seems to have an inhibitory effect in the differentiation of MSC and also in the mineralization capacity of mature OBs, since MSC derived from $Y_1R$ germline KO mice showed an increased capacity to differentiate into OB when compared to MSC from wild-type mice[56]. Concerning mineralization, however, only Bone marrow stromal cells (BMSC) derived from mice with a mature OB-specific deletion of $Y_1R$ demonstrated an increase in mineral deposition *in vitro*, BMSC obtained from $Y_1R$ germline KO showed a decreased mineralization capacity[56]. The different *in vitro* responses of OB

derived from $Y_1R$ germline KO mice and from conditional OB-specific $Y_1R$ deletion indicate that NPY might be involved in maturation-dependent actions in the OB lineage.

It is generally accepted that $Y_1R$ signalling inhibits OB bone forming activity, primarily due to evidence obtained from $Y_1R$ germline KO mice that showed a general increased cortical and cancellous bone formation[57]. In these experiments, Baldock et al demonstrated a significant increase in cancellous volume, with an increase in trabecular number and volume, cortical thickness and overall augmented bone formation and mineralization rates without changes in mineralization surfaces in both male and female mice, pointing to an intensified OB activity. Interestingly, OC surface was also increased in $Y_1R$ germline KO mice even though the overall balance of bone formation/resorption was shifted towards bone formation, which was not verified in $Y_2R$ germline KO mice[57]. Moreover, hypothalamic specific $Y_1R$ deletion did not alter bone homeostasis, suggesting that $Y_1R$ acts on bone formation through a peripheral pathway, independent of hypothalamic $Y_1R$ signalling[57]. The effect of an $Y_1R$ germline and hypothalamic deletion is illustrated in Figure 6.

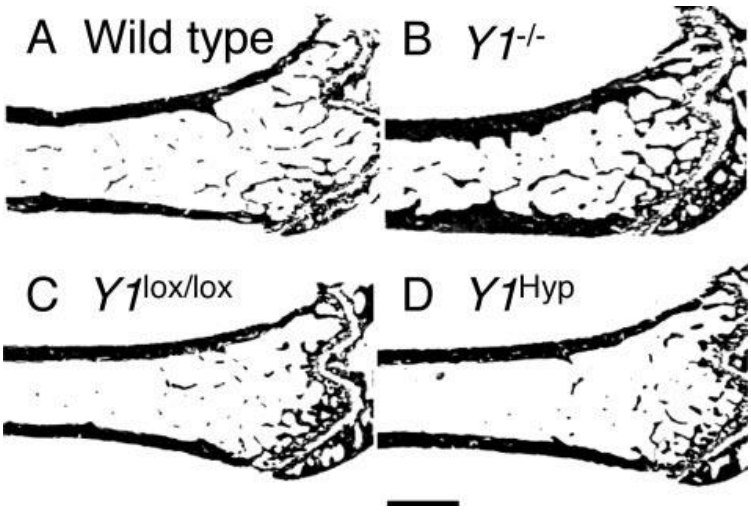


**Figure 6 –** Stained sections of the distal femoral metaphysis of (B) $Y_1R$ germline KO mice which show an increased cancellous volume and cortical thickness compared to (A) a Wild type phenotype. (D) Hypothalamic specific $Y_1R$ deletion did not displayed significant differences in cancellous volume and cortical thickness when compared to an empty vector control (C). Bar – 1mm. Adopted from [57].

These results are consistent with the findings of Lee et al where a conditional deletion of OB $Y_1R$ resulted in increased cancellous bone volume, trabecular number and thickness and enhanced OB activity, suggesting that OB-specific $Y_1R$ are primarily responsible for the $Y_1R$-mediated regulation of bone metabolism [58]. The extent of these changes, however, was not as great as in germline $Y_1R$ KO mice, which might point to an $Y_1R$ inhibition effect on pre-OB differentiation and consequent bone formation, since the deletion was specific to mature OBs in these mice[58].

In the regulation of bone formation, $Y_1R$ and $Y_2R$ seem to be involved through a common signalling pathway since the deletion of both $Y_1R$ and $Y_2R$ does not lead to significant changes in cancellous bone formation when compared to $Y_1R$ KO or $Y_2R$ KO single mutants, despite

resulting in a significant increase in bone formation compared to wild-type mice[57]. The mineral deposition seems to be slightly decreased in double mutant mice compared to $Y_2R$ KO mice, but no significant changes in cortical bone were reported[57]. Interestingly, OC surface was not increased in double mutant mice, contrarily to what was observed in $Y_1R$ KO mice[57]. Due to this lack of additive effects on bone metabolism, the involvement of Y1R and Y2R in

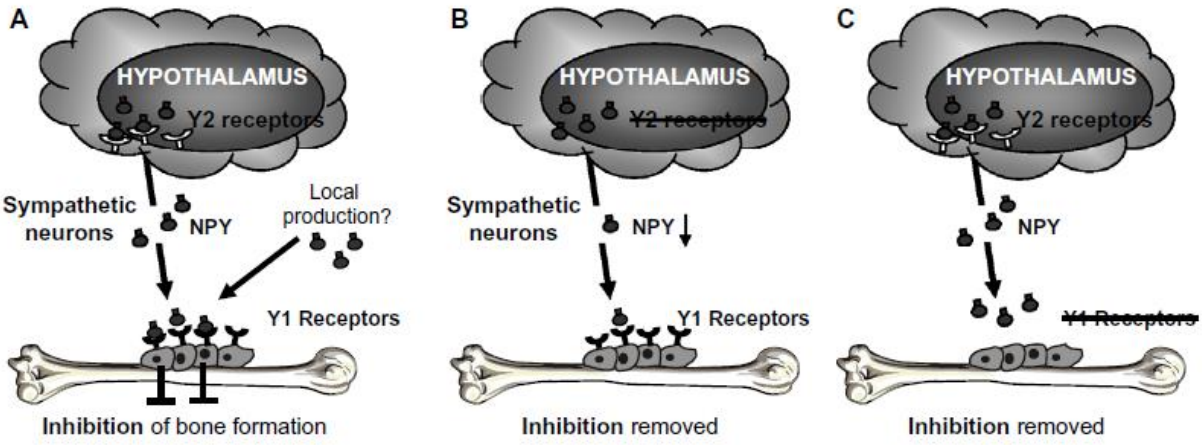


**Figure 7 -** Proposed pathway for the regulation of bone formation by hypothalamic $Y_2R$ and OBs $Y_1R$. $Y_2R$ in the hypothalamus mediate NPY inhibition of bone formation through OB $Y_1R$ (A). Central $Y_2R$ specific deletion (B) or OBs $Y_1R$ specific deletion (C) revert bone formation inhibition. Adopted from [55].

bone metabolism through a common pathway was hypothesized and a proposed mechanism of NPY action on bone is explicit in Figure 7.

*In vitro* studies have also revealed new insights on the regulation of NPY and $Y_1R$ and their influence on bone metabolism. NPY is secreted by neuronal cells in the proximity of the bone but can also be secreted by cells of the OB lineage. Of the latter, Osteocytes are the main producers of NPY, as revealed through NPY immunostaining studies using GFP expression to differentiate between the bone cell types[59]. This NPY expression was shown to be modulated by glucocorticoids, since NPY mRNA expression was upregulated in osteocyte-like cells exposed to corticosterone[60], and also by mechanical stimuli, leading to a decrease in NPY expression[59].

*In vitro*, similarly with an *in vivo* scenario, NPY interacts with $Y_1R$. $Y_1R$ expression in both calvarial OB and in OB-like MC3T3-E1 cells increases as the osteoprogenitor cells differentiate and mineralize in culture [59, 61, 62]. There is some controversy on whether NPY signalling modulates $Y_1R$ expression in culture, a decrease in expression under NPY signalling and also the maintenance of control levels were reported, although in these studies different cell types were used[54, 63]. Overall, NPY leads to the downregulation of OB specific markers such as BSP and osteocalcin and to a decrease in mineral deposition, according to studies using exogenous

NPY and also OB obtained from NPY overexpressing mice[59, 63]. Furthermore, cellular cAMP levels were decreased upon NPY stimulation[59]. This might be due to a G-protein receptor mediated adenylate cyclase inhibition and could be the underlying mechanism of modulation of OB differentiation, although other undiscovered signalling pathways cannot be excluded.

On the other hand, data on the effect of NPY and $Y_1R$ signalling on OCs is still scarce. *In vitro*, in an isoprenaline stimulated OC/stromal cell co-culture model, NPY seems to inhibit osteoclastogenesis in a dose dependent manner, decreasing the number of TRAP positive Multinucleate Cells ($TRAP^+$ MNCs) and decreasing the resorptive capacity of OC cultured in dentine slices. However, when stromal cells were stimulated with VitD3 or RANKL, the NPY inhibition was abrogated and $TRAP^+$ MNCs number was similar to the control[64]. These results might be explained by the different RANKL expression pathways on stromal cells, since VitD3 induces RANKL production through binding to an intracellular receptor that functions as a transcription factor whether PTH and isoprenaline induce this expression through cAMP/PKA signalling pathway[65], and $Y_1R$ seems to inhibit cAMP production. Nonetheless, the effect of $Y_1R$ signalling in osteoclastogenesis and OC gene expression remains poorly understood.

## $Y_1R$ antagonists and their therapeutic potential

Due to its effect on bone turnover and having a peripheral action pathway instead of a central one, $Y_1R$ has demonstrated a great potential as a drug target to prevent or revert bone loss and treat certain bone disorders such as osteoporosis[43]. Some antagonists were developed through the study of NPY hormone family peptides, but they had limitations due to its proteic origin[51]. Synthetic $Y_1R$ antagonists circumvent those limitations, and in 1994 Rudolf and his team described for the first time the molecule *((R)-N*2-(diphenylacetyl)-N-[(4-hydroxyphenyl)methyl]-argininamide) (BIBP3226), a promising $Y_1R$ synthetic antagonist[66]. BIBP3226 is a non-peptidic low molecular weight molecule that binds $Y_1R$ potently and selectively counteracting its normal signalling cascade, both *in vitro* and *in vivo*[67]. Despite the systemic administration of this compound might having serious disadvantages, a local and controlled release of these antagonists in the desired location through a drug carrier that allows cell targeting, controlled release and an extended half-life of the drug can be a good solution to overcome these problems.

Besides BIBP3226, other $Y_1R$ antagonists were developed. Daniels et al developed an extremely potent $Y_1R$ antagonist (GR231118) that demonstrated significant effects on the food intake in animal models[68]. However, it is not specific because it is also an $Y_4$ receptor agonist.

BIBO3304 is another promising potent compound that is highly specific for $Y_1R$ and is slightly less toxic than BIBP3226, and recent evidence show that an oral administration of BIBO3304 resulted in an increased bone formation *in vivo*[69]. Some synthetic $Y_1R$ antagonists are listed in Table II.

These compounds can prove valuable in the study of the role of the $Y_1R$ in bone homeostasis and they have shown great potential as therapeutic applications in bone disorders. In addition to $Y_1R$ KO experiments where the $Y_1R$ central role in bone regulation was highlighted [54, 55, 57, 58], *in vivo* and *in vitro* studies with $Y_1R$ antagonists may reveal possible therapeutic applications in the prevention or treatment of degenerative skeletal diseases. $Y_1R$ antagonists can also have potential applications in several other disorders including feeding disorders, seizures, intestinal disorders and even in cancer[70].

**Table II –** List of synthethic $Y_1R$ antagonists

| **Compounds** | **Description** |
|---|---|
| GR231118 | Extremely potent, however it is also a potent $Y_4$ agonist |
| BVD-11 | Highly selective and potent |
| BVD-42 | Highly selective and potent |
| BIBP3226 | Highly selective and potent, solubility/toxicity problems |
| BIBO3304 | Highly selective and potent, less toxic than BIBP3226 |
| SR 120819A | Selective and potent, does not penetrate the Blood Brain Barrier |
| LY357897 | Selective and potent |
| Benzazepine analog | Selective and potent |
| J-104870 | Highly selective and potent |

# Aims of the Project

The main objective of the current work is to study the effect of $Y_1R$ in OC differentiation and resorption activity. In order to achieve this goal, this project was focused in three specific aims:

- Study the influence of $Y_1R$ in OC differentiation and bone resorption using an $Y_1R$ KO animal model.
- Evaluate if the $Y_1R$ pathway is responsible for the observed results in OC derived from $Y_1R$ KO mice through $Y_1R$ blockage with a specific antagonist, BIBP3226.
- Study the influence of OB and the $Y_1R$ pathway in osteoclastogenesis through the establishment of an OB/OC direct co-culture.

# Materials and Methods

## 1 – Cell Culture

### 1.1 OC monocultures

- Cell Extraction

To generate primary OC, bone marrow cells were isolated from tibiae and femur of either 6-8 week old C57/Bl6 Wild Type (WT) mice or $Y_1R$ germline KO mice. Mice were euthanized through $CO_2$ asphyxiation, followed by femur dislocation from the hip by applying pressure on the joint. The skin was cut around the thigh and peeled down over the foot and both legs were cut over the femur and washed in PBS. The ankle was cut and both tibiae and femur were isolated and washed on PBS + 10% Penicillin/Streptomycin + 10% Fungizone after muscle and fat removal. Bone extremities were cut and cells were obtained by flushing the bone marrow with α-MEM supplemented with 10% v/v Fetal Bovine Serum (FBS), 10U/mL Penicillin and 10µg/mL Streptomycin (α-MEM Complete Medium). The resulting cell suspension was filtered through a 70µm cell strainer (Falcon) and centrifuged for 5 minutes at 1200 rpm and 4°C. Cells were ressuspended in 4mL α-MEM Complete Medium, plated in untreated petri dishes (1mL cell suspension + 4mL fresh α-MEM Complete Medium) and incubated for 3 days at 37°C in the presence of 30 ng/mL MCSF (PeproTech). Adherent cells were then detached with 0.05M EDTA in PBS for 20 minutes at 37°C, collected and centrifuged at 1200 rpm for 5 minutes at 4°C.

- OC monoculture

OC precursors were seeded at a density of $3.1x10^5$ cells/$cm^2$ of growth area in α-MEM Complete Medium. M-CSF and RANKL were added in every well at a concentration of 30ng/mL and 100ng/mL, respectively. Cells were incubated for 14 days changing medium every 3-4 days.

### 1.2 OB/OC direct co-cultures

- Cell Extraction

OCs precursors were obtained as described in section 1.1.

OBs were harvested from new-born mouse calvaria. Neonatal mouse pups with up to 6 days were rinsed in 70% ethanol and quickly euthanized through decapitation, followed by washing the heads with sterile PBS to remove blood. A cut was made in the base of the skull followed by a perpendicular cut on top of the skull and the removal of the skin. Calvaria was dissected and rinsed in α-MEM. 5 calvaria were put in 5 mL α-MEM complemented with 0.1% Collagenase, 0.2% Dispase II and 1% Penicillin/Streptomycin and were incubated for 10

minutes with agitation at 37°C. The digestion products were discarded and fresh 5mL α-MEM solution was added, incubating again for 10 minutes at 37°C under agitation. This second fraction was collected and the incubation step was repeated another 3 times, collecting fractions 2 to 5 in a single tube. The cell suspension was dissociated with a pipette and was filtered through a 70µm cell strainer to remove blood clots and cellular debris. The cell suspension was then centrifuged for 5 minutes at 1200 rpm at 4°C, the supernatant was discarded and the cells were ressuspended in 5mL of fresh α-MEM Complete Medium. Cells were seeded in 75cm$^2$ flasks at a cellular density of 10x10$^4$ cells/cm$^2$ and expanded at 37°C.

- OB/OC direct Co-cultures

After expansion, primary OB were seeded at a density of 2.5x10$^4$ cells/cm$^2$ of growth area in α-MEM Complete Medium. 50µg/mL Ascorbic Acid 2-phosphate, 10mM β-glycerophosphate, 10nM dexamethasone, 1000nM PGE2 and 10nM VitD3 were added to each well and the cells were incubated at 37°C for 24h[71]. After incubation, OC precursors were seeded directly on top of the adhered OB at a density of 3.1x10$^5$ cells/cm$^2$ of growth area in α-MEM Complete Medium supplemented with 1000nM PGE2 and 10nM VitD3 (Figure 8). Cells were incubated for 21 days changing medium every 3-4 days.

**1.3 Treatment with $Y_1R$ antagonist (BIBP3226)**

Cells were seeded at a density of 3.1x105 cells/cm2 of growth area in α-MEM Complete Medium. M-CSF and RANKL (PreproTech) were added in every well at a concentration of 30ng/mL and 100ng/mL, respectively, and cells were treated with 60 and 1000 nM BIBP3226. Untreated cells were used as control. Cells were then incubated for 14 days, and the medium was changed every 3-4 days. All conditions were established in triplicates.

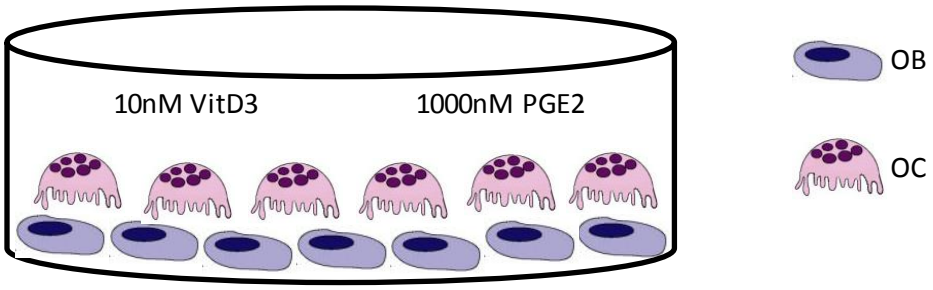


**Figure 8 – OB/OC direct co-culture model.** After cell extraction and expansion, OC were seeded directly on top of OB in the presence of VitD3 and PGE2.

## 2 - Dentine Resorption Assay

- **Dentine substrate resorption**

Resorbable Dentine Substrate Discs (OsteoSite Dentine Discs, IDS) were used for the OC resorption assay. Each disc was placed in an individual well of a 96-well plate and was incubated in α-MEM for 30 minutes at 37°C to wet the discs and facilitate cell adherence. WT

and $Y_1R$ KO OC precursors were directly seeded on top of the Dentine substrate at a density of $3.1x10^5$ cells/$cm^2$ of growth area in α-MEM Complete Medium, as described in section 1.1. Cells were then incubated for 21 days changing medium every 3-4 days.

- **Scanning Electron Microscope (SEM) analysis**

Dentine discs were washed thoroughly with PBS and transferred to 24-well plates. Each sample was fixed in 2.5% (v/v) glutaraldheyde (Agar) in 0.1M Sodium Cacodylate (Fluka) for 30 minutes at RT while shaking. After fixation, Dentine discs were washed with 0.1M Sodium Cacodylate three times. Finally, the discs were dehydrated in serial diluted ethanol solutions of 50, 60, 70, 80, 90 and 99% v/v, 10 minutes in each dilution, and stored in absolute ethanol. Each sample was then critical point dried, sputtered-coated with gold and examined by SEM. Pictures with a magnification of 50, 100, 500, 2000 and 5000x were obtained using back-scattered electrons, as well as an EDS spectra of the chemical composition of the Dentine disc surface. Image acquisition was done at the CEMUP facilities of the Universidade do Porto.

- **3D reconstruction of the resorption pits**

After washing with PBS, Dentine discs were incubated in a 2mM EDTA solution in PBS for 10 minutes at 37°C to remove adherent cells. They were then washed thoroughly with PBS and transferred to a new 96-well plate. The Dentine Discs were stained with 10µg/mL calcein in PBS for 30 min in the dark at RT, washed in PBS, air dried and stored at 4°C until Confocal Microscope analysis.

Images were obtained in a TCS SP2 Spectral Confocal and multiphoton system (Leica) at a resolution of 1024x1024 pixels with a 40x oil objective. The sample was exposed to radiation with a wavelength of 488nm through a pinhole setting of 1 airy. Images of resorption pits acquired were averaged twice and stacked images with a voxel size of 0.3662x0.3662x0.2849µm were generated.

Resorption pit 3D reconstruction was performed with Matlab 2013a (MathWorks, USA) software. Stacked images were loaded into the program and the resorption pit outline was manually inputted in every stack. A mask containing every outline was then generated and used to reconstruct the resorption pit and to calculate the resorption pit volume, depth, top section area and aspect ratio. Volume was calculated by multiplying the number of pixels contained in the outlines by the voxel size.

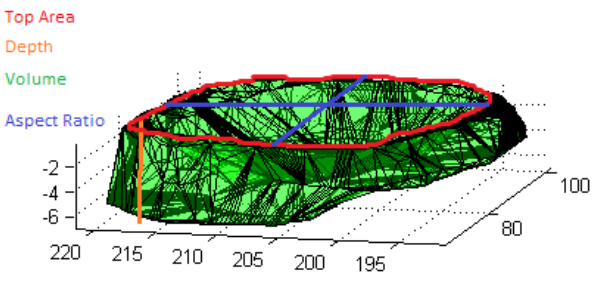


**Figure 9 – Resorption pit measurements.** Top Section Area (red), Depth (orange), Volume (green) and aspect ratio (blue) were calculated in each reconstructed resorption pit.

Depth was obtained by calculating the difference between the maximum layer index and the minimum layer index and multiplying by the step size (0.2849µm), the top section area was calculated by multiplying the pixels in the first layer by the voxel area and finally the aspect ratio was defined as the ratio between the maximum length and the perpendicular maximum width of the pit (Figure 9).

Resorption pits were defined as a single entity when consisting of one contiguous area at the surface of the dentine lacking fluorescence. Only isolated pits with clear boundaries were reconstructed. If the site pinched off into two or more entities at a depth greater than 50% of its total depth, they were still considered as a single pit. Otherwise, they were treated as separate pits with no clear boundaries, and therefore were not reconstructed. 3D reconstruction was performed by plotting the 3D point set of the mask obtained with the resorption pit outlines and by connecting each dot with the neighbouring 6 dots. The generated mesh was filled and a 3D image was generated.

## 3 - Staining procedures

### 3.1 TRAP Staining

TRAP Staining was performed using a Leukocyte Acid Phosphatase Kit (3-86A-1KT SIGMA) according to manufacturer's instructions. Briefly, the cells were washed with PBS and fixed with Citrate/Acetone Solution for 30 seconds at Room Temperature (RT). They were then rinsed with deionized water, air dried and incubated with warm TRAP Solution (water, acetate, naphtol, tartrate and 1 capsule of fast garnet salt GBC) for 1h at 37°C in the dark. After washing with water, the cells were incubated with Acid Hematoxylin solution for 5 minutes at RT. Finally, the samples were washed with water and air dried. Cells were then analyzed with a Stereomicroscope (SZX10, Olympus) coupled to a digital camera (DP21, Olympus) or with the Inverted Fluorescence Microscope (Zeiss Axio Vert), where images were acquired with AxioCam HRc (Zeiss) and using AxioVision SE64 Rel. 4.8. software.

### 3.2 F-Actin Staining

To analyse cell morphology, culture medium was removed from monoculture experiments and the cells were washed with PBS, followed by cell fixation with Paraformaldheyde (PFA) (Sigma-Aldrich) 4% for 10 minutes at RT. Cells were then washed with PBS and permeabilized with cold Triton X-100 0.1% (v/v)(Sigma) for 5 minutes. After washing twice with PBS, the wells were incubated with 1% (w/v) Bovine Serum Albumine (BSA)(Sigma) in PBS for 1h at 37°C to block antibody unspecific binding. The cells were incubated with Alexa-

Fluor 488 (green) Phalloidin (Life Technologies) 1:100 in PBS for 30 minutes at RT in the dark. At the end of the incubation time, the cells were washed with PBS and mounted using Vectashield with DAPI (Vector). The samples were kept at 4°C until analysis in the Inverted Fluorescence Microscope (Zeiss Axio Vert), where images were acquired with AxioCam HRc (Zeiss) and using AxioVision SE64 Rel. 4.8. software.

OC area measurements were performed using the "measure outline" tool of the AxioVision SE64 Rel. 4.8. software as depicted in Figure 10. Six representative images were obtained from each triplicate and every cell with more than 3 nuclei and with clearly defined boundaries was measured as an OC.

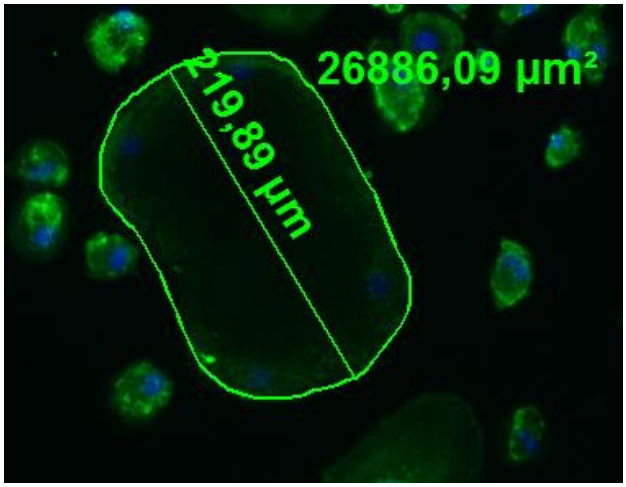


**Figure 10 –** Example of OC surface area measurement. Cells were stained with Alexa-Fluor 488 Phalloidin and DAPI and surface area was calculated using the "measure outline" tool of the AxioVision SE64 Rel. 4.8. software. Only cells with more than 3 nuclei and with clear boundaries were measured.

### 3.3 Alizarin Red staining and Quantification

Calcium deposition in OB produced matrix in OB/OC co-cultures was quantified by alizarin red staining. Medium was removed from the wells and the cells were washed twice with cold PBS. Cells were then fixed in ice-cold 70% ethanol for 1 hour at -20°C, followed by air drying. The wells were washed twice with water and stained with fresh 2% alizarin red (Sigma) solution in water (pH 4.2) for 15 minutes at RT on gentle agitation. After washing the wells twice, they were photographed using a Stereomicroscope (SZX10, Olympus) coupled to a digital camera (DP21, Olympus). The stain was eluted with 10% (w/v) cetylpyridinium chloride (CPC)(Sigma) in sodium phosphate solution (pH 7.0) for 20 minutes at RT on gentle agitation. The absorbance was measured at 570nm and compared to an alizarin red standard curve.

## 4 – Gene Expression Analysis

### 4.1 RNA extraction and purification

Culture media from 24-well plates was discarded and 100µL of TRIzol reagent (AMBION, Life Technologies) were added to each triplicate. The cells were incubated for 1 minute for cell lysis and the sample homogenate from each triplicate was put together. RNA was purified using a Direct-zol RNA Miniprep kit (Zymo Research) according to manufacturer's instructions. Briefly, 1 volume of ethanol (100%) was added to the sample homogenate in TRIzol, it was mixed by vortexing and loaded directly into a Zymo-Spin IIC Column in a Collection Tube. A series of washing procedures with Wash Buffers followed by centrifugation at 12000 rpm for 1 minute were performed. The RNA was eluted using DNase/RNase-Free water and stored at -80°C.

### 4.2 Reverse Transcriptase Polymerase Chain Reaction (RT-PCR)

The SuperScript II First Strand Synthesis Kit (Invitrogen) was used to synthetize cDNA. RNA concentration was normalized for 250ng (OC monoculture RNA) and for 500ng (OB/OC co-culture RNA) and filled up to 8µL with DEPC-treated water. 1µL of 10mM oligo(dTs) primer and 1µL of 10mM dNTPs were added to the RNA mix. Denatured the RNA/primer mixture at 65°C for 5 minutes and placed the samples on ice for 1 minute. Added 9µL of a reaction mix composed of 2µL of 10x RT-Buffer, 4µL of 25mM $MgCl_2$, 2µL of 0.1M DTT and 1µL of RNase out (40U/µL). Incubated the samples at 42°C for 2 minutes, after which 1µL of SuperScript II RT was added to each tube. cDNA synthesis was carried out for 50 minutes at 42°C. The reaction was then terminated at 70°C for 15 minutes, followed by chilling on ice. 1µL of RNase H was added to each tube and they were further incubated at 37°C for 20 minutes to eliminate reminiscent RNA. cDNA was stored at -20°C.

### 4.3 Polymerase Chain Reaction (PCR)

cDNA was amplified using the HotStarTaq PCR kit (Qiagen) according to manufacturer's instructions. Briefly, a reaction mix was prepared using 5µL of 10x concentrated PCR buffer containing 15mM $MgCl_2$, 1µL of 10mM dNTPs, 1µL of primer pairs (10µM), 0.25µL of HotStarTaq DNA Polymerase and filled up to 49µL of sterile distilled water. Primers were designed using the NCBI Primer-BLAST tool and synthetized by Invitrogen (Table III). All primer pairs were located in different exons to only ensure the amplification of correctly spliced mRNA. 1µL of template DNA was added to the previous mix. PCR was carried out in a

TPersonal Thermocycler (Biometra) with the following cycling conditions: enzyme was activated at 95°C for 15 min, followed by 35 cycles of sequential cDNA denaturation at 94°C for 1 min, annealing at 58°C for 1 min and extension at 72°C for 1 min. A final extension step at 72°C for 6 min was performed in the end and the samples were kept at 4°C.

PCR products were run on Ethidium Bromide stained 3.5% agarose (Lonza) gels using a PowerPac Basic Electrophoresis System (Bio-Rad) together with a HyperLadder V (Bioline) molecular weight marker. Gels were scanned on a GelDoc XR+ imaging system (Bio-Rad) under UV light and analysed using ImageLab Software (Bio-Rad).

**Table III –** Primer pair sequences for murine gene analysis.

| Gene | Forward Primer (5'->3') | Reverse Primer (5'->3') | Genbank Acession Number | Annealing Temperature (°C) | Product Length |
|---|---|---|---|---|---|
| GADPH | GCCTTCCGTGTTCCTACC | AGAGTGGGAGTTGCTGTTG | NM_008084 | 58 | 183 |
| TRAP5 | CGACCATTGTTAGCCACATACG | TCGTCCTGAAGATACTGCAGGTT | NM_001102405.1 | 58 | 77 |
| CTR | AGTTGCCCTCTTATGAAGGAGAAG | GGAGTGTCGTCCCAGCACAT | NM_007588.2 | 58 | 76 |
| (OSCAR) | TGGCGGTTTGCACTCTTCA | GATCCGTTACCAGCAGTTCCAGA | NM_175632 | 58 | 199 |
| CATK | ATATGTGGGCCAGGATGAAAGTT | TCGTTCCCCACAGGAATCTCT | NM_007802.4 | 58 | 90 |
| RANK | GGACAACGGAATCAGATG | CCACTACTACCACAGAGAT | NM_009399.3 | 58 | 123 |
| RANKL | CCCATCGGGTTCCCATAAAGT | AGCAAATGTTGGCGTACAGG | NM_011613.3 | 58 | 114 |
| OPG | GTGGAATAGATGTCACCCTGTGT | TTTGGTCCCAGGCAAACTGT | NM_008764.3 | 58 | 110 |
| DC-STAMP | AAGCGGAACTTAGACACAGGG | CAGCTAGGGCTTCGTGGAAA | NM_029422 | 58 | 101 |
| Atp6v0d2 | TTCTTGAGTTTGAGGCCGAC | CAGCTTGAGCTAACAACCGC | NM_175406 | 58 | 144 |
| CD9 | GCTGGGATTGTTCTTCGGGT | GCTTTGAGTGTTTCCCGCTG | NM_007657 | 58 | 171 |
| CD47 | CGATGCCATGGTGGGAAACT | TCAGTGTTGAAGGCCGTGC | NM_010581 | 58 | 99 |
| MCP1 | AGCCAACTCTCACTGAAGCC | GCGTTAACTGCATCTGGCTG | NM_011333 | 58 | 131 |
| $Y_1R$ | CTCGCTGGTTCTCATCGCTGTGGAACGG | GCGAATGTATATCTTGAAGTAG | NM_010934.4 | 60 | 325 |

### 4.4 Real-Time quantitative Polymerase Chain Reaction (RT-qPCR)

RT-qPCR was performed in a iCycler iQ5 Real-Time PCR Detection System (Bio-Rad) and data was analysed using iQ5 software (Bio-Rad). RT-qPCR was carried out in a 20µL reaction volume containing 10µL of iQ SYBR Green supermix (Bio-Rad), 1µL of cDNA template and 10µM primer pairs. The used supermix was composed of dNTPs, SYBR Green I dye, hot-start iTaq DNA Polymerase, qPCR buffer solution and stabilizers.

The following cycling conditions were performed: the enzyme was activated at 95°C for 3.30 min, followed by 40 cycles of sequential cDNA denaturation at 95°C for 30s, annealing at 58°C for 30s and extension at 72°C for 30s. The final step was the determination of the melting curve at 55-95°C for 10s/step.

For data analysis, the comparative threshold (CT) cycle values for constitutively expressed Glyceraldehyde 3-phosphate dehydrogenase (GADPH) to normalize loading variations. The expression fold difference was calculated according to Eq.1.

$$\text{mRNA relative Expression} = 2^{(CT_{control} - CT)} \quad \text{(Eq.1)}$$

Primer efficiency was assessed by a linear regression of the CT values of a cDNA template serial dilution and primers were considered efficient with efficiency values of 90-105%.

## 5 - Statistical Analysis

All results are expressed as mean ± SEM. Normal distribution of the data was assessed through Shapiro-Wilk test. Statistical differences between groups were compared using a two-way ANOVA and *post hoc* comparisons were performed with an Independent-samples t-test. When normal distribution was not verified, the non-parametric Kruskal-Wallis test followed by the Mann-Whitney U-test to assess statistical significance were performed. Statistical analysis was carried out with SPSS for Windows, version 20 (SPSS Inc., Chicago, IL, USA) and a $p<0.05$ was accepted as being statistically significant.

# Results and Discussion

## 1 – The role of $Y_1R$ in Osteoclastogenesis and OC resorption capacity

### 1.1 Expression of $Y_1R$ during Osteoclastogenesis

$Y_1R$ presence in WT OC was confirmed by PCR and RT-qPCR, which revealed an increase in $Y_1R$ expression during OC differentiation (Figure 11). Undifferentiated pre-OC do not show measurable levels of $Y_1R$ mRNA, while $Y_1R$ expression is non significantly increased at day 7 and day 14 of culture. Since $Y_1R$ expression was verified in these cells, further testing with this receptor ensued.

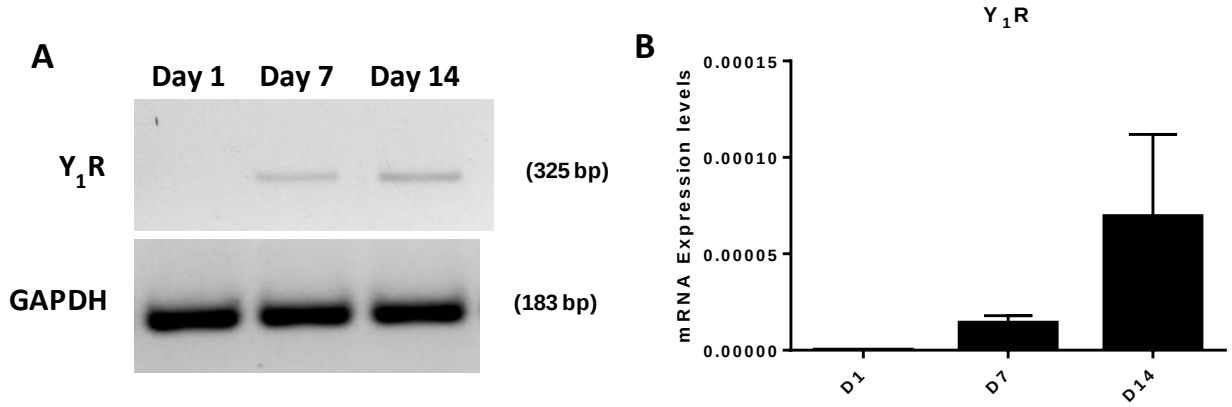


**Figure 11 - Expression of $Y_1R$ in WT cells**. Maturation of bone marrow derived pre-OC was induced with M-CSF and RANKL for 14 days in 24-well culture plates. mRNA was collected at the given time points from 3 replicates. (A) Expression of $Y_1R$ at day 1, 7 and 14 of culture. (B) Quantification of $Y_1R$ expression in WT cells relative to GADPH constitutive expression. Results are expressed as mean ± SEM from 2 independent experiments.

### 1.2 The effect of $Y_1R$ gene deletion on Osteoclastogenesis

$Y_1R$ KO mice demonstrated an increase in OC surface on cancellous bone when compared to control animals, suggesting an effect of $Y_1R$ signalling on the modulation of osteoclastogenesis[57]. However, the impact of $Y_1R$ deficiency on OC maturation is still unknown. Therefore, primary bone marrow flushed cells either from WT or $Y_1R$ KO mice were cultured for 14 days in the presence of M-CSF and RANKL to promote OC maturation. TRAP expression and morphology analysis was performed at culture day 7 and 14, where cells with more than 3 nuclei were considered OC.

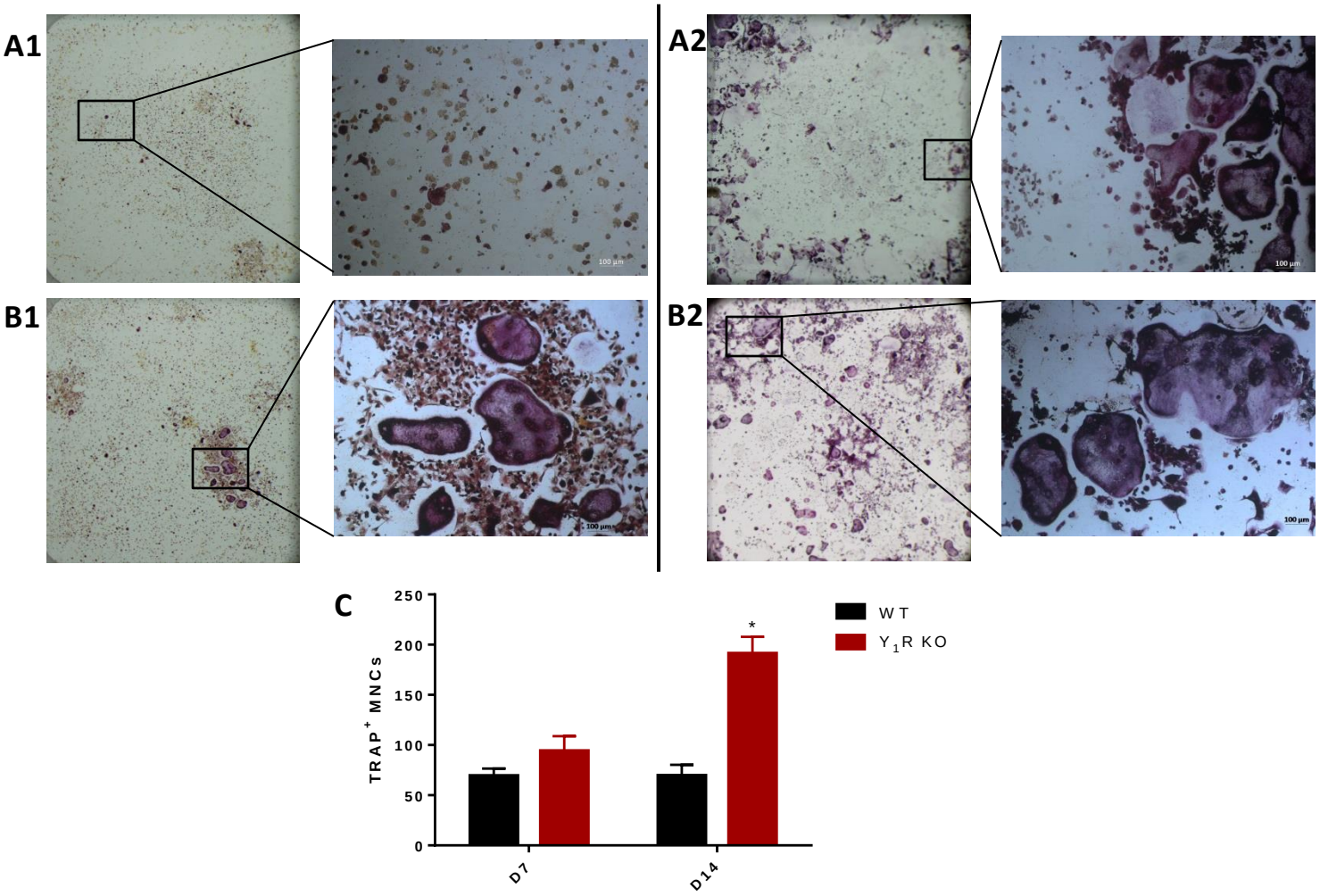


**Figure 12 – TRAP Staining of $Y_1$R KO OCs.** Maturation of bone marrow derived pre-OC was induced with M-CSF and RANKL for 14 days. Representative images of (A) WT and (B) Y1R KO cells at (1) day 7 and (2) day 14 time points are presented. Whole well images are shown on the left and images taken with the microscope with a 10x objective are shown on the right. Scale bar, 100 µm. (C) Number of $TRAP^+$ MNCs. $TRAP^+$ OC with more than 3 nuclei were counted. Results are expressed as mean ± SEM from 3 independent experiments. Groups were compared through ANOVA and independent-samples t-test with * $p<0.05$.

TRAP staining results are shown in Figure 12. At day 7, $Y_1$R KO wells revealed a relative increase in number of $TRAP^+$ MNCs compared to control conditions, albeit statistically non-significant (Figure 12C). After 14 days, however, $TRAP^+$ MNC numbers increased significantly in $Y_1$R KO wells. Microscopic analysis also shows a relative increase in size of $Y_1$R KO OCs compared to WT OCs (Figure 12B). These results are consistent with previous reports of a decrease in $TRAP^+$ MNC numbers with NPY stimulation[64], thus the increase in $TRAP^+$ MNCs is to be expected in the absence of NPY signalling through $Y_1$R in $Y_1$R KO OCs. NPY is therefore a negative regulator of pre-OC fusion such as OPG and Calcitonin[72], which also revealed a decrease in TRAP+ MNCs[73, 74], , although these changes might be implemented through different signalling pathways.

Similarly to other NPY receptors, it is generally accepted that $Y_1$R signalling cascade triggering leads to adenyl cyclase and $Ca^{2+}$ channel inhibition and to PI3K and ERK1 activation, promoting transcriptional regulation[75]. Interestingly, Hotokezaka and co-workers reported an

increase in osteoclastogenesis and TRAP intensity in OC-like cells incubated with specific Mitogen-activated protein kinase (MAPK) ERK kinase (MEK) inhibitors, which would inhibit MEK from phosphorylating and activating ERK1[76]. Thus, a decrease in osteoclastogenesis and $TRAP^+$ MNC numbers could be due to ERK1 activation, which is part of the $Y_1R$ signalling pathway. ERK1 inhibition is consistent with the results observed in the absence of $Y_1R$.

In addition, immunostaining of cytoskeletal F-actin was used to analyse $Y_1R$ KO OC morphology in comparison to control samples (Figure 13). Day 7 time point images revealed few and relatively small OC when compared to those of day 14 time point, suggesting that 7 days it is not enough to allow differentiation of pre-OC using this protocol. Pre-OC are rounded cells with a diameter around 30-50µm that are visible throughout the surface of the wells in every image, whereas other cells with fibroblast-like aspect such as the ones pointed with a red arrow (Figure 13A2, 13B2) might be BMSCs or MSCs that differentiated towards other cell types than pre-OC. A primary cell culture is mostly heterogeneous since it is hard to purify the cell types extracted from the bone marrow, which might explain the presence of the different cell types in culture (red arrows). Protocol modifications should be implemented in order to reduce these cell contaminations. Analysis of the wells at the day 14 time point showed an obvious increased size of mature $Y_1R$ KO OCs when compared to WT OCs, suggesting an increased fusion capacity of $Y_1R$ KO pre-OC. Differences in differentiation capacity cannot be concluded since cells from both genotypes were capable of differentiating, with comparable cell numbers. Mature OC pointed with a white arrow show typical OC morphology: a multinucleated cell with a characteristic actin ring in the sealing zone, with higher concentration of F-actin in the perimeter of the cell when compared to the cytoplasm.

Interestingly, measurement of OC section area revealed a statistically significant increase in the area of $Y_1R$ KO mature OCs when compared to WT cells, but only on day 14 time point (Figure 13C). This increased section area is probably due to increased motility or fusion protein expression by $Y_1R$ KO pre-OC.

### 1.3 The effect of $Y_1R$ KO on OC Resorption Capacity

A previous study with isoprenaline treated stromal cell/OC co-culture has shown a decreased OC resorption of dentin slices upon NPY stimulation[64]. In order to verify the effect of $Y_1R$ on OC resorption capacity, primary bone marrow flushed cells from WT and $Y_1R$ KO mice were seeded directly on top of dentine substrates on 96-well plates and were cultured for 21 days under M-CSF and RANKL stimulation. After fixation, critical-point drying and gold-

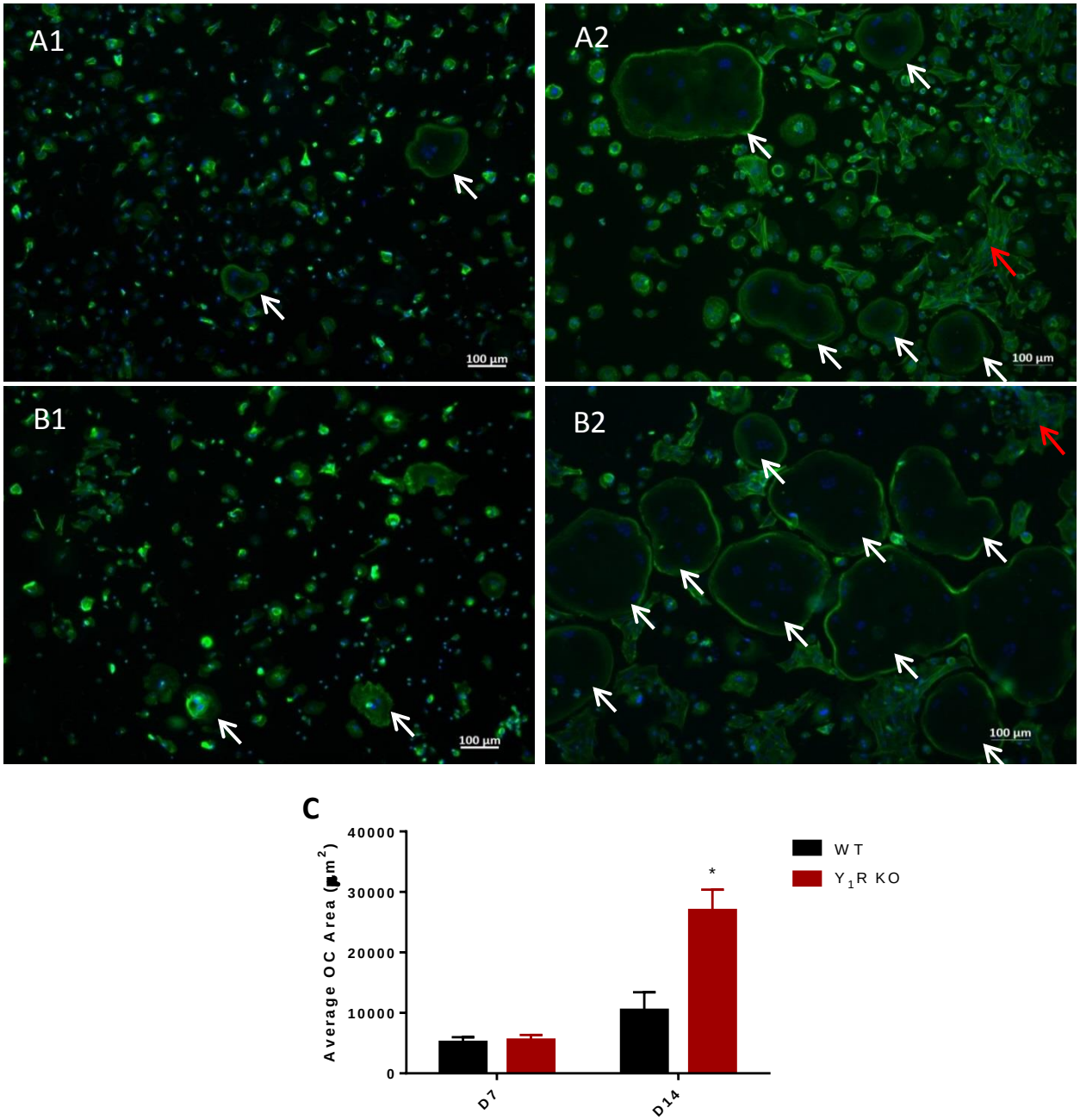


**Figure 13 – Morphological analysis and section area quantification of $Y_1$R KO OCs.** Maturation of bone marrow derived pre-OC was induced with M-CSF and RANKL for 14 days. Representative images of (A) WT and (B) $Y_1$R KO cells at (1) day 7 and (2) day 14 time points are presented, taken with a 10x objective. F-actin and nuclei were labelled with green and blue, respectively. Large, multinucleated cells were considered mature OC (white arrows). Other cell types were also present in culture (red arrows). Scale bar, 100µm. (C) Quantification of the mature OC section area by genotype. Results are expressed as mean ± SEM from 3 independent experiments with a total day 7 n = 179, 62, 109 ; 123, 126, 119 (WT; $Y_1$R KO) and day 14 n = 170, 39, 145 ; 90, 148, 166 (WT; $Y_1$R KO) cells measured. Groups were compared through Kruskal-Wallis and Mann-Whitney U-test with * $p<0.05$.

sputtering, each dentine disc was analysed at the SEM (Figure 14). A control dentine disc without cultured cells can be found in the Annex (Figure 32).

Back-scattered electron images revealed a decrease in number and area of resorption pits on dentine discs cultured with $Y_1$R KO OC when compared to WT controls. In addition, this back-scattered electron image formation mode is based on the collection of back-scattered

electrons from the sample, which are released with discrete and defined energy depending on the atomic number of the atoms excited by the electron beam. Thus, as atoms with low atomic number require higher energy to release surface electrons, these electrons are released with lower energy and originate darker points in the image. Contrarily, surface electrons from high atomic number atoms are easily released (farther away from the atom's protons) and are collected with a higher energy, originating brighter points in the image [77]. Dentine discs are constituted by a mineralized collagen matrix, where collagen is covered by a hydroxyapatite layer. After resorption, the bright phosphate and calcium of the dentine's surface (higher atomic number) is replaced by darker regions of collagen (carbon, lower atomic number). An image of the collagen fibres exposed by the resorption can be found in the Annex. Carbon-rich cellular remains might be found in some areas, such as the ones signalled by white arrows (Figure 14B), and they seem to cover parts of the dentine surface, probably due to errors occurred in the critical-point drying of the samples.

The dentine disc surface can be analysed with an EDS spectra, where the discrete energy of the back-scattered electrons is used to obtain the surface atomic composition up to few nanometers deep. As expected, Phosphate and Calcium peaks are higher in dentine surfaces and the carbon peak is higher in the pit surface than in dentine surface due to the exposure of collagen fibres, mainly constituted by carbon.

Considering that darker regions correspond to exposed collagen, WT resorption pits seem to be deeper than $Y_1$R KO ones since the latter are relatively brighter. This is consistent with the EDS spectra of the resorption pits, where the difference between the oxygen, phosphate and calcium peaks in the surface of the dentine disc and in the pits derived from WT OCs is steeper than in those derived from $Y_1$R KO OCs (Figure 14C, D). This might suggest a higher exposure of collagen fibres and more successful demineralization in dentine discs derived from WT OCs when compared to those derived from $Y_1$R KO OCs.

In order to obtain more quantifiable results, OC-generated resorption pits were reconstructed from Confocal Microscopic images using an original Matlab program. The results are demonstrated in Figure 15.

The measurements of resorption pits revealed a marked difference between WT and $Y_1$R KO OC resorption pits, with a statistically significant decrease in either Volume, Top Section Area and Depth of $Y_1$R KO derived resorption pits when compared to WT ones. 3D reconstruction confirmed that WT resorption pits are deeper and wider than $Y_1$R KO resorption pits, and therefore a greater volume. $Y_1$R KO pits are shallower, which could indicate an impaired resorption capacity. These results are consistent with the previous SEM analysis.

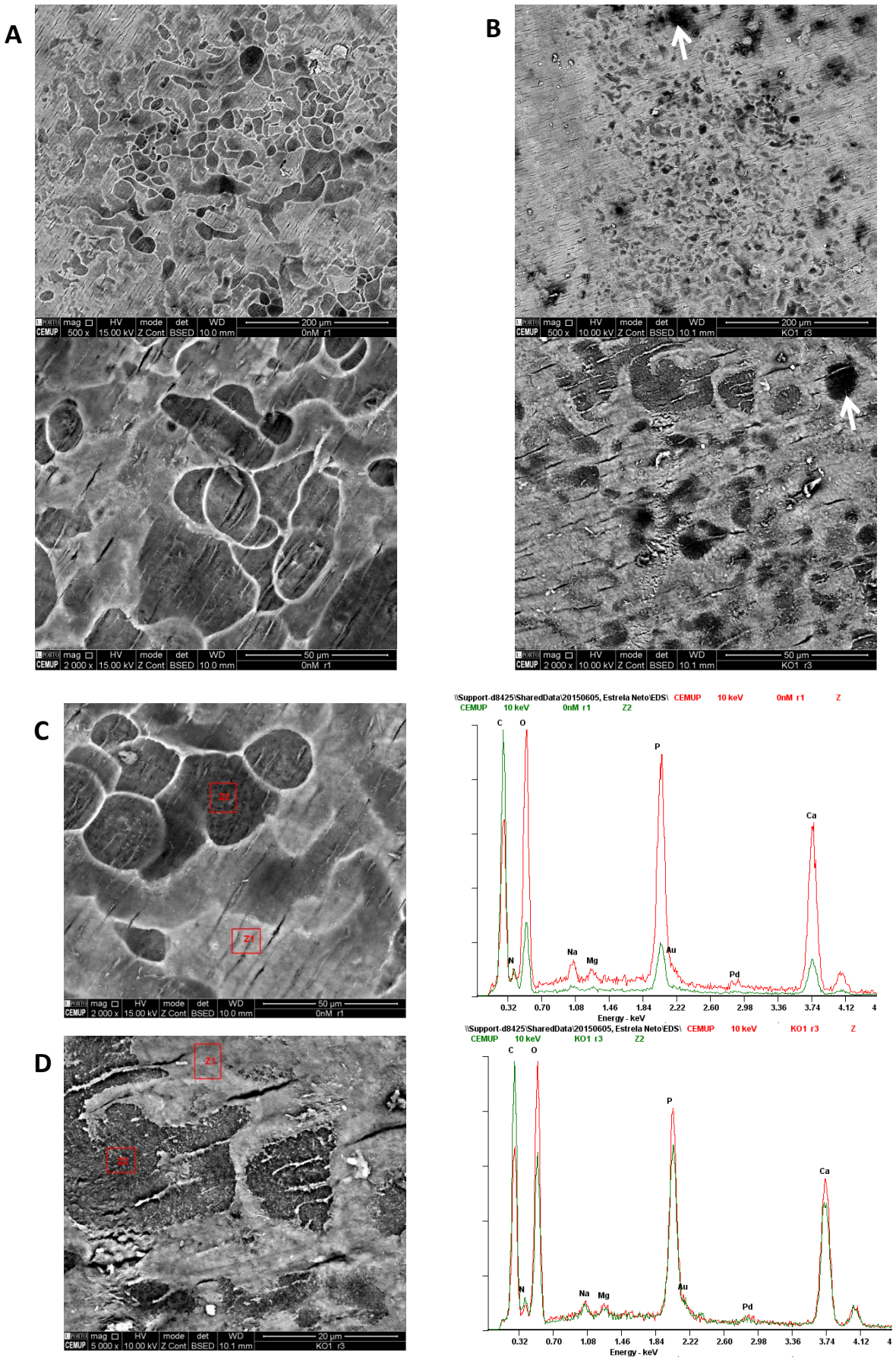


**Figure 14 – SEM analysis and EDS spectra of dentine discs after culture with WT and $Y_1$R KO OCs.** Bone marrow derived pre-OC were seeded directly on dentine discs and stimulated with M-CSF and RANKL for 21 days. Representative SEM images of (A) WT and (B) $Y_1$R KO OC cultured dentine discs were taken after 21 days of culture with 500x and 2000x magnification. There are some cellular remains visible on $Y_1$R KO OC cultured dentine discs (white arrows). Images were obtained through the collection of back-scattered electrons. (C) WT and (D) Y1R KO OC cultured dentine disc EDS spectra where dentine surface (Z1-red) and pit surface (Z2-green) are compared.

Interestingly, by plotting the Top Section Area vs Resorption Pit Depth it is clear that with increasing Depth the Top Section Area does not increase as much in $Y_1R$ KO pits, resulting on a graphic distribution shifted to the bottom (Figure 15F). In WT samples, measurements are more evenly distributed. This could mean that impairment in OC resorption capacity is more significant in lateral resorption than in vertical resorption, although both are affected. A similar distribution can be seen in a Depth vs Volume scatter, where the distribution of dots is shifted to an increasing Depth rather than homogenous distribution such as the one verified in WT OC

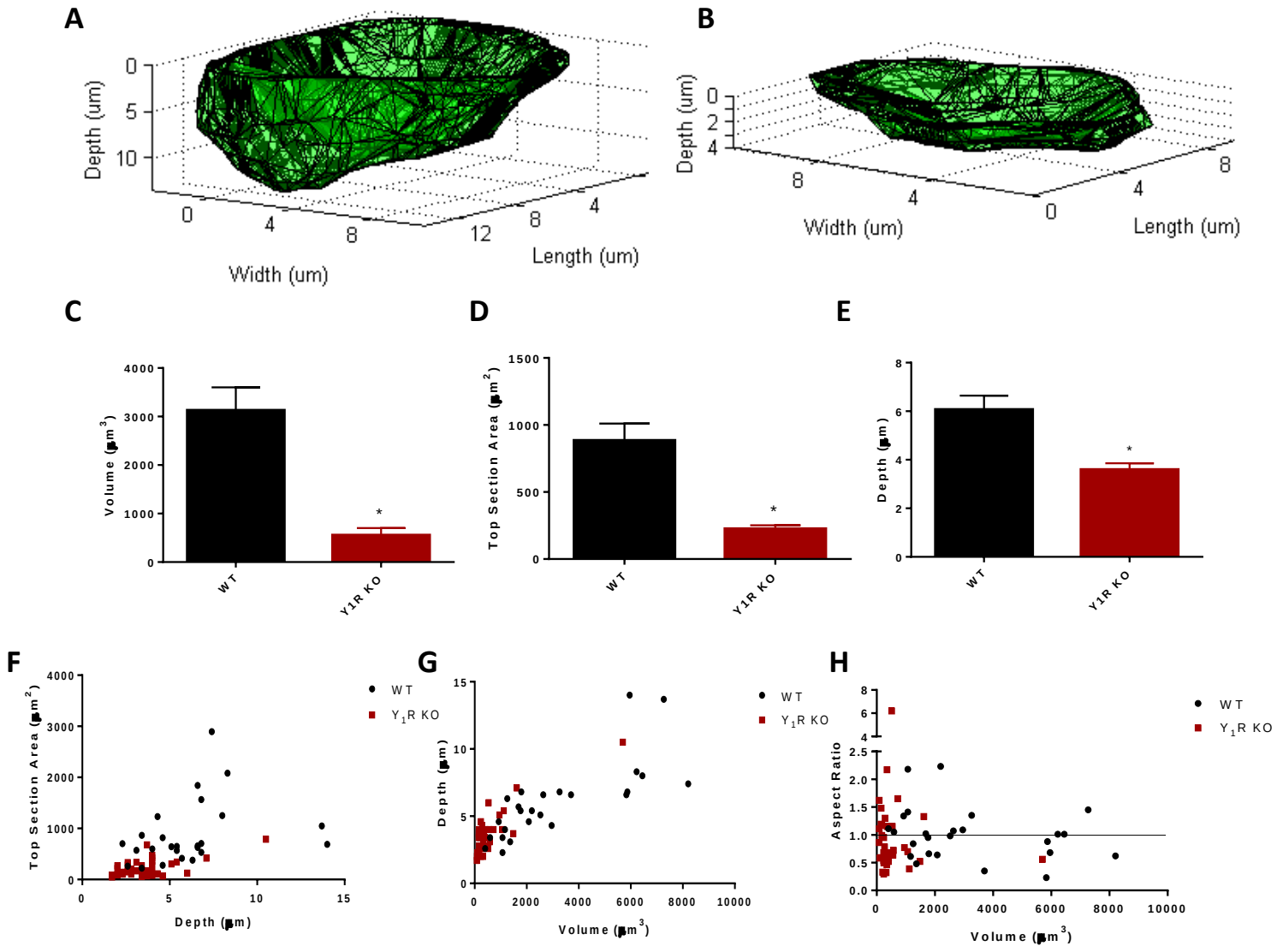


**Figure 15 – $Y_1R$ KO resorption pit 3D reconstruction.** Bone marrow derived pre-OC were seeded directly on dentine discs and stimulated with M-CSF and RANKL for 21 days. Dentine discs were stained with calcein and observed at the Confocal Microscope under 488nm radiation. Representative reconstruction of (A) WT and (B) $Y_1R$ KO resorption pits. 3D reconstruction was performed with Matlab software using the stacked images obtained at the microscope with a 40x objective. Images had a resolution of 1024x1024 pixels and a z-step of 0.2849 µm. (C) Resorption pit Volume, (D) Top section area and (E) Depth. Results are expressed as mean ± SEM from N (WT; $Y_1R$ KO) = 2; 3 independent experiments. n = 13 resorption pits were used from each mouse. Groups were compared through Kruskal-Wallis test and Mann-Whitney test with * $p<0.05$ (F) Scatter plot of resorption pit Top Section Area against Depth and (G) Depth and (H) Aspect Ratio against resorption pit Volume.

resorption pits.

Another interesting measure is the Aspect Ratio of the resorption pits. Aspect ratio is calculated by dividing the maximum Length of a resorption pit by the maximum perpendicular size and it can relate to the circularity of the resorption pit section area, where an Aspect Ratio of 1 corresponds to an approximately circular section area. As observed in Figure 15H, $Y_1$R KO resorption pits seem to be distributed far from the 1 value (black line), where WT pits are distributed around the 1 value, with some values farther from 1. This could point to a preferable direction of resorption by $Y_1$R KO OC leading to elliptical resorption pits rather than circular ones.

Dentine resorption could be influenced by either intrinsic factors such as genomic expression or by extrinsic factors such as the composition and topography of the material to be resorbed. Goldberg and her team studied the influence of the Rho GTPases Rac1 and Rac2 on the resorption behaviour of mice OC[78]. Rac1 and Rac2 regulate motility and cytoskeleton rearrangement and a decrease in resorption pit volume was reported in Rac1 and Rac2 KO mice. Interestingly, Rac1 KO mice demonstrated reduced pit depth and surface area while Rac2 KO mice only demonstrated reduced pit depth, suggesting different roles of these proteins on the process of bone resorption. Goldberg also reported a WT mean resorption pit volume of approximately 11000 $\mu m^3$, which is far greater than the one obtained in this project. This was probably due to the use of dentine discs from different origins.

On the other hand, resorption can be influenced by the resorption substrate[79] and Rumpler and co-workers demonstrated that dentine substrates suffer higher resorption than bone substrates[80]. This difference seems to be due to increased osteoclastogenesis in dentine surfaces and not due to increased resorption, since resorption pit size is similar in both substrates[80]. In this work, material composition cannot be the influencing factor since the resorbed material was the same in each condition. Rumpler also proposed a resorption trail formation model, which leads to the formation of trails with a preferential direction and constant depth. In addition, Rumpler observed that actin ring organization was different in resorption pit and trail formation, leading to different resorption orientation[80]. Therefore, a different actin rearrangement could be responsible for the observed differences in resorption pit shape.

### 1.4 $Y_1R$ KO OC Gene Expression

In order to have a better understanding on changes observed in previous morphology and resorption analysis, the expression of several key markers for OC differentiation, fusion and bone resorption were studied. Primary bone marrow flushed cells were seeded on 24-well plates under M-CSF and RANKL stimulation for 14 days. mRNA was extracted at day 7 and day 14 time points, following cDNA synthesis and amplification.

**Differentiation Markers**

The analysis of specific OC differentiation markers in $Y_1R$ KO cells has revealed an apparent decrease in their expression when compared to their WT counterparts (Figure 16). TRAP expression exhibited a slight decrease in expression in the first 7 days of culture in $Y_1R$ KO OCs. At day 14, however, the decrease in TRAP expression in $Y_1R$ KO OCs is more pronounced, with a decreasing trend when compared to WT OCs. Although non-significant, this result is consistent with the previous resorption assays, where $Y_1R$ KO OCs demonstrated

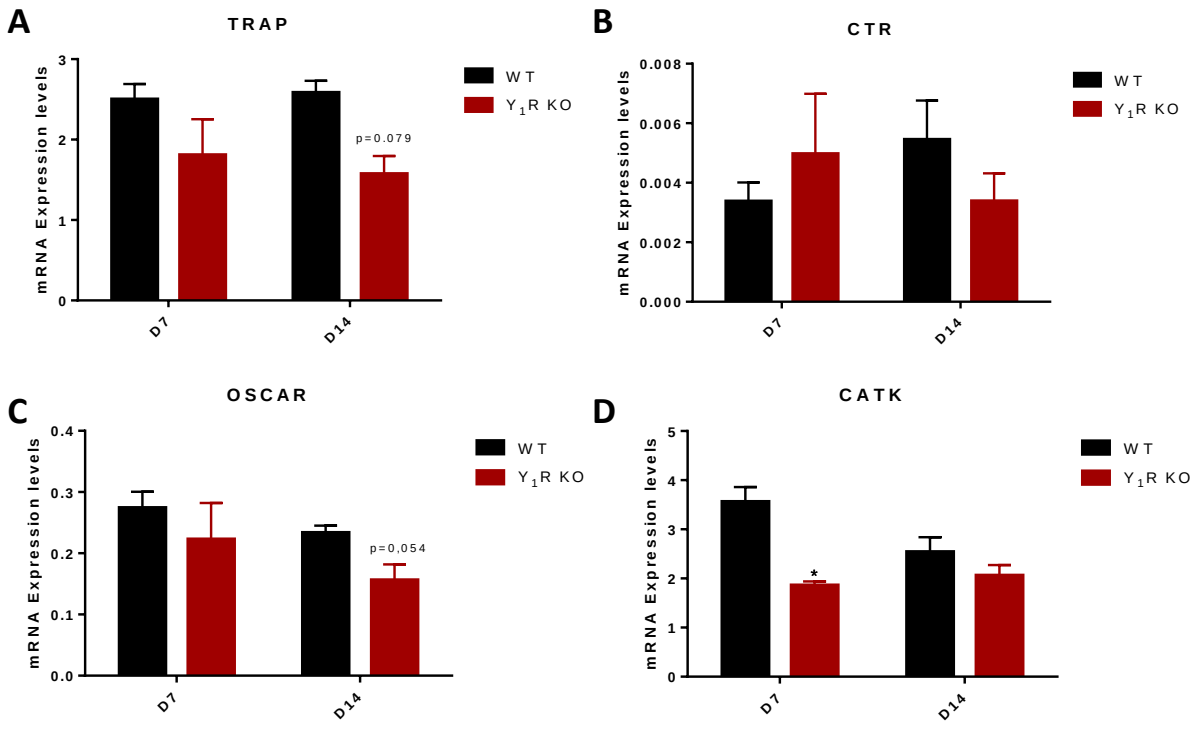


**Figure 16 – Expression of OC differentiation markers in $Y_1R$ KO OC.** Maturation of bone marrow derived pre-OC was induced with M-CSF and RANKL for 14 days in 24-well culture plates. mRNA was collected at the given time points from 3 replicates. (A) TRAP, (B) CTR, (C) OSCAR and (D) CATK gene expression quantification relative to GADPH constitutive expression. Results are expressed as mean ± SEM from 3 independent experiments. Groups were compared through ANOVA and independent-samples t-test, except CTR expression that was compared through Kruskal-Wallis and Mann-Whitney U-test, with * $p<0.05$.

an inferior resorption capacity. TRAP is an acidic phosphatase released into the resorption sealing zone and is partially responsible for the bone demineralization process, thus its downregulation could explain the observed reduced bone resorption. Other studies also reported a deficient OC resorption activity due to TRAP inhibition [81] and a correlation between cell size and TRAP activity, where larger osteoclastic giant cells had a decreased TRAP activity[82], which is consistent with the increased OC area and decreased TRAP expression observed.

CTR is another typical OC marker, and its expression did not significantly change during 14 days of culture and OC differentiation. CTR exerts an inhibitory action upon activation and its expression is very low in comparison to the housekeeping gene. CTR expression in $Y_1R$ KO cells did not show statistically significant differences during OC differentiation, with a high associated error between experiments. Thus, CTR expression does not seem to be influenced by the absence of $Y_1R$.

OSCAR is a transmembrane receptor specific for OC that is expressed during early stages of OC differentiation and it is required for osteoclastogenesis together with M-CSF and RANKL stimulation[83]. OSCAR expression displayed a decreasing trend in Day 14 time point, although it was not statistically significant. Since OSCAR expression is induced by NFATc1[84], a transcription factor that is in turn involved in the RANK signalling cascade [85], changes in the RANK/RANKL signalling pathway could be responsible for the slight decreasing trend observed in OSCAR expression.

Finally, CATK is expressed in a RANKL dependent manner during OC differentiation and it is a fundamental enzyme in the resorption process, being responsible for bone matrix collagen degradation. $Y_1R$ KO OCs show a significant downregulation of CATK expression at day 7 time point, where the production of CATK mRNA is nearly halved when compared to the expression in WT controls. However, no statistical differences were found at day 14 time point, which point to a slight recovery in CATK levels. CATK levels in $Y_1R$ KO cells remained constant throughout the experiment, while WT levels decreased with time. This could result from a time-dependent decrease in resorption capacity of WT cells, however no evidence of such decrease is apparent in the resorption assays performed previously. Similarly to TRAP expression, these results are consistent with those obtained in the dentine resorption assays, which might be explained by CATK downregulation and subsequent collagen degradation impairment. Interestingly, J.H. Kang and co-workers reported an increase in OC area and a decrease in resorption capacity after OC produced OPG silencing[74]. These authors have shown that OC can produce OPG to intrinsically limit osteoclastogenesis, and that the OPG silencing

resulted in a downregulation of TRAP and CATK even though there was an increase in OC area, similar results to those shown in this project. Thus, the absence of $Y_1R$ signalling might interfere with the RANK/RANKL axis with similar end results as OPG signalling, although other signalling pathways must be explored. For instance, calcitonin was shown to downregulate OC resorption through Protein Kinase A(PKA) and PKC activation in mice[86]. The latter results are consistent with the absence of $Y_1R$ signalling since $Y_1R$ activation leads to adenyl cyclase and $Ca^{2+}$ channel inhibition, which then decreases PKA and PKC activity and therefore an increased resorption compared to $Y_1R$ KO mice.

**Fusion Proteins**

To complement the TRAP staining and morphological analysis, the expression of several genes responsible for pre-OC fusion was explored (Figure 17). Of the genes analysed, only MCP1 has been significantly upregulated in $Y_1R$ KO cells. DC-STAMP expression has shown a

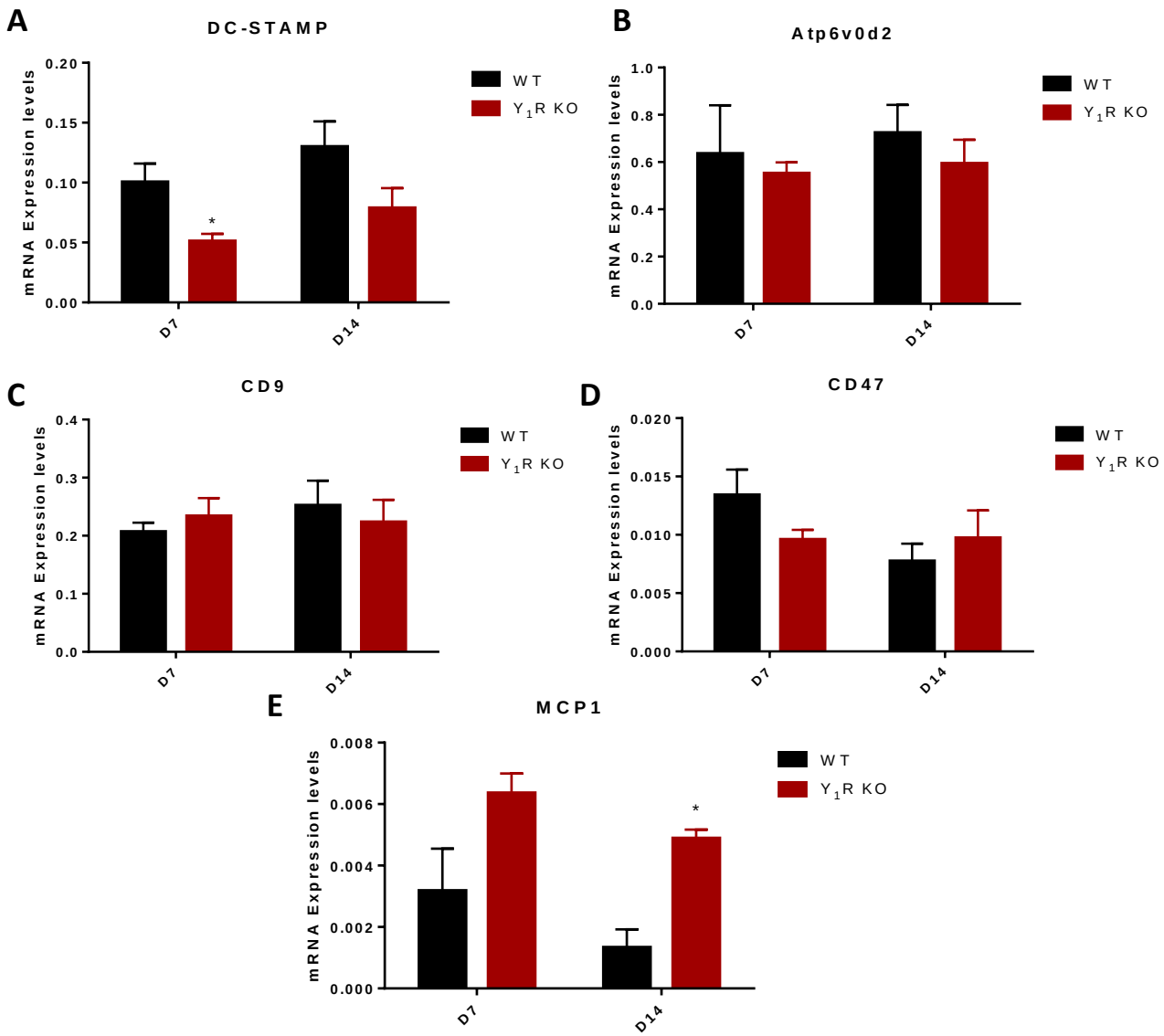


**Figure 17 – Expression of pre-OC fusion genes in $Y_1R$ KO cells.** Maturation of bone marrow derived pre-OC was induced with M-CSF and RANKL for 14 days in 24-well culture plates. mRNA was collected at the given time points from 3 replicates. (A) DC-STAMP, (B) Atp6v0d2, (C) CD9, (D) CD47 and (E) MCP1 gene expression quantification relative to GADPH constitutive expression. Results are expressed as mean ± SEM from 3 independent experiments. Groups were compared through ANOVA and independent-samples t-test with * $p<0.05$.

statistically significant downregulation in $Y_1$R KO cells, which is unexpected taking in to account the increased OC area and $TRAP^+$ MNCs observed in previous results.

DC-STAMP is a RANKL-dependent transmembrane protein which is fundamental in pre-OC fusion but it is not directly involved in OC differentiation [25, 87]. Its expression is regulated primarily by the RANKL-induced transcription factors NFATc1 and c-Fos and they promote cell-to-cell fusion by binding to a yet unknown ligand[88]. Since $Y_1$R signalling might interfere with RANKL pathway, this decrease in expression could be explained by the DC-STAMP dependence of RANKL signalling, but the decrease in expression was not verified for CD9 and Atp6v0d2 which are also RANKL-dependent[23]. Furthermore, a decrease in resorption pit formation was reported in an OC-like RAW-D cell line after the addition of an anti-DC-STAMP antibody[89], suggesting a role of DC-STAMP in the resorption activity which could explain the decreased resorption observed previously in this work. However, $TRAP^+$ MNC number was also decreased with the addition of the same antibody, which is disagreeing with the increase in $TRAP^+$ MNCs verified in $Y_1$R KO OCs.

Atp6v0d2, CD9 and CD47 gene expression by Y1R KO cells was similar to control levels in all time points, with the exception of a slight decreasing trend of the expression of CD47 at day 7.

Atp6v0d2 is a component of the v-ATPase involved in pre-OC fusion that exerts its function through direct cell-to-cell contact but not directly involved in the proton pump activity[26]. Nonetheless, the similar Atp6v0d2 levels between $Y_1$R OCs and WT OCs might also point to similar levels of v-ATPase, which could mean that a deficient acidification of the sealing zone is not the factor responsible for the impaired resorption activity observed in $Y_1$R OCs. Confirmation is required in future studies, though. Likewise, the increase in OC area and fusion in $Y_1$R KO cells is not accountable to an increase in Atp6v0d2 expression levels.

CD9 and CD47 are membrane proteins involved in cell fusion and cell recognition, respectively. CD9 expression is enhanced by RANKL signalling and it is located at lipid rafts in the cellular membrane, being involved in cell fusion[23]. CD9 mRNA expression in $Y_1$R KO OCs was similar to control levels, thus it does not seem to be responsible for the increased fusion observed in those cells. CD47 is an integrin-associated protein that binds to another receptor involved in cell fusion, the Macrophage Fusion Receptor (MFR), and it mediates cell-cell recognition instead of cell-cell fusion[23]. Similarly to CD9 and despite the slight decreasing trend in CD47 expression in $Y_1$R KO cells at day 7, CD47 does not seem to be responsible for the increased fusion in $Y_1$R OC cells.

Lastly, at day 7 there is a non-significant, slight increase in the expression of MCP1 in $Y_1R$ KO cells. Moreover, MCP1 expression was significantly increased in $Y_1R$ KO OC at the day 14 time point. MCP1 is a chemokine that binds C-C Receptor 2 and is involved in the recruitment of leukocytes during acute inflammation but it has also been reported to be involved in OC differentiation in a RANKL dependent manner[90]. Several studies with MCP1 KO mice have shown that MCP1 facilitates OC fusion and maturation, since the absence of MCP1 signalling led to decreased TRAP+ MNC counts *in vitro* and decreased bone resorption *in vivo*[91-93]. In addition, MCP1 together with M-CSF is able to induce the formation of $CTR^+$ $TRAP^+$ MNCs without RANKL stimulation, although the obtained OCs are not able to resorb bone[94]. Furthermore, OC express MCP1 and it regulates OC fusion and differentiation in an autocrine/paracrine way, although its action is not independent from other factors such as DC-STAMP[95]. Hence, MCP1 upregulation in $Y_1R$ KO cells might be responsible for an increased motility and cell fusion, leading to increased OC area and $TRAP^+$ MNC numbers in these cells.

A study using monocytes where MCP1 was downregulated after Janus kinase (JAK)/signal transducer and activator of transcription (STAT) and p38 MAPK inhibition could enlighten the mechanism underlying RANKL-dependent upregulation of MCP1[96]. Considering that DC-STAMP and MCP1 are regulated by different transcription factors, although both being RANKL dependent, and that MCP1 is a soluble chemokine which acts independently of cell-cell contact, the decrease in DC-STAMP mRNA levels and increase in MCP1 mRNA observed in $Y_1R$ KO OCs is not contradictory and could explain the increase in OC section area. However, other factors involved in OC fusion such as a disintegrin and metalloprotease (ADAM) 8 and 12, MFR and triggering receptor expressed on myeloid cells 2 (TREM2) should not be excluded and should be analysed in future studies.

## 2 - $Y_1R$ antagonism in Osteoclastogenesis and OC resorption capacity

To verify if the $Y_1R$ pathway is responsible for the observed results in $Y_1R$ KO OCs, OC behaviour was analysed after $Y_1R$ blockage. Non-peptidic $Y_1R$ antagonists have shown promising results in *in vivo* experiments regarding an increase in bone formation, similarly to a $Y_1R$ KO phenotype[69]. To achieve this specific aim, the $Y_1R$ antagonist BIBP3226 was chosen due to its high specificity.

### 2.1 The effect of $Y_1R$ antagonist stimulation in Osteoclastogenesis

To assess the effect of $Y_1R$ antagonism on Osteoclastogenesis, primary bone marrow flushed cells from WT mice were cultured for 14 days in the presence of M-CSF and RANKL to promote OC maturation. Soluble $Y_1R$ antagonist BIBP3226 was added to cultures at increasing concentrations of 0, 60 and 1000nM. Untreated cells were used as control. TRAP staining and morphological analysis was performed at day 7 and day 14 time points, where cells with more

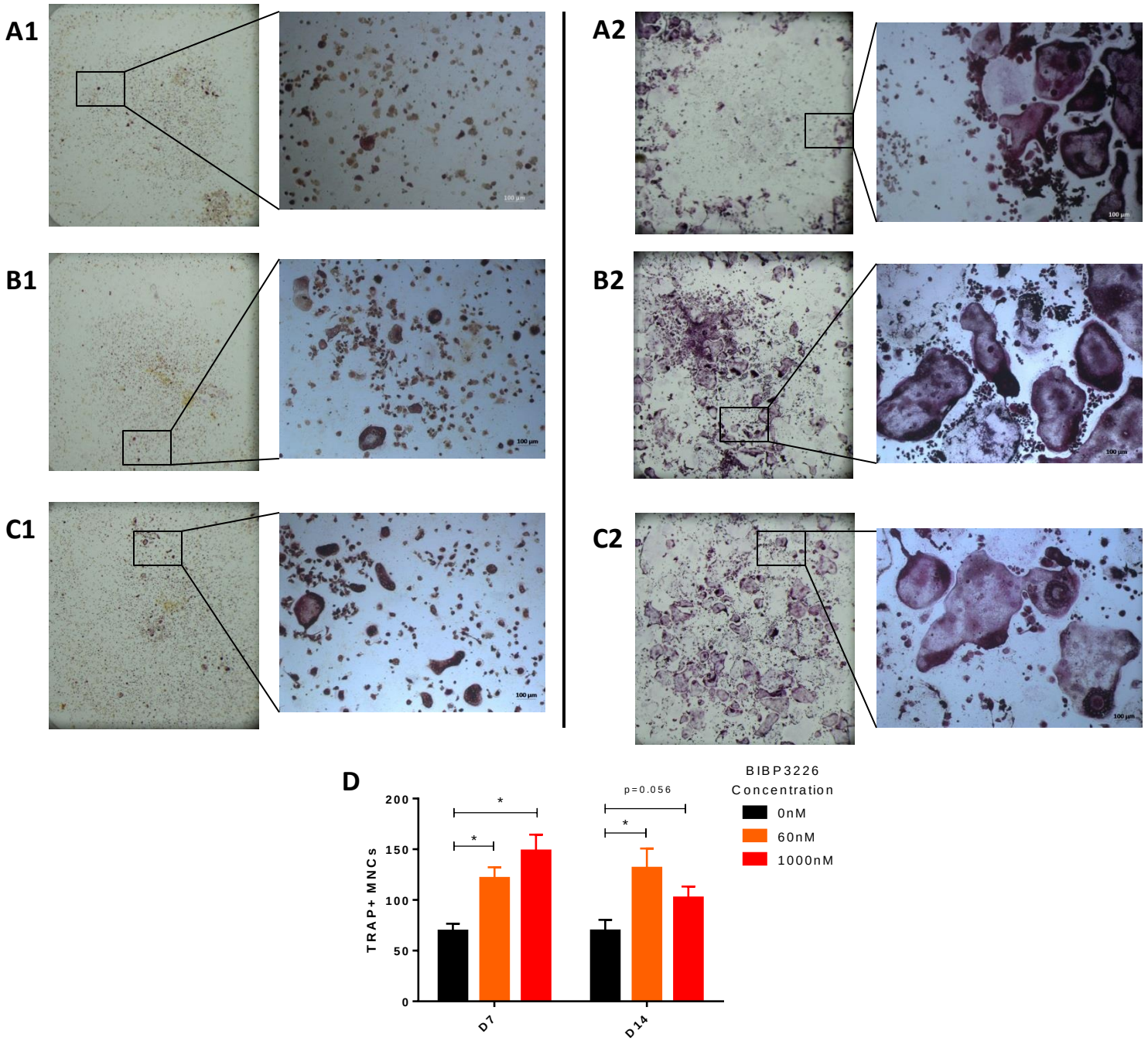


**Figure 18 - TRAP Staining of BIBP3226 treated cells.** Maturation of bone marrow derived pre-OC was induced with M-CSF and RANKL for 14 days in the presence of 60nM and 1000nM BIBP3226. Untreated cells were used as control. Representative images of (A) 0nM, (B) 60nM and (C) 1000nM BIBP3226 treated cells at (1) day 7 and (2) day 14 time points are presented. Whole well images are shown on the left and images taken with the microscope with a 10x objective are shown on the right. Scale bar, 100µm. (D) Number of $TRAP^+$ MNCs. $TRAP^+$ OC with more than 3 nuclei were counted. Results are expressed as mean ± SEM from 3 independent experiments. Groups were compared through paired t-test with * $p<0.05$.

than 3 nuclei were considered mature OC.

BIBP3226 treatment led to a statistically significant increase in $TRAP^+$ MNC numbers in day 7 time point, independently of the tested concentration (Figure 18). However, at day 14 cells treated with 1000nM BIBP3226 only revealed a non-significant increasing trend when compared to control levels, while treatment with 60nM BIBP3226 maintained a significant increase in $TRAP^+$ MNCs. Microscopic images revealed an increase in size and number of differentiated OC after BIBP3226 treatment when compared to control conditions (Figure 18B-C). These results suggest that $Y_1R$ specific antagonism lead to an upregulation of OC differentiation and fusion, similarly to the increased fusion observed in $Y_1R$ KO OCs. However, this increase in $TRAP^+$ MNCs seems to develop at an earlier stage than in $Y_1R$ KO OCs, since at day 7 there is already an increase in $TRAP^+$ MNCs. Furthermore, at day 14 there seems to be a decrease in $TRAP^+$ MNCs in wells treated with 1000nM BIBP3226, which might point to a inhibitory mechanism of BIBP3226 in high doses at later stages of differentiation or a recovery towards control levels. Toxicity of 1µM BIBP3226 in a kidney cell line has been reported previously[97]. Nevertheless, since the affinity of BIBP3226 to $Y_1R$ is extremely high with a Ki of less than 8nM (which means that a concentration of 8nM would bind to 50% of the available $Y_1R$, displacing the natural agonists)[98], total antagonism can be achieved with low BIBP concentrations and thus decrease BIBP3226 toxic effects, if existent. However, a cytotoxicity evaluation using rezazurin assay was performed previously and did not show any significant differences between BIBP3226 treated cells and controls (Data not shown).

As performed with $Y_1R$ KO cells, immunostaining of cytoskeletal F-actin was used to analyse the effect of BIBP3226 in cell morphology (Figure 19). At day 7, there are no striking differences between BIBP3226 treated cells and control ones, with many undifferentiated pre-OC and few OCs visible (white arrows). Day 14 time point images show large differentiated OC in both 60nM and 1000nM BIBP3226 treated cells, where60nM BIBP3226 treated OCs seem to be larger. Morphological traits do not seem to be different between OC subjected to different treatments.

OC section area analysis has shown no differences at both the analysed time points between treatments but there is a slight increase in 60nM BIBP3226 treated OCs in comparison with controls at day 14 (Figure 19C), although in a much lesser extent than what was verified in $Y_1R$ KO OCs. Interestingly, antagonist overstimulation of $Y_1R$ with1000nM BIBP3226 led to a decrease in OC area compared to 60nM BIBP3226 treatment at day 14. These results are consistent with the TRAP staining performed previously, where the same pattern of OC differentiation after BIBP3226 treatment is observed at day 14.

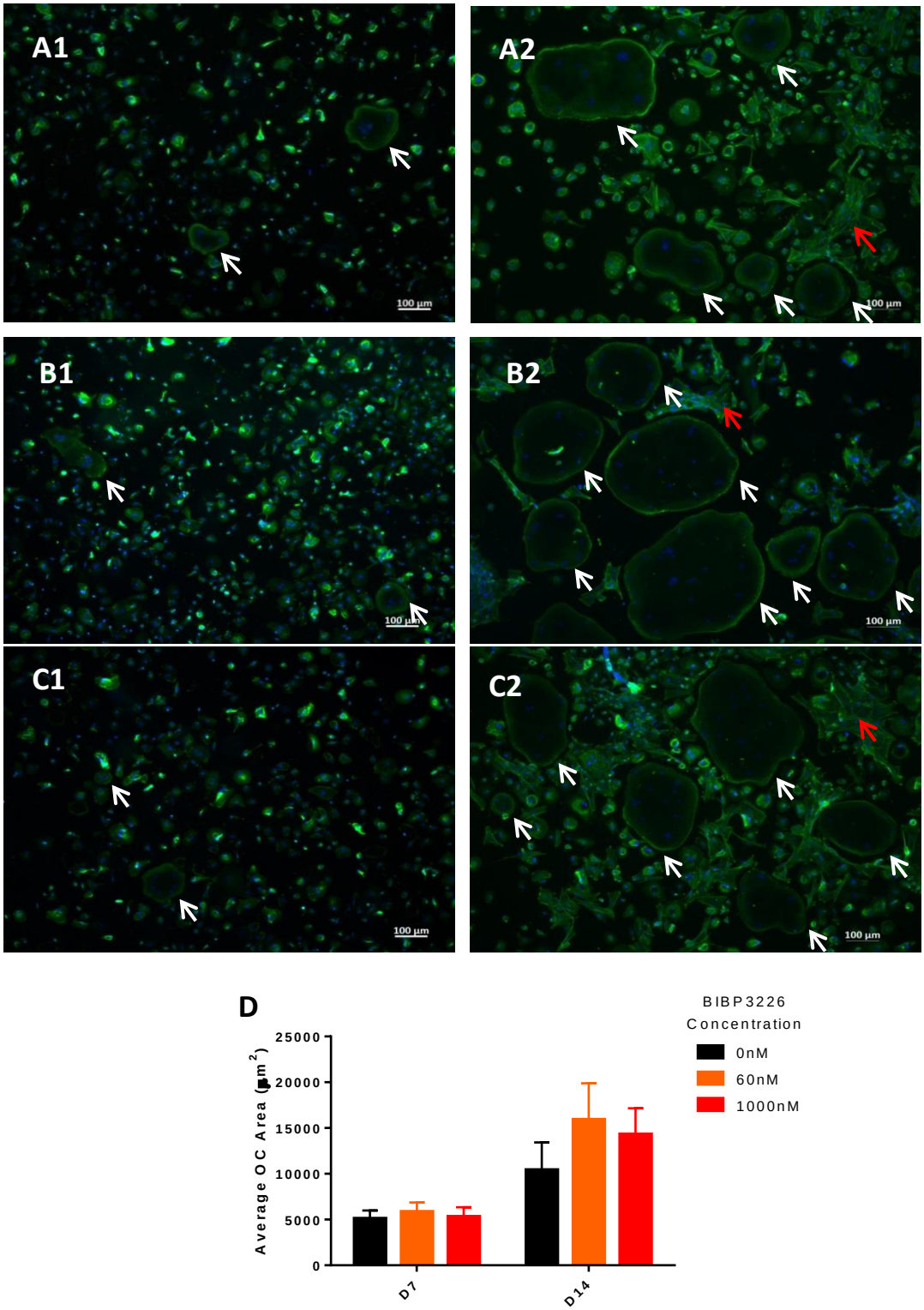


**Figure 19 – Morphological analysis and section area quantification of BIBP3226 treated cells.** Maturation of bone marrow derived pre-OC was induced with M-CSF and RANKL for 14 days in the presence of BIBP3226. Untreated cells were used as control. Representative images of (A) 0nM, (B) 60nM and (C) 1000nM BIBP3226 treated cells at (1) day 7 and (2) day 14 time points are presented, taken with a 10x objective. F-actin and nuclei were labelled with green and blue, respectively. Large, multinucleated cells were considered mature OC (white arrows). Other cell types were also present in culture (red arrows). Scale bar, 100µm. (C) Quantification of the mature OC section area by treatment. Results are expressed as mean ± SEM from 3 independent experiments with a total day 7 n (0nM; 60nM; 1000nM) = 179, 62, 109 ; 224, 108, 110; 239, 164, 113 and day 14 n (0nM; 60nM; 1000nM) = 170, 39, 145; 148, 41, 125; 181, 62, 115 cells measured. Groups were compared through Wilcoxon signed-ranked test with * $p<0.05$.

NPY binds to $Y_1R$ leading to adenyl cyclase inhibition, among other effects. BIBP3226 treatment was shown in previous studies to counteract NPY driven cAMP inhibition, consistent

with $Y_1R$ antagonism[99]. Therefore, an abrogation of the inhibitory signalling of $Y_1R$ by BIBP3226 antagonism might be responsible for the observed TRAP staining and morphological analysis results.

### 2.2 The effect of Y1R antagonist stimulation in OC resorption activity

To assess if an $Y_1R$ antagonist treatment of WT OCs would yield similar results to those verified in $Y_1R$ KO cells, primary bone marrow flushed cells from WT mice were seeded directly on top of dentine substrates on 96-well plates and were cultured for 21 days under M-CSF and RANKL stimulation. Moreover, soluble BIBP3226 was added to culture at a final concentration of 60nM and 1000nM. Untreated cells were used as control. Back-scattered electron SEM images revealed resorption at a lesser extent than the control dentine discs in both conditions, although the 1000nM BIBP3226 treated resorption pits seem to be deeper than those of 60nM BIBP3226 treatment (Figure 20). Resorption in 60nM BIBP3226 treated dentine discs is apparently more distributed throughout the dentine surface but at a shallow depth, while 1000nM BIBP3226 treated dentine discs suffered resorption within a smaller area, as can be seen in Figure 20B.

EDS spectra analysis revealed identical Oxygen, Phosphate and Calcium peaks observed at the dentine surface and shift to a high Carbon peak at the resorption pit as in control samples. The difference between phosphate and calcium peaks at the surface and in the resorption pit seem to be steeper in 1000nM BIBP3226 treated samples than in 60nM BIBP3226 treated samples, suggesting that the latter resorption pits are shallow, resembling $Y_1R$ KO OC derived resorption pits. However, both BIBP3226 concentrations seem to diminish the resorption capabilities of OC when compared to untreated controls.

Resorption pits derived from BIBP3226 treated cells were also reconstructed using Matlab software, to quantify and compare the resorption pit formation behaviour of these cells. Measurement and 3D reconstruction of resorption pits is demonstrated in Figure 21. Pit reconstruction revealed a statistically significant volume decrease in either 60nM or 1000nM BIBP3226 resorption pits. Interestingly, there is an increasing trend in the volume of 1000nM BIBP3226 treated pits compared to 60nM BIBP3226 treated ones, suggesting a non-significant small recovery towards control levels.

There is a statistically significant decrease in Top Section Area in both 60nM and 1000nM BIBP3226 treatments when compared to control resorption pits, while no significant

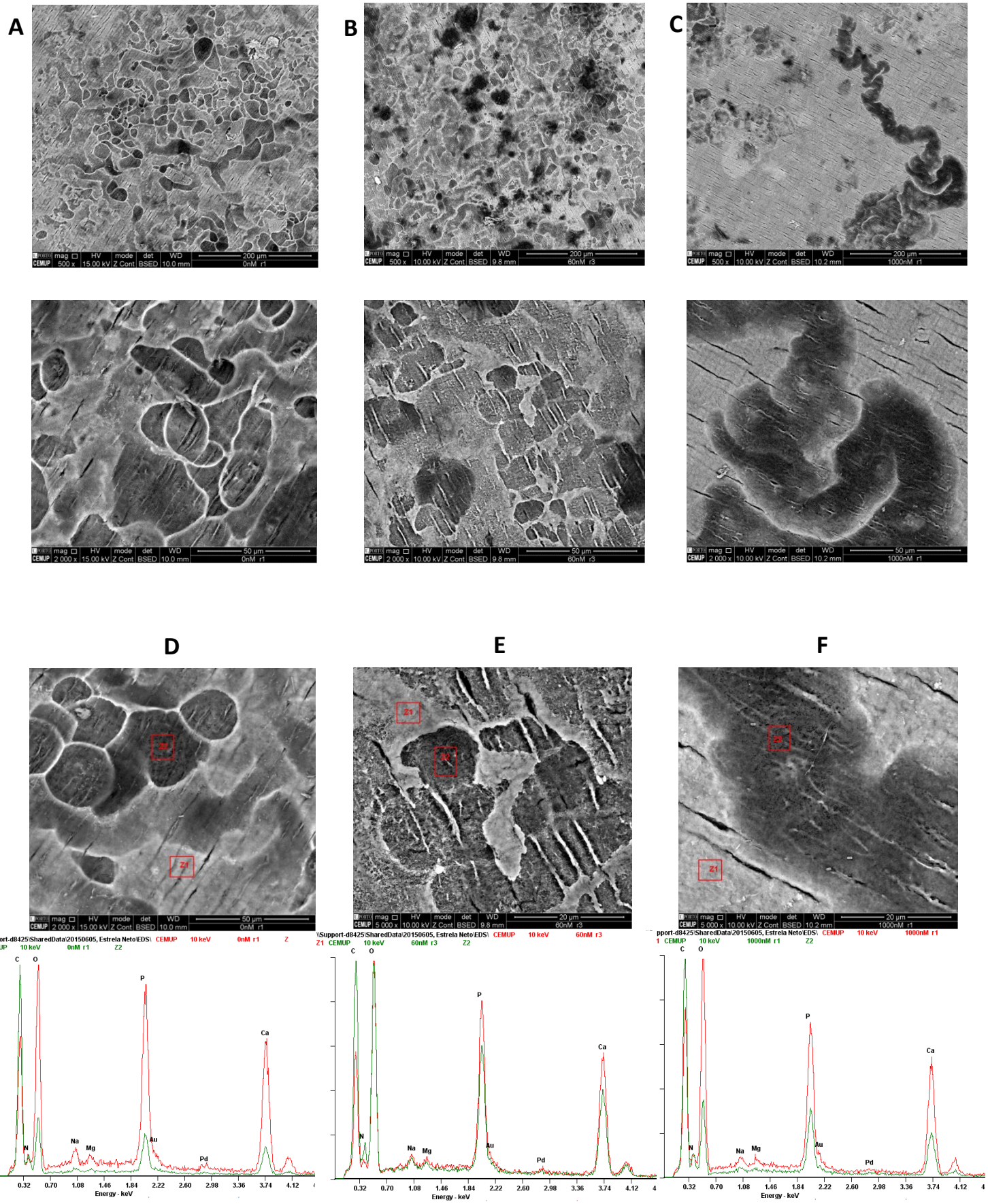


**Figure 20 - SEM analysis and EDS spectra of dentine discs after culture with BIBP3226 treated OC.** Bone marrow derived pre-OC were seeded directly on dentine discs and stimulated with M-CSF and RANKL for 21 days in the presence of 60nM and 1000nM BIBP3226. Representative SEM images of (A) 0nM, (B) 60nM and (C) 1000nM BIBP3226 treated dentine discs were taken after 21 days of culture with 500x and 2000x magnification. Images were obtained through the collection of back-scattered electrons. (D) 0nM, (E) 60nM and (F) 1000nM BIBP3226 treated dentine disc EDS spectra where dentine surface (Z1-red) and pit surface (Z2-green) are compared.

differences were observed between both treatments. Regarding Depth, however, there is only a statistically significant decrease in depth on 60nM BIBP3226 treated wells compared to control pits. Surprisingly, no significant differences were observed between 1000nM BIBP3226 and control resorption pits, with only a decreasing trend in 1000nM BIBP3226 treated pits. There is a significant recovery towards control values in 1000nM BIBP3226 compared to 60nM BIBP3226, suggesting that the vertical resorption capacity of 1000nM BIBP3226 treated OCs is slightly improved. Thus, an increase in collagen degradation is possibly the mechanism of vertical resorption recovery.

Similarly to $Y_1R$ KO resorption pits, the plot of Top Section Area vs Depth revealed a shift

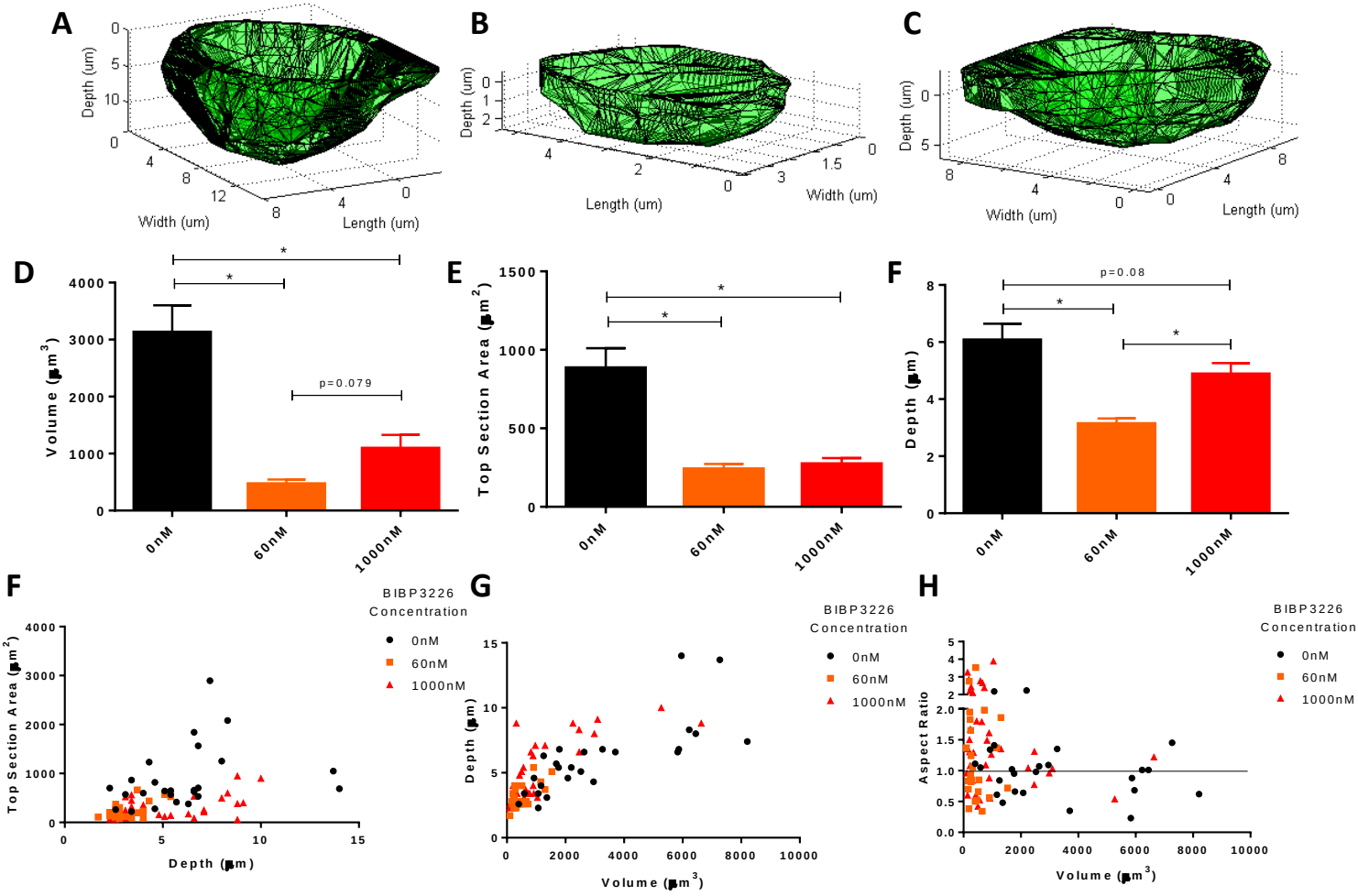


**Figure 21 - $Y_1R$ KO resorption pit 3D reconstruction.** Bone marrow derived pre-OC were seeded directly on dentine discs and stimulated with M-CSF and RANKL for 21 days in the presence of 60nM and 1000nM BIBP3226. Dentine discs were stained with calcein and observed at the Confocal Microscope under 488nm radiation. Representative reconstruction of (A) 0nM, (B) 60nM and (C) 100 0nM BIBP3226 treated resorption pits. 3D reconstruction was performed with Matlab software using the stacked images obtained at the microscope with a 40x objective. Images had a resolution of 1024x1024 pixels and a z-step of 0,2849 µm. (D) Resorption pit Volume, (E) Top section area and (F) Depth. Results are expressed as mean ± SEM from N (0nM; 60nM; 1000nM) = 2; 2; 3 independent experimen ts. n = 13 resorption pits were used from each mouse. Groups were compared through Kruskal-Wallis test and Mann-Whitney test with * p<0.05 (F) Scatter plot of resorption pit Top Section Area against Depth and (G) Depth and (H) Aspect Ratio against resorption pit Volume.

to the bottom of the graph and therefore there seems to be a more substantial impairment in lateral resorption than vertical resorption. A similar distribution can be observed in a Depth vs Volume plot, where an increase in depth does not lead to a proportional increase in volume in 60nM BIBP3226 samples. However, 1000nM BIBP3226 values are more evenly distributed and in an approximate manner to the control samples, consistent with the Depth quantification in Figure 21F.

Aspect Ratio analysis revealed that 60nM and 1000nM BIBP3226 treated pits might be formed in a preferential direction. These pits have an Aspect Ratio somewhat different from the value 1, as can be seen by analysing the distance between each dot and the black line. This suggests an elliptical configuration of the 60nM and 1000nM BIBP3226 treated resorption pits, slightly different from control resorption pits. Similarly to Y1R KO resorption pits, BIBP3226 treated OC might have a different actin ring organization which could lead to different resorption pit appearance.

An increase in Osteoclastogenesis followed by a decrease in the volume and depth of resorption pits after incubation with 25-dihydroxyvitamin-D3 was previously reported in tumour OC-like cells[100]. These results are similar to those observed after BIBP3226 incubation, although the extent of resorption impairment is much higher in BIBP3226 treatment.

In conclusion, $Y_1$R antagonism leads to impaired resorption, which is more apparent in 60nM BIBP3226 treated OC than in 1000nM BIBP3226 treated OC.

### 2.3 The effect of $Y_1$R antagonist treatment on OC Gene Expression

$Y_1$R antagonism during Osteoclastogenesis and bone resorption yielded similar results to those obtained in $Y_1$R KO experiments, yet the genetic background and cell signalling pathways behind them could be distinct. To assess the effect of $Y_1$R antagonism on gene expression, the expression of the OC specific genes and fusion involved genes was studied. Primary bone marrow flushed cells were seeded on 24-well plates under M-CSF and RANKL stimulation for 14 days, in the presence of 60nM and 1000nM BIBP3226. mRNA was extracted at day 7 and day 14 time points, following cDNA synthesis and amplification.

**Differentiation Markers**

The analysis of OC specific markers of differentiation in BIBP3226 treated cultures revealed an increasing trend in the TRAP expression in 60nM BIBP3226 treated cells and a statistically significant increase in early stages of differentiation of 1000nM BIBP3226 treated cells (Figure 22). Interestingly, TRAP expression followed an increasing trend from 60nM to 1000nM BIBP3226 treatment, suggesting that OC behave differently with different

concentrations of $Y_1R$ antagonists. However, at day 14 of differentiation, TRAP levels were similar in the different conditions. These results seem contradictory with the previous resorption assays, since an increase in TRAP expression could lead to augmented resorption capacity. Nevertheless, it could explain the slight recovery in vertical resorption observed in 1000nM BIBP3226 treated resorption pits, where the resorption impairment verified in these

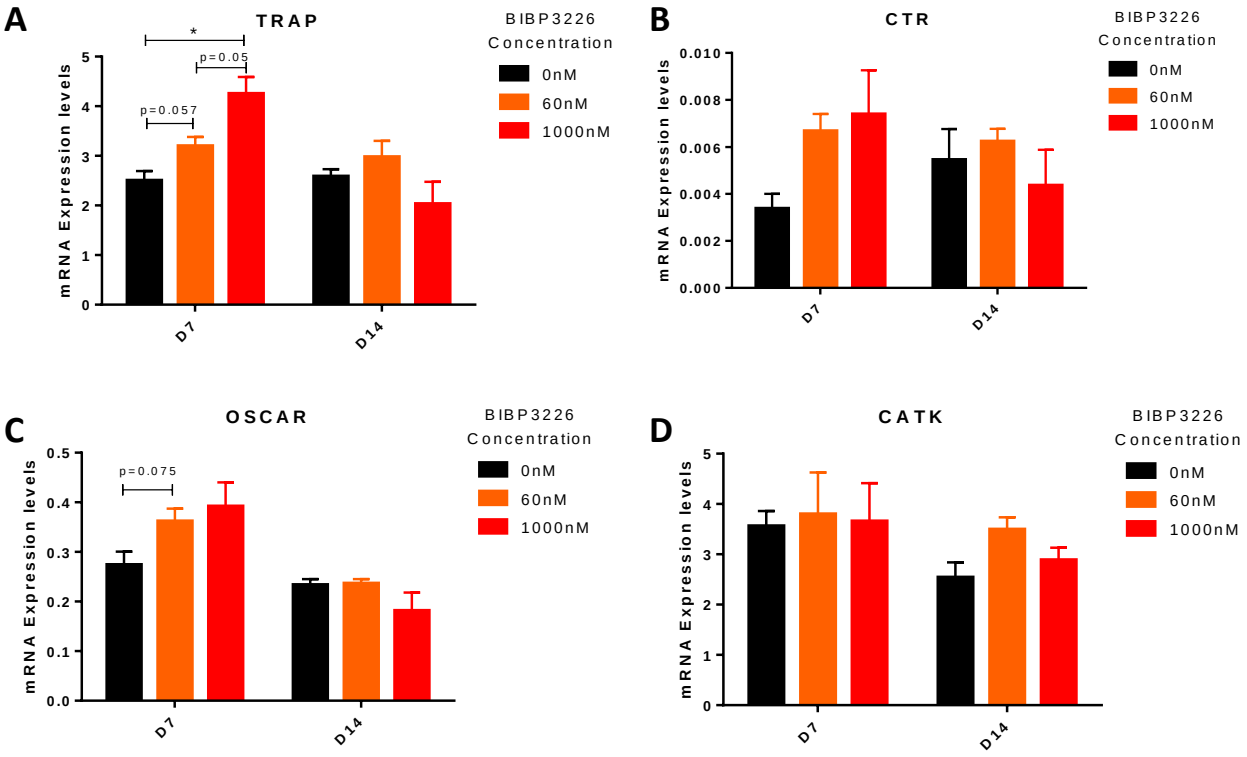


**Figure 22 - Expression of OC differentiation markers in BIBP3226 treated OC.** Maturation of bone marrow derived pre-OC was induced with M-CSF and RANKL for 14 days in 24-well culture plates in the presence of 60nM and 1000nM BIBP3226. mRNA was collected at the given time points from 3 replicates. (A) TRAP, (B) CTR, (C) OSCAR and (D) CATK gene expression quantification relative to GADPH constitutive expression. Results are expressed as mean ± SEM from 3 independent experiments. Groups were compared through ANOVA and independent-samples t-test with * $p<0.05$.

cells could be caused by other factors yet unknown.

CTR expression was increased in BIBP3226 treated cells in early stages of differentiation, although ANOVA analysis did not show any statistical significance. OSCAR was slightly upregulated at day 7 in both BIBP3226 treatments, although it was not statistically significant.

Strikingly, CATK levels were the same as control mRNA levels, with a slight increasing trend at day 14 in 60nM BIBP3226 treated cells. Similarly to TRAP expression, these results are quite unexpected since resorption assays were comparable to the $Y_1R$ KO genotype, where CATK downregulation seems to be one of the causing factors. $Y_1R$ antagonism must therefore cause resorption impairment through different signalling pathways than the ones prompted by the absence of $Y_1R$.

OC differentiation markers were only increased in earlier stages of differentiation after BIBP3226 treatment, with the exception of CATK. At day 14 no differences were observed in every OC marker tested. Thus, the increase in OC differentiation resulting from BIBP3226 treatment previously demonstrated by $TRAP^+$ MNC counting cannot be explained by increased expression of OC differentiation markers. Yet, as mRNA levels do not always reflect the protein levels, this increase in OC differentiation markers at day 7 may not reflect the actual protein synthesis, which could be confirmed by ELISA in future studies.

**Fusion Proteins**

Pre-OC fusion gene expression has shown no differences in all genes analysed (Figure 23). However, there is a slight increase in CD47 expression in BIBP3226 treated cells when compared to control levels. Thus, the slightly increased OC area and $TRAP^+$ MNC numbers

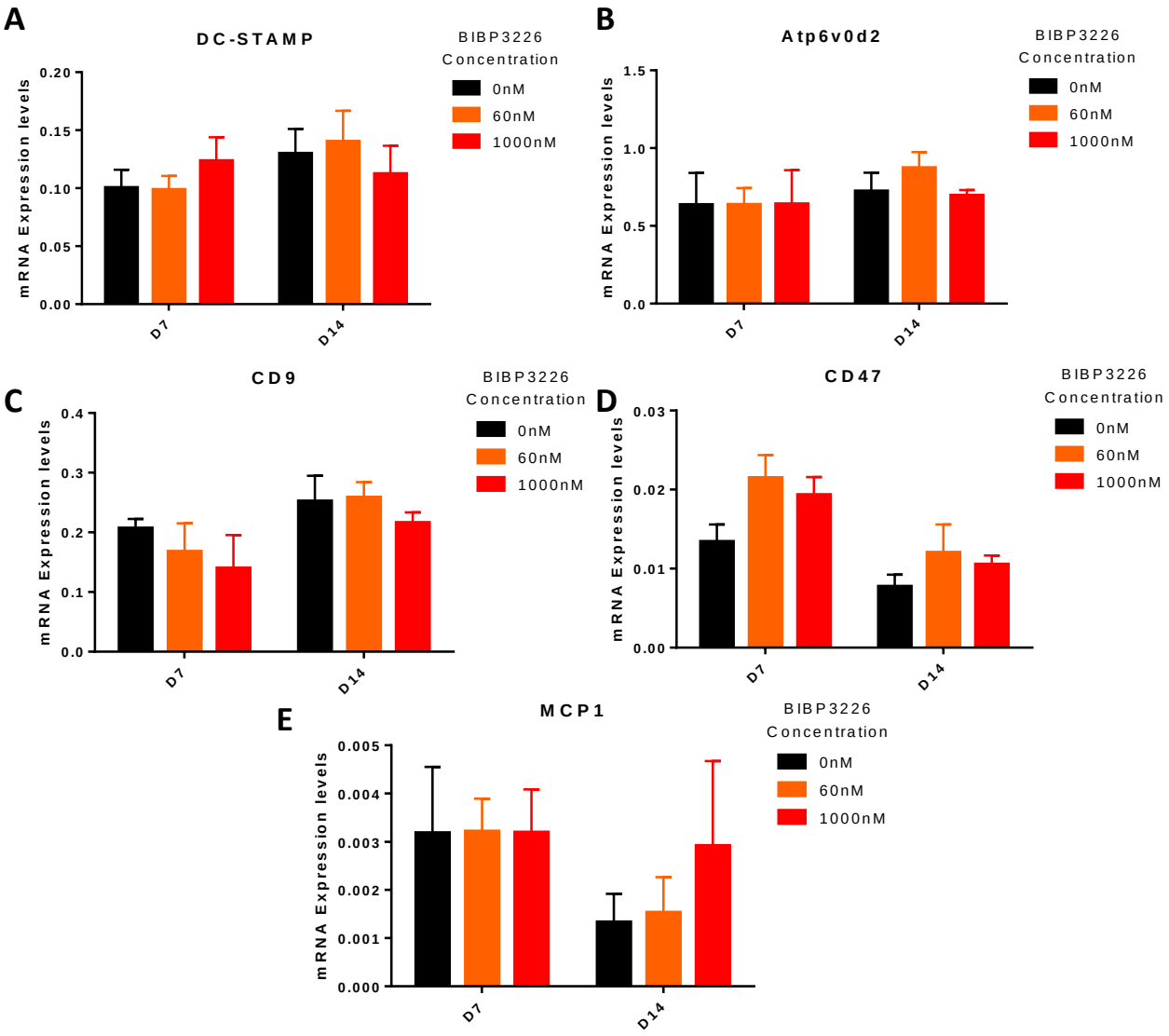


**Figure 23 - Expression of pre-OC fusion genes in BIBP3226 treated cells.** Maturation of bone marrow derived pre-OC was induced with M-CSF and RANKL for 14 days in 24-well culture plates in the presence of 60nM and 1000nM BIBP3226. mRNA was collected at the given time points from 3 replicates. (A) DC-STAMP, (B) Atp6v0d2, (C) CD9, (D) CD47 and (E) MCP1 gene expression quantification relative to GADPH constitutive expression. Results are expressed as mean ± SEM from 3 independent experiments. Groups were compared through paired t-test with * $p<0.05$.

observed in BIBP3226 treated cells might be due to an increase in CD47 expression at the cellular membrane, in contrast of what was verified in $Y_1R$ KO OCs. Once again, it seems that the regulatory pathways leading to the same results are different whether $Y_1R$ is absent or it suffers antagonist stimulation. Regarding pre-OC fusion, $Y_1R$ antagonist treatment could lead to an upregulation of CD47 instead of the MCP1 increased expression observed in $Y_1R$ KO samples. Nevertheless, the number of samples should be increased in future studies to confirm these results and to reduce the associated error to these measures.

Upon NPY stimulation, $Y_1R$ is rapidly internalized through a clathrin-dependent endocytic pathway as part of a desensitization process, as Gicquiaux and co-workers demonstrated using endocytic inhibitors. $Y_1R$ agonist internalization is also partially dependent on G protein activation, since internalization was reduced after treatment with G protein inhibitor pertussis toxin[99]. However, antagonist receptor internalization was not affected by pertussis toxin treatment and it has shown reduced sensitivity to endocytic inhibitors, although its internalization was still significantly reduced after endocytic inhibition[97]. Furthermore, $Y_1R$ is recycled back to the cellular membrane after internalization contrarily to what occurs after antagonist binding. Antagonist $Y_1R$ internalization led to a non-recoverable loss of 50% of total binding sites at the cellular surface[97], which point to a marked difference between agonist and antagonist binding and internalization. Therefore, antagonist stimulation of $Y_1R$ could lead to different signalling pathways besides inhibition of the normal cellular response to NPY, which could explain the different mRNA expression observed in BIBP3226 treated and $Y_1R$ KO cells.

In addition, in CHO-K1 cells BIBP3226 was reported to cause an increase in cAMP and $Ca^{2+}$ cellular levels, as well as Phospholipase C (PLC) activation, when present at concentrations higher than 1μM[101, 102]. The presence of G protein inhibitors did not prevent these cellular responses, which point to an $Y_1R$ independent effect. However, this seems to be a cell-type dependent response, since no calcium elevation was observed after BIBP3226 incubation in SK-N-MC cells. Nonetheless, a receptor-independent BIBP3226 response in OC such as diffusion through the cellular membrane and intracellular signalling should not be ruled out in the analysis of the previous differentiation, resorption and mRNA expression results and testing the specificity of the antagonist signalling should be a priority in future studies.

## 3 - Osteoclastogenesis on an OB/OC co-culture model

As bone remodelling occurs in a highly regulated manner with a close interaction between different cells, a co-culture model could replicate in an approximate way the myriad of signalling processes that takes place between the main cell types of the bone, OBs and OCs. Furthermore, it would be of interest to study the $Y_1R$ pathway in this interaction since the influence of OB on osteoclastogenesis in an $Y_1R$ deletion model is still poorly understood.

### 3.1 – Osteoclastogenesis on an $Y_1R$ KO OB/OC co-culture model

A direct co-culture model using calvarial OB and primary bone marrow flushed cells was established in order to allow direct coupling and integrin signalling between OB and OC. OB adhesion, growth and expression of OC differentiation cytokines was stimulated by dexamethasone, ascorbic acid, β-glycerophosphate, PGE2 and VitD3 for 1 day before the direct seeding of M-CSF stimulated pre-OC. Co-culture was maintained for 21 days under PGE2 and VitD3 stimulation. TRAP expression was assessed at day 7 and 14, genetic expression of OBs and OCs was analysed at day 1 and 14 and late calcium deposition was assessed at day 21. TRAP staining results are presented in Figure 24. No statistically significant differences were found between Y1R KO and WT $TRAP^+$ MNC numbers. Microscopic analysis show differentiated OCs in both conditions at day 7 time point, although WT OCs are larger at this early stage. At day 14, differentiated OC are present in similar number and size in both conditions. Unfortunately, OBs seem to stain with a light pink colour and the high cellular density hampers the $TRAP^+$ MNC counting, which could result in an error-prone evaluation. In fact, TRAP expression and internalization by OB was previously reported [103]. In addition, TRAP+ MNC counting was performed in an inverted microscope, thus the OBs in the bottom of the well were visualized on top of the OC. Furthermore, at day 14 loose OB matrix can be observed which could mean that some of the cells present on top were released and discarded in medium changes. OB-produced collagenous matrix is clearly visible over the differentiated OC at later stages of differentiation and this matrix seems to lose adhesion capacity because, instead of being spread throughout the entirety of the well as observed in OB monocultures (data not shown), it is retracted and only partially adhered. This could be due to the release of resorption enzymes by mature OC which would degrade the collagenous matrix.

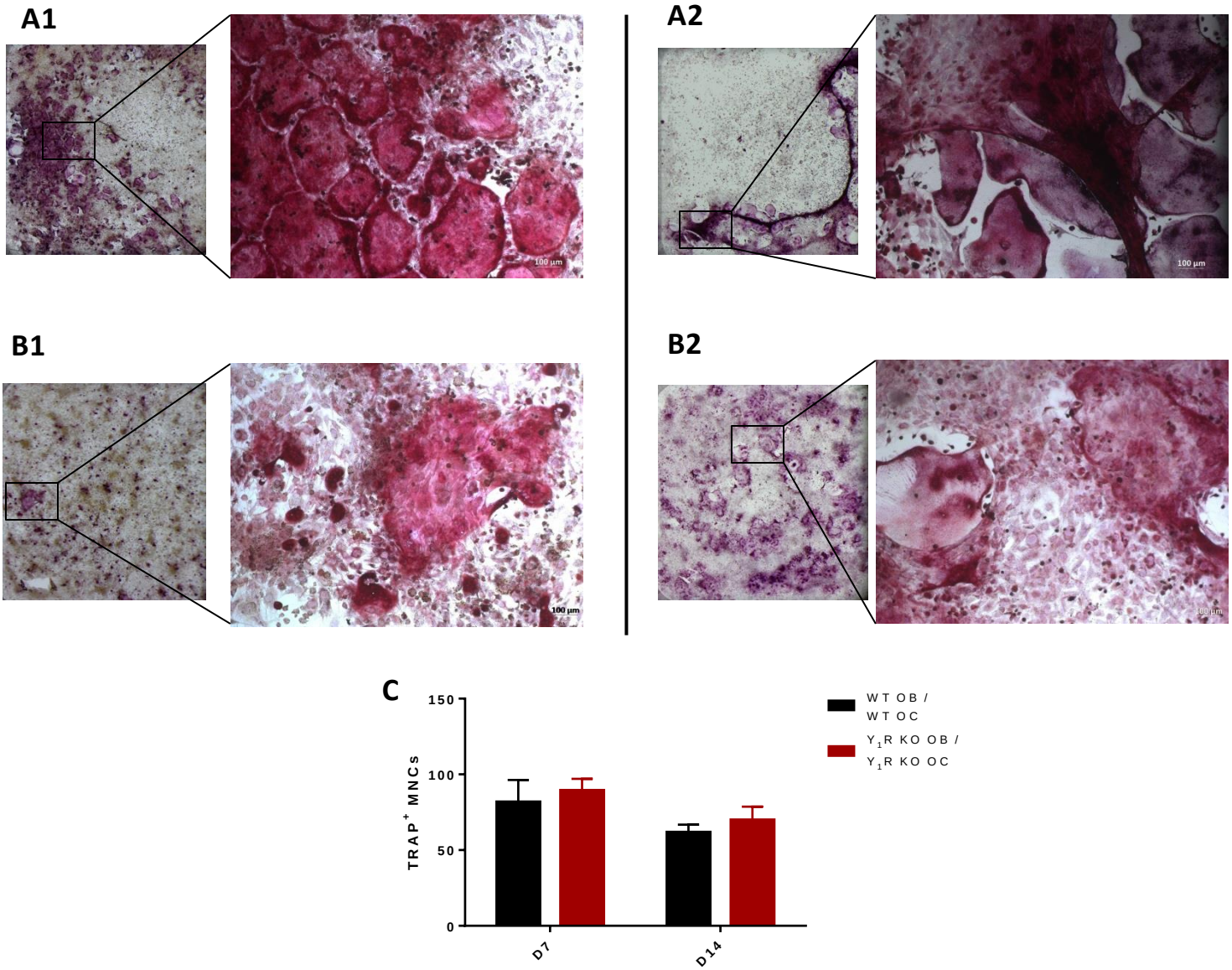


**Figure 24 – TRAP Staining of $Y_1$R KO co-cultures.** Bone marrow flushed pre-OC were seeded directly on top of calvarial OB and cultured for 14 days with 1000nM PGE2 and 10nM VitD3. Representative images of (A) WT and (B) $Y_1$R KO co-cultures at (1) day 7 and (2) day 14 time points are presented. Whole well images are shown on the left and images taken with the microscope with a 10x objective are shown on the right. Scale bar, 100µm. (C) Number of $TRAP^+$ MNCs. $TRAP^+$ OC with more than 3 nuclei were counted. Results are expressed as mean ± SEM from 2 independent experiments. Groups were compared through ANOVA and independent-samples t-test with * $p<0.05$.

Compared to OC monocultures, OCs co-cultured with OBs apparently differentiate faster with an increased size, because cell size at day 7 seems comparable to OC monoculture cells at day 14. No marked differences were observed between $Y_1$R KO and WT OC when in co-culture, suggesting that the absence of $Y_1$R signalling in OC was partially countered by OB stimulus. Further experiments should be conducted to confirm these results, since only two independent experiments were performed. A different counting method should also be employed to reduce errors.

**OC Differentiation Markers**

OB and OC specific gene expression was also analysed, with focus on genes involved in Osteoclastogenesis. $Y_1R$ KO co-cultures have shown a general increase in OC specific differentiation marker expression at day 14 time point, with exception of CATK (Figure 25). Expression of TRAP, CTR, OSCAR and CATK genes at day 1 was negligible, no differentiation occurred at this early stage as expected. At day 14, TRAP expression revealed a non-significant increasing trend in $Y_1R$ KO co-culture while OSCAR expression was significantly upregulated. CTR expression apparently increased in $Y_1R$ KO co-culture but the high associated error did not

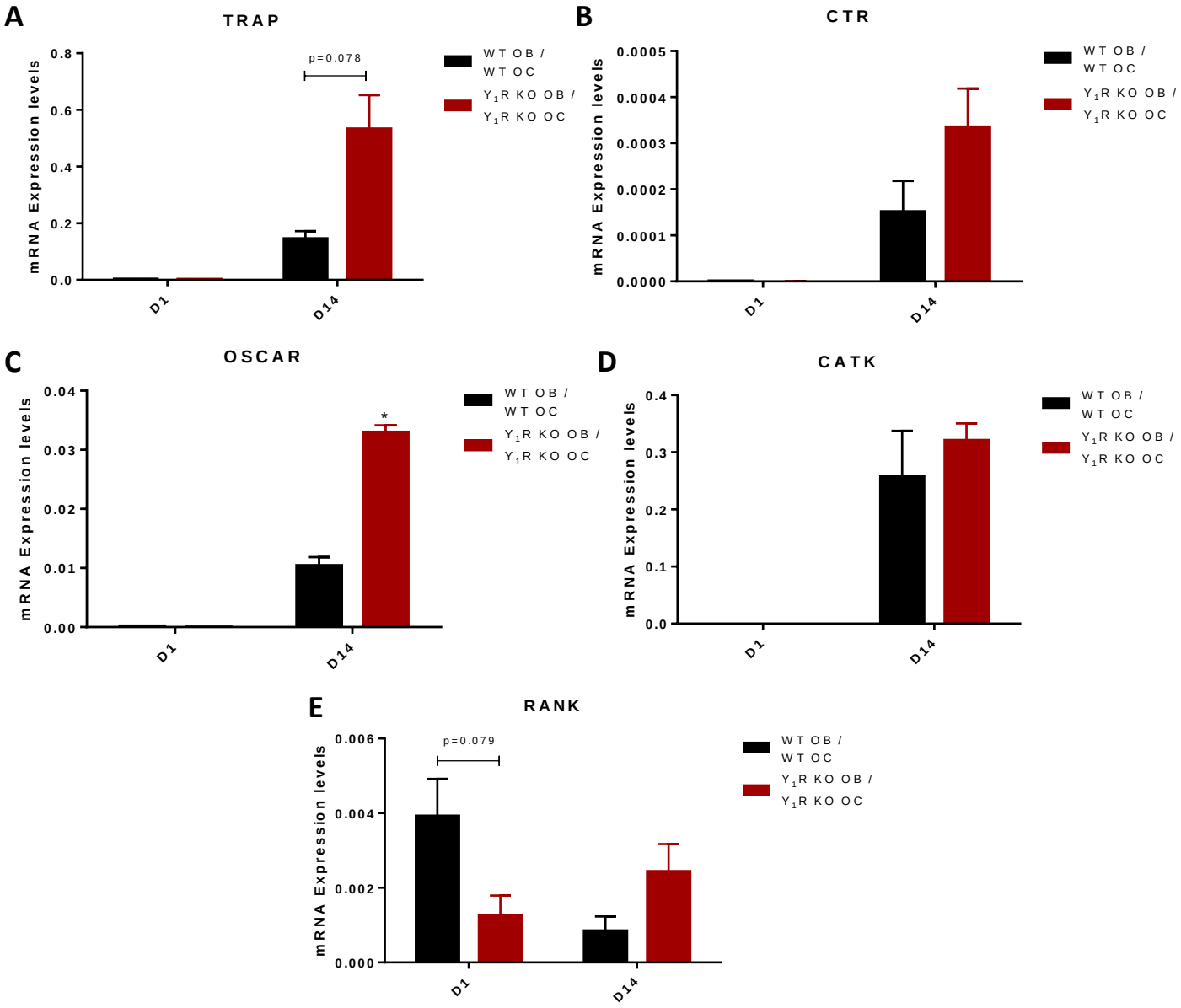


**Figure 25 – Expression of OC-specific differentiation markers in Y1R KO co-cultures.** Bone marrow flushed pre-OC were seeded directly on top of calvarial OB and cultured for 14 days with 1000nM PGE2 and 10nM VitD3. mRNA was collected at the given time points from 3 replicates. (A) TRAP, (B) CTR, (C) OSCAR, (D) CATK, and (E) RANK gene expression quantification relative to GADPH constitutive expression. Results are expressed as mean ± SEM from 3 independent experiments. Groups were compared through ANOVA and independent-samples t-test with * $p<0.05$.

allow any definite conclusion. CATK expression showed no significant differences but given the increase in the other OC differentiation markers and the expression decrease observe d in $Y_1R$ KO OC monoculture, this result is not unexpected. Interestingly, RANK expression revealed a decreasing trend at day 1 time point in $Y_1R$ KO co-culture, with a non-significant increase at day 14. This could explain the increase in size of WT OC at day 7 compared to $Y_1R$ KO OC observed in the TRAP staining, since RANK signalling might be decreased.

**OB Specific Genes Involved in Osteoclastogenesis**

Contrarily to the results obtained from OC monocultures, OC-specific differentiation markers were generally upregulated, which could point to a stimulatory effect of OB when $Y_1R$ signalling is absent. To further explore this possibility, RANKL and OPG expression by OBs was analysed. Interestingly, RANKL expression by $Y_1R$ KO OBs was non-significantly decreased in comparison to WT values at day 1 (Figure 26). However, at day 14, RANKL expression had a statistically significant 4-fold increase compared to WT expression.

OPG levels were constant in WT cells throughout the 14 days of co-culture. $Y_1R$ KO OBs had a decreasing trend in OPG expression compared to WT OBs, but at day 14 expression of

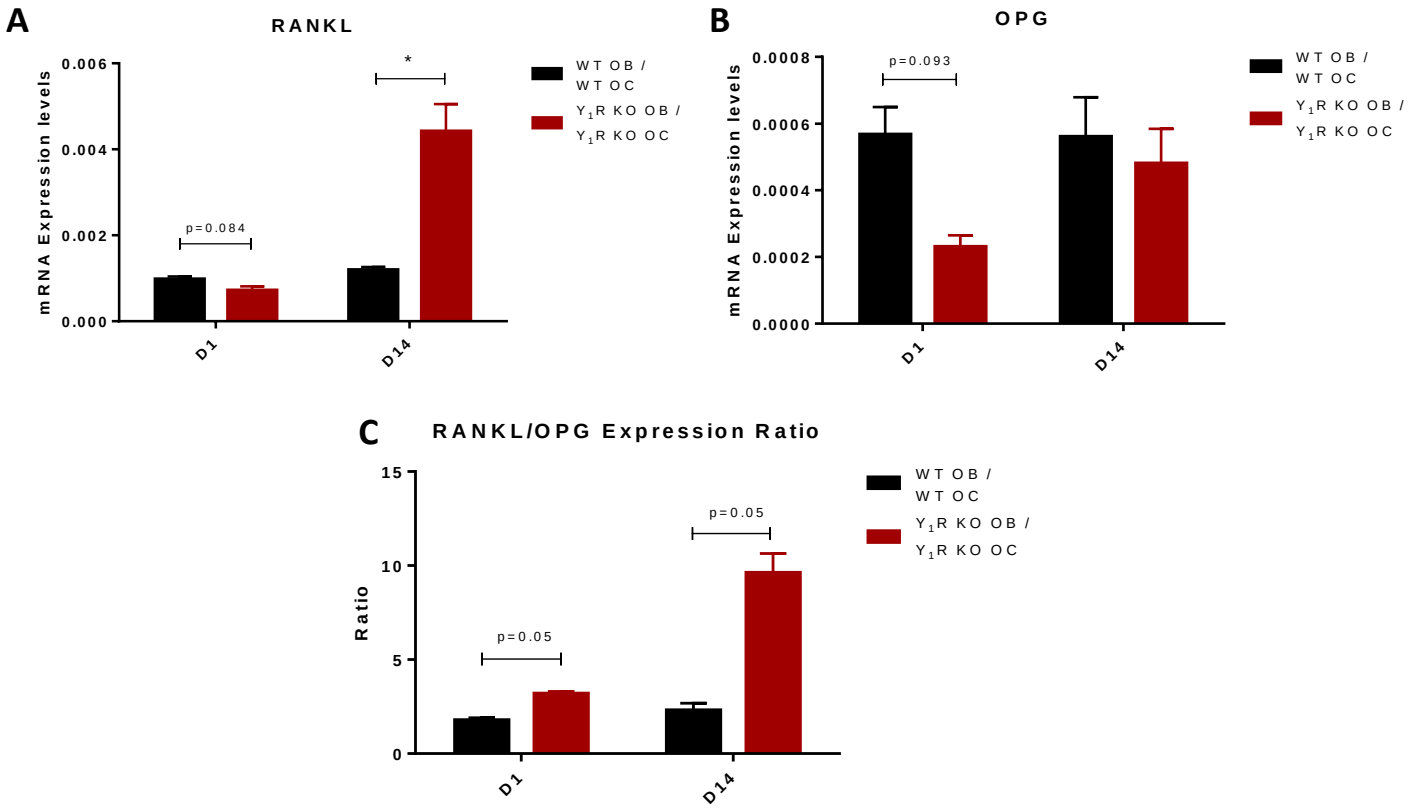


**Figure 26 – Expression of OB-specific RANKL and OPG genes in $Y_1R$ KO co-cultures.** Bone marrow flushed pre-OC were seeded directly on top of calvarial OB and cultured for 14 days with 1000nM PGE2 and 10nM VitD3. mRNA was collected at the given time points from 3 replicates. (A) RANKL and (B) OPG gene expression quantification relative to GADPH constitutive expression. Results are expressed as mean ± SEM from 3 independent experiments. Groups were compared through ANOVA and independent-samples t-test with * $p<0.05$. (C) RANKL/OPG expression ratio. Groups were compared through Kruskal-Wallis test and Mann-Whitney U-test with * $p<0.05$.

OPG was similar to control levels. As OPG sequestrates RANKL and inhibits osteoclastogenesis, RANKL/OPG ratio was calculated and compared. RANKL/OPG ratio was increased at every time point studied. This is consistent with the findings of Teixeira and co-workers that NPY inhibits RANKL expression and stimulates OPG release from OBs[54]. Therefore, RANKL mRNA increase and OPG mRNA decrease is expected in $Y_1R$ KO OBs due to the absence of $Y_1R$ signalling.

This increased RANKL/OPG ratio is probably responsible for the general increase in OC-specific differentiation marker expression. Since RANKL expression is higher in $Y_1R$ KO co-cultures, an increase in osteoclastogenesis and differentiation marker expression is expected compared to WT co-cultures. However, these results are not consistent with the TRAP staining assays performed previously, since no increase in $TRAP^+$ MNCs were observed. TRAP staining assays should be repeated in the future to clarify if an increase in $TRAP^+$ MNCs is verified or if there is some inhibitory factor in $Y_1R$ KO cultures.

To study the influence of $Y_1R$ signalling in OB driven matrix mineralization on the co-culture model, calcium deposition was quantified by Alizarin Red staining at later stages of culture. Alizarin Red stains free and mineralized calcium and it is widely used to determine the presence of calcium deposits by OBs. Alizarin Red staining did not reveal significant differences between $Y_1R$ KO and control samples (Figure 27). An increase in mineralization would be expected since $Y_1R$ signalling was previously shown to inhibit mineral deposition *in vitro* and *in vivo*[54, 57].

These are preliminary results since few experiments were conducted in order to obtain reliable data. Van Kossa Staining could alternatively be used to detect phosphate deposits and complement this analysis.

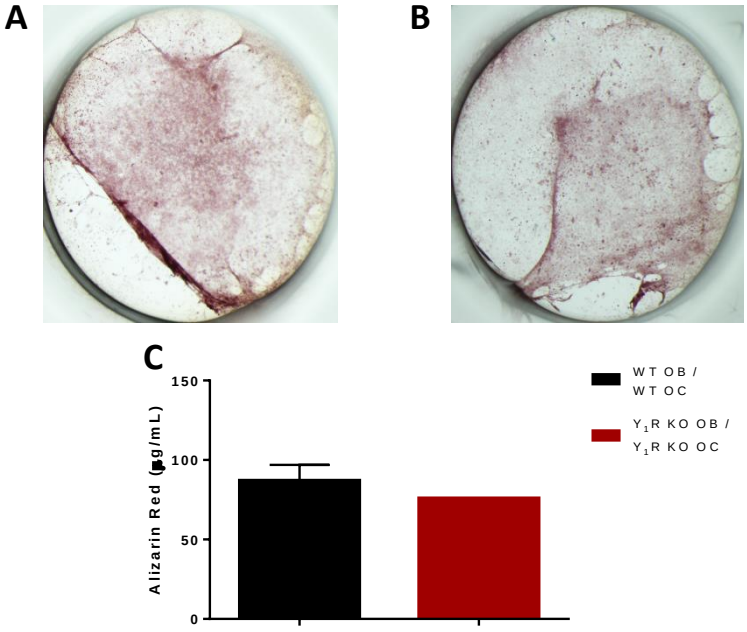


**Figure 27 – Calcium deposition quantification by Alizarin Red staining in $Y_1R$ KO co-cultures.** Bone marrow flushed pre-OC were seeded directly on top of calvarial OB and cultured for 21 days with 1000nM PGE2 and 10nM VitD3. Representative images of (A) WT and (B) $Y_1R$ KO OB calcified matrix staining with Alizarin Red. (C) Quantification of the calcium-associated Alizarin Red. Results are expressed as mean ± SEM from N (WT; $Y_1R$ KO) = 2; 1 independent experiments.

### 3.2 The effect of $Y_1R$ antagonism on Osteoclastogenesis in an OB/OC co-culture model

In order to study the influence of $Y_1R$ antagonism in Osteoclastogenesis in an OB/OC co-culture model. OB adhesion, growth and expression of OC differentiation cytokines was stimulated by dexamethasone, ascorbic acid, β-glycerophosphate, PGE2 and VitD3 for 1 day before the direct seeding of M-CSF stimulated pre-OC. Co-culture was maintained for 21 days under PGE2 and VitD3 stimulation, with the presence of 60nM and 1000nM BIBP3226. TRAP expression was assessed at day 7 and 14, genetic expression of OBs and OCs was analysed at day 1 and 14 (Day 1 without BIBP3226) and late calcium deposition was assessed at day 21.

TRAP staining revealed no differences in $TRAP^+$ MNC number at day 7 time point (Figure 28). Microscopic images show OC present in similar number and size in both treatments compared to control samples. At day 14 there is a slight decreasing trend in $TRAP^+$ MNCs in 60nM BIBP3226 treated OCs compared to control OCs. No differences were observed in $TRAP^+$ MNCs between 1000nM BIBP3226 treated OCs and control cells. Once again, co-cultured OC do not show the same behaviour as OC in monoculture, no increase in $TRAP^+$ MNCs is observed contrarily to the increase observed in monocultures. Further experiments should be conducted to decrease errors and strengthen the observed results, yet there seems to be an inhibitory stimulus when $Y_1R$ is antagonized. It is generally accepted that $Y_1R$ signalling inhibits osteoblast growth and RANKL production; thus $Y_1R$ antagonism should stimulate osteoclastogenesis. Therefore, this co-culture model should be further optimized in future studies.

**OC Differentiation Markers**

In addition, the expression of OC specific differentiation markers was studied. Results were very similar to those observed in $Y_1R$ KO co-cultures, with a generalized increase in OC marker expression in both BIBP3226 treatments with the exception of CATK (Figure 29). Since it was expected that no differences would be observed in such a short time, no BIBP3226 was added to the day 1 wells to avoid wasting resources. Expression of TRAP, CTR, OSCAR and CATK genes at day 1 was negligible, no differentiation occurred at this early stage as expected. TRAP expression was significantly increased in 60nM BIBP3226 treated OCs and an increasing tre nd was observed in 1000nM BIBP3226 treated OCs compared to control cells. CTR and OSCAR had very similar expression profiles, with a non-significant increasing trend in 1000nM BIBP3226 treated cells. Expression of these genes was also increased in 60nM BIBP3226 treated OCs, but no conclusions were made due to the high associated error. CATK expression showed no differences in BIBP3226 treated cells compared to the controls.

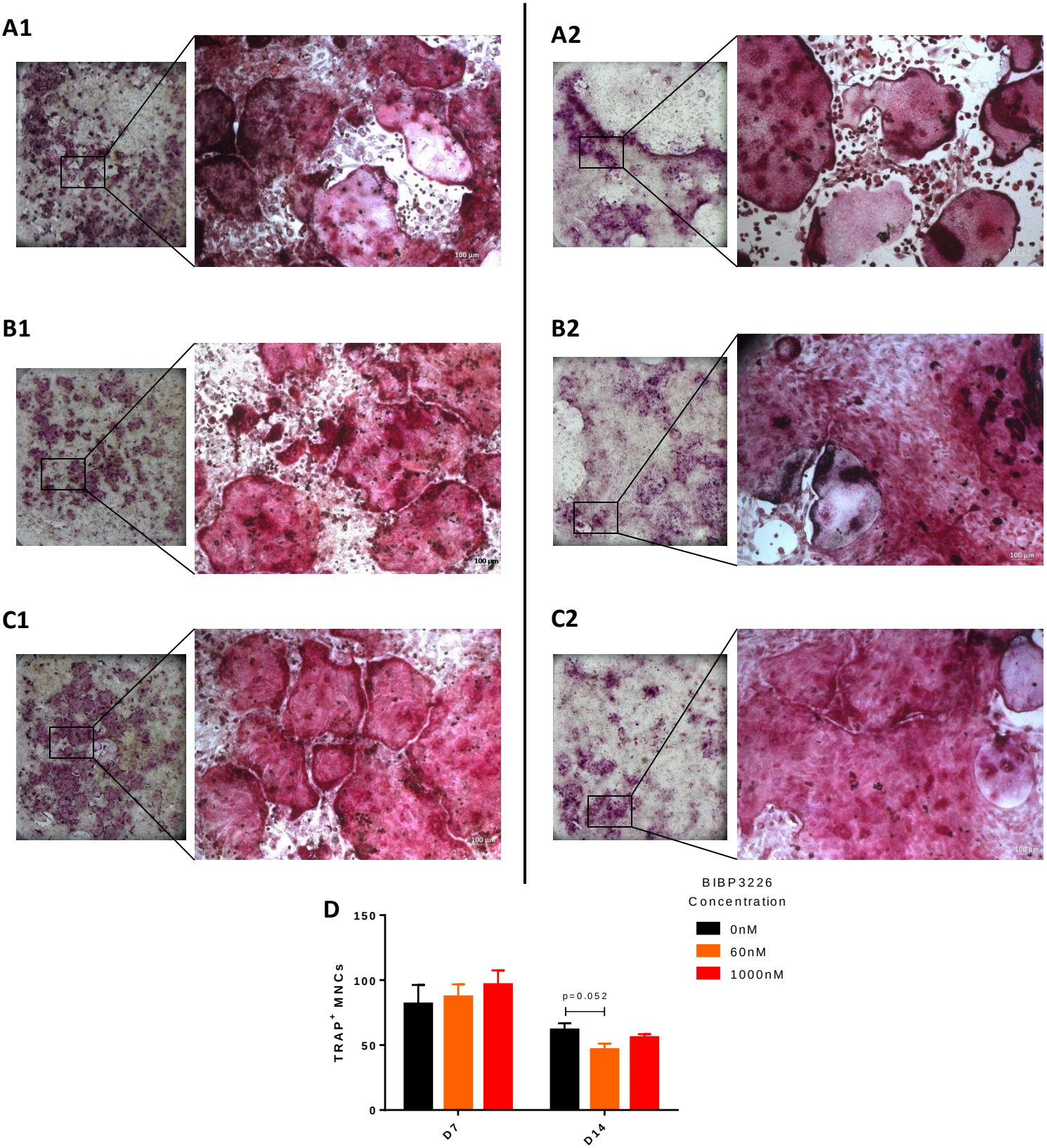


**Figure 28 - TRAP Staining of BIBP3226 treated co-cultures.** Bone marrow flushed pre-OC were seeded directly on top of calvarial OB and cultured for 14 days with 1000nM PGE2 and 10nM VitD3 in the presence of 60nM and 1000nM BIBP3226. Representative images of (A) 0nM, (B) 60nM and (C) 1000nM BIBP3226 treated co-cultures at (1) day 7 and (2) day 14 time points are presented. Whole well images are shown on the left and images taken with the microscope with a 10x objective are shown on the right. Scale bar, 100µm. (D) Number of $TRAP^+$ MNCs. $TRAP^+$ OC with more than 3 nuclei were counted. Results are expressed as mean ± SEM from 2 independent experiments. Groups were compared through ANOVA and independent-samples t-test with * $p<0.05$.

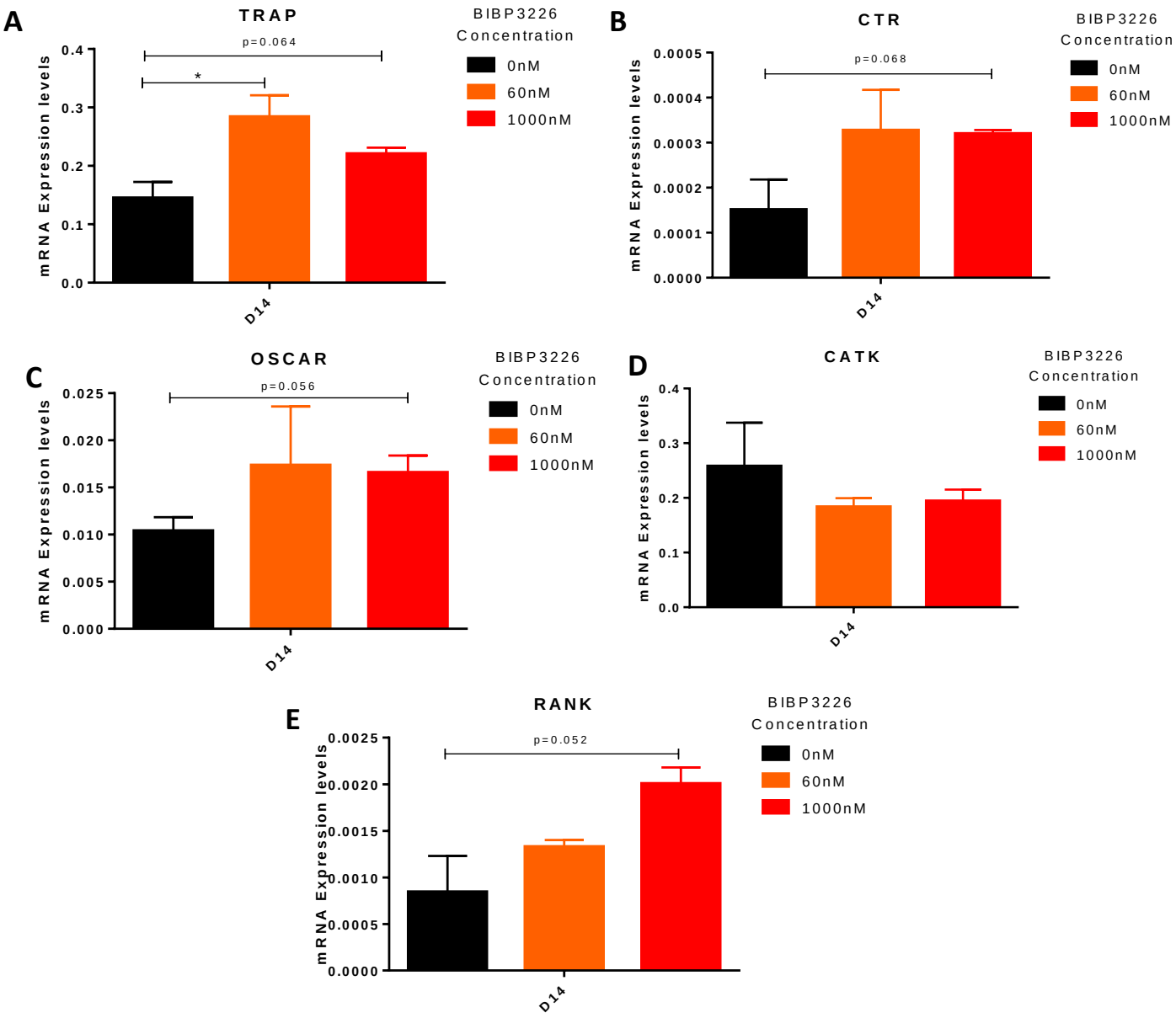


**Figure 29 – Expression of OC-specific differentiation markers in BIBP3226 treated co-cultures.** Bone marrow flushed pre-OC were seeded directly on top of calvarial OB and cultured for 14 days with 1000nM PGE2 and 10nM VitD 3 in the presence of 60nM and 1000nM BIBP3226. mRNA was collected at the given time points from 3 replicates. (A) TRAP, (B) CTR, (C) OSCAR, (D) CATK, and (E) RANK gene expression quantification relative to GADPH constitutive expression. Results are expressed as mean ± SEM from 3 independent experiments. Groups were compared through ANOVA and independent-samples t-test with * $p<0.05$.

### OB Specific Genes Involved in Osteoclastogenesis

RANKL and OPG expression was also analysed. Interestingly, only 1000nM BIBP3226 treated OBs had a statistically significant increase in RANKL expression, 60nM BIBP3226 treated OBs RANKL expression was similar to the controls (Figure 30). OPG expression was similar in every condition, with no statistically significant differences observed. Thus, the increased RANKL expression in 1000nM BIBP3226 led to an increased RANKL/OPG ratio. This increasing trend was not statistically significant ($p=0.05$) probably due to the non-parametrical

statistical test used. RANKL/OPG ratio of 60nM BIBP3226 treated OBs was similar to control levels.

These results were not consistent with the TRAP staining previously performed. Considering the genetic expression profile observed, it was expected that 1000nM BIBP3226

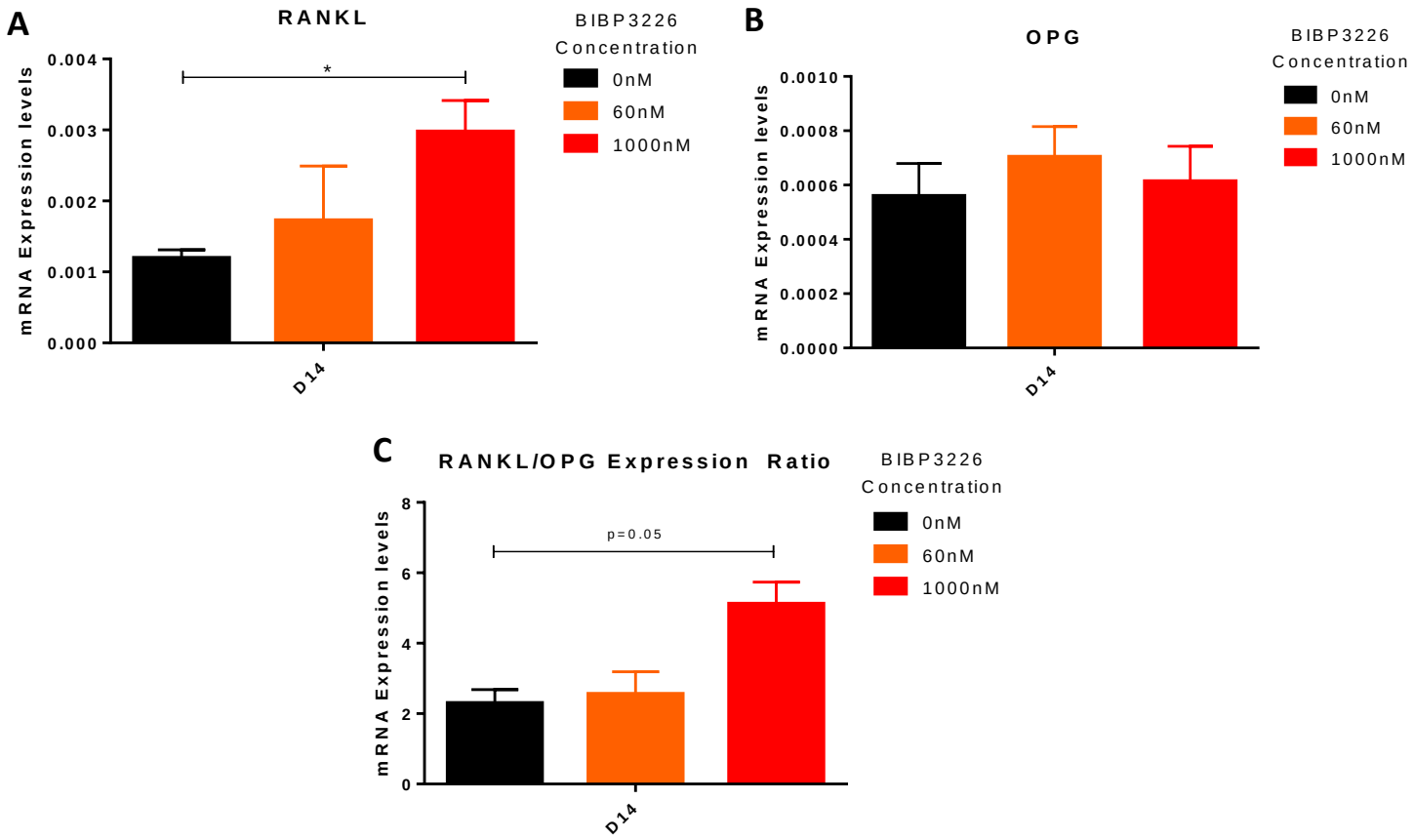


**Figure 30 - Expression of OB-specific RANKL and OPG genes in BIBP3226 treated co-cultures.** Bone marrow flushed pre-OC were seeded directly on top of calvarial OB and cultured for 14 days with 1000nM PGE2 and 10nM VitD3 in the presence of 60nM and 1000nM BIBP3226. mRNA was collected at the given time points from 3 replicates. (A) RANKL and (B) OPG gene expression quantification relative to GADPH constitutive expression. Results are expressed as mean ± SEM from 3 independent experiments. Groups were compared through ANOVA and independent-samples t-test with * $p<0.05$. (C) RANKL/OPG expression ratio. Groups were compared through Kruskal-Wallis test and Mann-Whitney U-test with * $p<0.05$.

treated cells would have increased $TRAP^+$ MNC numbers. In order to verify these results, further experiments should be conducted to produce statistically solid results.

Since RANKL expression is elevated in $Y_1R$ KO and BIBP3226 treated co-cultures, an inhibiting factor should be counteracting the RANKL stimulation, resulting in similar control and treated $TRAP^+$ MNCs. Nitrous Oxide was shown to inhibit Osteoclastogenesis in previous studies after stimulation by Interferon gamma and Fibronectin [104, 105]. Interleukins (IL) are cytokines involved in the regulation of inflammation and immune response but they also modulate bone resorption, such as the osteoclastogenesis inhibitor IL-4[106, 107] or the osteoclastogenic IL-1[108] and IL-11[109]. IL-33 and IL-18 were reported to be produced by OB and

to inhibit osteoclastogenesis[110, 111]. In future studies the influence of these inhibitory factors should be investigated if the TRAP staining results are confirmed.

Calcium deposition in BIBP3226 treated co-cultures was assessed through Alizarin Red Staining (Figure 31). No statistically significant differences between calcium deposition in 60nM and 1000nM BIBP3226 treated co-cultures compared to control deposition. However, conflicting results were obtained in the two independent experiments performed, where in one of the experiments Alizarin Red was slightly decreased in BIBP3226 treated co-cultures and in the other it was slightly increased. Further optimization should be done in order to

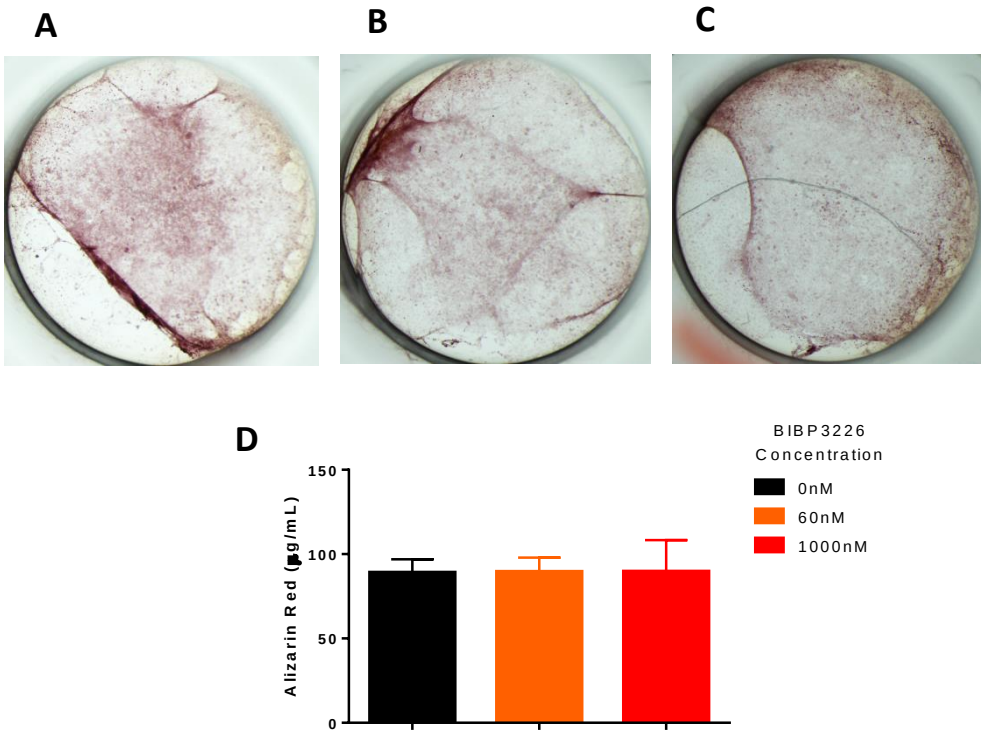


**Figure 31 - Calcium deposition quantification by Alizarin Red staining in BIBP3226 treated co-cultures.** Bone marrow flushed pre-OC were seeded directly on top of calvarial OB and cultured for 21 days with 1000nM PGE2 and 10nM VitD3 in the presence of 60nM and 1000nM BIBP3226. Representative images of (A) 0nM, (B) 60nM and (C) 1000nM BIBP3226 treated OB-calcified matrix staining with Alizarin Red. (D) Quantification of the calcium-associated Alizarin Red. Results are expressed as mean ± SEM from 2 independent experiments with * $p<0.05$.

clarify these results. Performing the Alizarin Red staining in larger wells and increasing the number of replicates should improve measurement quality.

In conclusion, there seem to be no differences in $TRAP^+$ MNC formation between either $Y_1R$ KO or BIBP3226 treated co-cultures and WT controls, in spite of the genetic expression profile of OBs and OCs. No differences in matrix mineralization were observed in Y1R KO co-cultures and after BIBP3226 treatment. More experiments as well as further optimization are required to clarify these results.

# Concluding remarks and perspectives

1. An upregulated osteoclastogenesis was observed in bone marrow derived pre-OC from $Y_1R$ KO mice, with increased $TRAP^+$ MNC numbers and OC section area and increased MCP1 expression, consistent with an augmented pre-OC fusion. However, $Y_1R$ KO OC exhibited impaired bone resorption capacity, with decreased TRAP and CATK expression. Thus, $Y_1R$ absence led to significant changes in OC behaviour, probably due to changes in RANK/RANKL signalling or a stimulation of previously inhibited secondary messengers. Future studies are proposed on the assessment of the role of MMPs in the decreased resorption capacity of $Y_1R$ KO OCs and the study of other fusion regulatory proteins such as ADAM8, MFR and TREM2. In addition, OC resorption assays in dentine slices should be repeated to strengthen the obtained results in the pit 3D reconstruction.

2. Secondly, BIBP3226 treated cells revealed an increase in osteoclastogenesis, with higher number of $TRAP^+$ MNCs but no differences were observed in regards to OC section area. OC differentiation marker expression was upregulated after BIBP3226 treatment. Resorption capacity of BIBP3226 treated cells also demonstrated a significant decrease in pit volume and top section area. In addition, future studies with GPCR inhibitors should be conducted to verify if the observed results are $Y_1R$ dependent. The same questions are posed regarding other OC fusion and resorption proteins as in $Y_1R$ KO cells.

3. Finally, an OB/OC co-culture model was established, with successful osteoclastogenesis in all conditions. However, no changes were observed in TRAP+ MNC numbers. Genetic expression analysis revealed an increase in OC specific differentiation markers in $Y_1R$ KO co-cultures. This increase in OC marker expression was probably due to a significant increase in RANKL production by $Y_1R$ KO OBs. However, this genetic expression analysis was not consistent with TRAP staining results. This could point to the presence of an OB secreted OC inhibitor upregulated upon $Y_1R$ deletion. BIBP3226 treatment yielded the same results as the ones obtained after $Y_1R$ gene deletion but in a smaller extent, with increased OC marker expression and no differences in $TRAP^+$ MNCs and mineralization. In future studies, it would be interesting to establish WT OB/$Y_1R$ KO OC and $Y_1R$ KO OB/WT OC co-cultures in order to perceive which cell type could have the most influence on osteoclastogenesis after $Y_1R$ deletion. The influence of OC on bone formation should also be analysed through Alizarin Red, Van Kossa and ALP activity assays, but in larger wells and with more replicates to generate reliable data.

In summary, the present work contributes for the unravelling of the role of $Y_1R$ signalling on OC behaviour while exploring the effect of BIBP3226. In addition, the first steps were taken towards the establishment of a co-culture model that could approximate an *in vitro* setting to *in vivo* conditions.

# References


[1] VanPutte, C.; Regan, J. and Russo, A. (2014), "Seeley's Anatomy & Physiology", McGraw-Hill

[2] Tech, M.: http://classes.midlandstech.edu/carterp/Courses/bio210/chap06/lecture1.html

[3] Bilezikian, J. P.; Raisz, L. G. and Rodan, G. A. (1996), "Principles of Bone Biology", 1st Edition, Academic Press

[4] Brandi, M. L. (2009), "Microarchitecture, the key to bone quality", Rheumatology, Vol. 48, iv3-iv8

[5] Rauner, M.; Sipos, W. and Pietschmann, P. (2007), "Osteoimmunology", International Archives of Allergy and Immunology, Vol. 143, 31-48

[6] Rosen, C. J.; Compston, J. E. and Lian, J. B. (2008), "Primer on the Metabolic Bone Diseases and Disorders of Mineral Metabolism", 7th Edition, American Society for Bone and Mineral Research

[7] Kular, J.; Tickner, J.; Chim, S. M. and Xu, J. (2012), "An overview of the regulation of bone remodelling at the cellular level", Clinical Biochemistry, Vol. 45, 863-873

[8] Panaroni, C.; Tzeng, Y.-s.; Saeed, H. and Wu, J. (2014), "Mesenchymal Progenitors and the Osteoblast Lineage in Bone Marrow Hematopoietic Niches", Current Osteoporosis Reports, Vol. 12, 22-32

[9] Taipaleenmäki, H.; Bjerre Hokland, L.; Chen, L.; Kauppinen, S. and Kassem, M. (2012), "MECHANISMS IN ENDOCRINOLOGY: Micro-RNAs: targets for enhancing osteoblast differentiation and bone formation", European Journal of Endocrinology, Vol. 166, 359-371

[10] Marie, P. J. (2008), "Transcription factors controlling osteoblastogenesis", Archives of Biochemistry and Biophysics, Vol. 473, 98 - 105

[11] Nakashima, K.; Zhou, X.; Kunkel, G.; Zhang, Z.; Deng, J. M.; Behringer, R. R. and de Crombrugghe, B. (2002), "The Novel Zinc Finger-Containing Transcription Factor Osterix Is Required for Osteoblast Differentiation and Bone Formation", Cell, Vol. 108, 17-29

[12] Titorencu, I.; Pruna, V.; Jinga, V. and Simionescu, M. (2014), "Osteoblast ontogeny and implications for bone pathology: an overview", Cell and Tissue Research, Vol. 355, 23-33

[13] Datta, N. S. and Abou-Samra, A. B. (2009), "PTH and PTHrP signaling in osteoblasts", Cellular Signalling, Vol. 21, 1245-1254

[14] Kubota, T.; Michigami, T. and Ozono, K. (2009), "Wnt signaling in bone metabolism", Journal of Bone and Mineral Metabolism, Vol. 27, 265-271

[15] Babij, P.; Zhao, W.; Small, C.; Kharode, Y.; Yaworsky, P. J.; Bouxsein, M. L.; Reddy, P. S.; Bodine, P. V.; Robinson, J. A.; Bhat, B.; Marzolf, J.; Moran, R. A. and Bex, F. (2003), "High Bone Mass in Mice Expressing a Mutant LRP5 Gene", Journal of Bone and Mineral Research, Vol. 18, 960-974

[16] Nakamura, H. (2007), "Morphology, Function, and Differentiation of Bone Cells", Journal of hard tissue biology, Vol. 16, 15-22

[17] Sapir-Koren, R. and Livshits, G. (2014), "Osteocyte control of bone remodeling: is sclerostin a key molecular coordinator of the balanced bone resorption–formation cycles?", Osteoporosis International, Vol. 25, 2685-2700

[18] Tonna, S. and Sims, N. (2014), "Talking among Ourselves: Paracrine Control of Bone Formation within the Osteoblast Lineage", Calcified Tissue International, Vol. 94, 35-45

[19] Tanaka, S.; Miyazaki, T.; Fukuda, A.; Akiyama, T.; Kadono, Y.; Wakeyama, H.; Kono, S.; Hoshikawa, S.; Nakamura, M.; Ohshima, Y.; Hikita, A.; Nakamura, I. and Nakamura, K. (2006), "Molecular Mechanism of the Life and Death of the Osteoclast", Annals of the New York Academy of Sciences, Vol. 1068, 180-186

[20] Boyce, B. F. (2013), "Advances in the Regulation of Osteoclasts and Osteoclast Functions", Journal of Dental Research, Vol. 92, 860-867

[21] Boyle, W. J.; Simonet, W. S. and Lacey, D. L. (2003), "Osteoclast differentiation and activation", Nature, Vol. 423, 337-342

[22] Asagiri, M. and Takayanagi, H. "The molecular understanding of osteoclast differentiation", Bone, Vol. 40, 251-264

[23] Xing, L.; Xiu, Y. and Boyce, B. F. (2012), "Osteoclast fusion and regulation by RANKL-dependent and independent factors", World Journal of Orthopedics, Vol. 3, 212-222

[24] Ishii, M.; Iwai, K.; Koike, M.; Ohshima, S.; Kudo-Tanaka, E.; Ishii, T.; Mima, T.; Katada, Y.; Miyatake, K.; Uchiyama, Y. and Saeki, Y. (2006), "RANKL-Induced Expression of Tetraspanin CD9 in Lipid Raft Membrane Microdomain Is Essential for Cell Fusion During Osteoclastogenesis", Journal of Bone and Mineral Research, Vol. 21, 965-976

[25] Yagi, M.; Miyamoto, T.; Toyama, Y. and Suda, T. (2006), "Role of DC-STAMP in cellular fusion of osteoclasts and macrophage giant cells", Journal of Bone and Mineral Metabolism, Vol. 24, 355-358

[26] Lee, S.-H.; Rho, J.; Jeong, D.; Sul, J.-Y.; Kim, T.; Kim, N.; Kang, J.-S.; Miyamoto, T.; Suda, T.; Lee, S.-K.; Pignolo, R. J.; Koczon-Jaremko, B.; Lorenzo, J. and Choi, Y. (2006), "v-ATPase V0 subunit d2-deficient mice exhibit impaired osteoclast fusion and increased bone formation", Nat Med, Vol. 12, 1403-1409

[27] Lacey, D. L.; Timms, E.; Tan, H. L.; Kelley, M. J.; Dunstan, C. R.; Burgess, T.; Elliott, R.; Colombero, A.; Elliott, G.; Scully, S.; Hsu, H.; Sullivan, J.; Hawkins, N.; Davy, E.; Capparelli, C.; Eli, A.; Qian, Y. X.; Kaufman, S.; Sarosi, I.; Shalhoub, V.; Senaldi, G.; Guo, J.; Delaney, J. and Boyle, W. J. "Osteoprotegerin Ligand Is a Cytokine that Regulates Osteoclast Differentiation and Activation", Cell, Vol. 93, 165-176

[28] Tamma, R. and Zallone, A. (2012), "Osteoblast and Osteoclast Crosstalks: From OAF to Ephrin", Inflammation & Allergy - Drug Targets, Vol. 11, 196-200

[29] Cappariello, A.; Maurizi, A.; Veeriah, V. and Teti, A. (2014), "The Great Beauty of the osteoclast", Archives of Biochemistry and Biophysics, Vol. 558, 70-78

[30] Hayman, A. R. and Cox, T. M. (2003), "Tartrate-Resistant Acid Phosphatase Knockout Mice", Journal of Bone and Mineral Research, Vol. 18, 1905-1907

[31] Teti, A. (2011), "Bone Development: Overview of Bone Cells and Signaling", Current Osteoporosis Reports, Vol. 9, 264-273

[32] Percival, C. J. and Richtsmeier, J. T. (2013), "Angiogenesis and intramembranous osteogenesis", Developmental Dynamics, Vol. 242, 909-922

[33] Staines, K. A.; Pollard, A. S.; McGonnell, I. M.; Farquharson, C. and Pitsillides, A. A. (2013), "Cartilage to bone transitions in health and disease", Journal of Endocrinology, Vol. 219, R1-R12

[34] Sims, N. A. and Martin, T. J. (2014), "Coupling the activities of bone formation and resorption: a multitude of signals within the basic multicellular unit", BoneKEy Rep, Vol. 3,

[35] Ikeda, K. and Takeshita, S. (2014), "Factors and Mechanisms Involved in the Coupling from Bone Resorption to Formation: How Osteoclasts Talk to Osteoblasts", J Bone Metab, Vol. 21, 163-167

[36] Kristensen, H. B.; Andersen, T. L.; Marcussen, N.; Rolighed, L. and Delaisse, J.-M. (2013), "Increased presence of capillaries next to remodeling sites in adult human cancellous bone", Journal of Bone and Mineral Research, Vol. 28, 574-585

[37] Takahashi, N.; Udagawa, N. and Suda, T. (2014), "Vitamin D endocrine system and osteoclasts", BoneKEy Rep, Vol. 3,

[38] Davey, R. A. and Findlay, D. M. (2013), "Calcitonin: Physiology or fantasy?", Journal of Bone and Mineral Research, Vol. 28, 973-979

[39] Spencer, G. J.; Hitchcock, I. S. and Genever, P. G. (2004), "Emerging neuroskeletal signalling pathways: a review", FEBS Letters, Vol. 559, 6-12

[40] Jones, K. B.; Mollano, A. V.; Morcuende, J. A.; Cooper, R. R. and Saltzman, C. L. (2004), "Bone and Brain: A Review of Neural, Hormonal, and Musculoskeletal Connections", The Iowa Orthopaedic Journal, Vol. 24, 123-132

[41] Elefteriou, F. (2005), "Neuronal signaling and the regulation of bone remodeling", Cellular and Molecular Life Sciences CMLS, Vol. 62, 2339-2349

[42] Tatemoto, K. (1982), "Neuropeptide Y: complete amino acid sequence of the brain peptide", Proceedings of the National Academy of Sciences of the United States of America, Vol. 79, 5485-5489

[43] Sousa, D. M.; Herzog, H. and Lamghari, M. (2009), "NPY Signalling Pathway in Bone Homeostasis: Y1 Receptor as a Potential Drug Target", Current Drug Targets, Vol. 10, 9-19

[44] Shi, Y.-C. and Baldock, P. A. "Central and peripheral mechanisms of the NPY system in the regulation of bone and adipose tissue", Bone, Vol. 50, 430-436

[45] Ducy, P.; Amling, M.; Takeda, S.; Priemel, M.; Schilling, A. F.; Beil, F. T.; Shen, J.; Vinson, C.; Rueger, J. M. and Karsenty, G. (2000), "Leptin Inhibits Bone Formation through a Hypothalamic Relay: A Central Control of Bone Mass", Cell, Vol. 100, 197-207

[46] Iwaniec, U. T.; Boghossian, S.; Lapke, P. D.; Turner, R. T. and Kalra, S. P. (2007), "Central leptin gene therapy corrects skeletal abnormalities in leptin-deficient ob/ob mice", Peptides, Vol. 28, 1012-1019

[47] Baldock, P. A.; Sainsbury, A.; Allison, S.; Lin, E.-J. D.; Couzens, M.; Boey, D.; Enriquez, R.; During, M.; Herzog, H. and Gardiner, E. M. (2005), "Hypothalamic Control of Bone Formation: Distinct Actions of Leptin and Y2 Receptor Pathways", Journal of Bone and Mineral Research, Vol. 20, 1851-1857

[48] Driessler, F. and Baldock, P. A. (2010), "Hypothalamic regulation of bone", Journal of Molecular Endocrinology, Vol. 45, 175-181

[49] Babilon, S.; Mörl, K. and Beck-Sickinger Annette, G. (2013), "Towards improved receptor targeting: anterograde transport, internalization and postendocytic trafficking of neuropeptide Y receptors", Biological Chemistry, Vol. 394, 921-936

[50] Nunes, A. F.; Liz, M. A.; Franquinho, F.; Teixeira, L.; Sousa, V.; Chenu, C.; Lamghari, M. and Sousa, M. M. (2010), "Neuropeptide Y expression and function during osteoblast differentiation – insights from transthyretin knockout mice", FEBS Journal, Vol. 277, 263-275

[51] Walther, C.; Mörl, K. and Beck-Sickinger, A. G. (2011), "Neuropeptide Y receptors: ligand binding and trafficking suggest novel approaches in drug development", Journal of Peptide Science, Vol. 17, 233-246

[52] Baldock, P. A.; Sainsbury, A.; Couzens, M.; Enriquez, R. F.; Thomas, G. P.; Gardiner, E. M. and Herzog, H. (2002), "Hypothalamic Y2 receptors regulate bone formation", The Journal of Clinical Investigation, Vol. 109, 915-921

[53] Lundberg, P.; Allison, S. J.; Lee, N. J.; Baldock, P. A.; Brouard, N.; Rost, S.; Enriquez, R. F.; Sainsbury, A.; Lamghari, M.; Simmons, P.; Eisman, J. A.; Gardiner, E. M. and Herzog, H. (2007), "Greater Bone Formation of Y2 Knockout Mice Is Associated with Increased Osteoprogenitor Numbers and Altered Y1 Receptor Expression", Journal of Biological Chemistry, Vol. 282, 19082-19091

[54] Teixeira, L.; Sousa, D. M.; Nunes, A. F.; Sousa, M. M.; Herzog, H. and Lamghari, M. (2009), "NPY revealed as a critical modulator of osteoblast function in vitro: New insights into the role of Y1 and Y2 receptors", Journal of Cellular Biochemistry, Vol. 107, 908-916

[55] Lee, N. J. and Herzog, H. "NPY regulation of bone remodelling", Neuropeptides, Vol. 43, 457-463

[56] Lee, N. J.; Doyle, K. L.; Sainsbury, A.; Enriquez, R. F.; Hort, Y. J.; Riepler, S. J.; Baldock, P. A. and Herzog, H. (2010), "Critical role for Y1 receptors in mesenchymal progenitor cell

differentiation and osteoblast activity", Journal of Bone and Mineral Research, Vol. 25, 1736-1747

[57] Baldock, P. A.; Allison, S. J.; Lundberg, P.; Lee, N. J.; Slack, K.; Lin, E.-J. D.; Enriquez, R. F.; McDonald, M. M.; Zhang, L.; During, M. J.; Little, D. G.; Eisman, J. A.; Gardiner, E. M.; Yulyaningsih, E.; Lin, S.; Sainsbury, A. and Herzog, H. (2007), "Novel Role of Y1 Receptors in the Coordinated Regulation of Bone and Energy Homeostasis", Journal of Biological Chemistry, Vol. 282, 19092-19102

[58] Lee, N. J.; Nguyen, A. D.; Enriquez, R. F.; Doyle, K. L.; Sainsbury, A.; Baldock, P. A. and Herzog, H. "Osteoblast specific Y1 receptor deletion enhances bone mass", Bone, Vol. 48, 461-467

[59] Igwe, J. C.; Jiang, X.; Paic, F.; Ma, L.; Adams, D. J.; Baldock, P. A.; Pilbeam, C. C. and Kalajzic, I. (2009), "Neuropeptide Y is expressed by osteocytes and can inhibit osteoblastic activity", Journal of Cellular Biochemistry, Vol. 108, 621-630

[60] Ma, Y.; Wu, X.; Li, X.; Fu, J.; Shen, J.; Li, X. and Wang, H. (2012), "Corticosterone Regulates the Expression of Neuropeptide Y and Reelin in MLO-Y4 Cells", Molecules and Cells, Vol. 33, 611-616

[61] Hosaka, H.; Nagata, A.; Yoshida, T.; Shibata, T.; Nagao, T.; Tanaka, T.; Saito, Y. and Tatsuno, I. (2008), "Pancreatic polypeptide is secreted from and controls differentiation through its specific receptors in osteoblastic MC3T3-E1 cells", Peptides, Vol. 29, 1390-1395

[62] Kurebayashi, N.; Sato, M.; Fujisawa, T.; Fukushima, K. and Tamura, M. (2013), "Regulation of neuropeptide Y Y1 receptor expression by bone morphogenetic protein 2 in C2C12 myoblasts", Biochemical and Biophysical Research Communications, Vol. 439, 506-510

[63] Matic, I.; Matthews, B. G.; Kizivat, T.; Igwe, J. C.; Marijanovic, I.; Ruohonen, S. T.; Savontaus, E.; Adams, D. J. and Kalajzic, I. (2012), "Bone-specific overexpression of NPY modulates osteogenesis", Journal of musculoskeletal & neuronal interactions, Vol. 12, 209-218

[64] Amano, S.; Arai, M.; Goto, S. and Togari, A. (2007), "Inhibitory effect of NPY on isoprenaline-induced osteoclastogenesis in mouse bone marrow cells", Biochimica et Biophysica Acta (BBA) - General Subjects, Vol. 1770, 966-973

[65] Takahashi, N.; Udagawa, N. and Suda, T. (1999), "A New Member of Tumor Necrosis Factor Ligand Family, ODF/OPGL/TRANCE/RANKL, Regulates Osteoclast Differentiation and Function", Biochemical and Biophysical Research Communications, Vol. 256, 449-455

[66] Rudolf, K.; Eberlein, W.; Engel, W.; Wieland, H. A.; Willim, K. D.; Entzeroth, M.; Wienen, W.; Beck-Sickinger, A. G. and Doods, H. N. (1994), "The first highly potent and selective non-peptide neuropeptide Y Y1 receptor antagonist: BIBP3226", European Journal of Pharmacology, Vol. 271, R11-R13

[67] Doods, H. N.; Wienen, W.; Entzeroth, M.; Rudolf, K.; Eberlein, W.; Engel, W. and Wieland, H. A. (1995), "Pharmacological characterization of the selective nonpeptide neuropeptide Y Y1 receptor antagonist BIBP 3226", Journal of Pharmacology and Experimental Therapeutics, Vol. 275, 136-42

[68] Balasubramaniam, A. (2003), "Neuropeptide Y (NPY) Family of Hormones: Progress in the Development of Receptor Selective Agonists and Antagonists", Current Pharmaceutical Design, Vol. 9, 1165-1175

[69] Sousa, D. M.; Baldock, P. A.; Enriquez, R. F.; Zhang, L.; Sainsbury, A.; Lamghari, M. and Herzog, H. "Neuropeptide YY1 receptor antagonism increases bone mass in mice", Bone, Vol. 51, 8-16

[70] Balasubramaniam, A. "Clinical potentials of neuropeptide Y family of hormones", The American Journal of Surgery, Vol. 183, 430-434

[71] Helfrich, M. H. and Ralston, S. H. (2012), "Bone Research Protocols", 2nd Edition, Humana Press

[72] CHAMBERS, T. J. and MOORE, A. (1983), "The Sensitivity of Isolated Osteoclasts to Morphological Transformation by Calcitonin", The Journal of Clinical Endocrinology & Metabolism, Vol. 57, 819-824

[73] Fu; Gu; Zhang; Tong; Zhao; Yuan; Liu; Bian and Liu (2013), "Osteoprotegerin influences the bone resorption activity of osteoclasts", International Journal of Molecular Medicine, Vol. 31, 1411-1417

[74] Kang, J. H.; Ko, H. M.; Moon, J. S.; Yoo, H. I.; Jung, J. Y.; Kim, M. S.; Koh, J. T.; Kim, W. J. and Kim, S. H. (2014), "Osteoprotegerin Expressed by Osteoclasts: An Autoregulator of Osteoclastogenesis", Journal of Dental Research, Vol. 93, 1116-1123

[75] Brothers, S. P. and Wahlestedt, C. (2010), "Therapeutic potential of neuropeptide Y (NPY) receptor ligands", EMBO Molecular Medicine, Vol. 2, 429-439

[76] Hotokezaka, H.; Sakai, E.; Kanaoka, K.; Saito, K.; Matsuo, K.-i.; Kitaura, H.; Yoshida, N. and Nakayama, K. (2002), "U0126 and PD98059, Specific Inhibitors of MEK, Accelerate Differentiation of RAW264.7 Cells into Osteoclast-like Cells", Journal of Biological Chemistry, Vol. 277, 47366-47372

[77]Cobham:
https://www.cobham.com/media/160745/rfa21_semedx_imaging_modes_4pg_041209.pdf

[78] Goldberg, S. R.; Georgiou, J.; Glogauer, M. and Grynpas, M. D. "A 3D scanning confocal imaging method measures pit volume and captures the role of Rac in osteoclast function", Bone, Vol. 51, 145-152

[79] Azari, A.; Schoenmaker, T.; de Souza Faloni, A. P.; Everts, V. and de Vries, T. J. (2011), "Jaw and long bone marrow derived osteoclasts differ in shape and their response to bone and dentin", Biochemical and Biophysical Research Communications, Vol. 409, 205-210

[80] Rumpler, M.; Würger, T.; Roschger, P.; Zwettler, E.; Sturmlechner, I.; Altmann, P.; Fratzl, P.; Rogers, M. J. and Klaushofer, K. (2013), "Osteoclasts on Bone and Dentin In Vitro: Mechanism of Trail Formation and Comparison of Resorption Behavior", Calcified Tissue International, Vol. 93, 526-539

[81] Harada, K.; Itoh, H.; Kawazoe, Y.; Miyazaki, S.; Doi, K.; Kubo, T.; Akagawa, Y. and Shiba, T. (2013), "Polyphosphate-Mediated Inhibition of Tartrate-Resistant Acid Phosphatase and Suppression of Bone Resorption of Osteoclasts", PLoS ONE, Vol. 8, e78612

[82] Metze, K.; Ciplea, A. G.; Hettwer, H. and Barckhaus, R. H. (1987), "Size Dependent Enzyme Activities of Multinucleated (Osteoclastic) Giant Cells in Bone Tumors", Pathology - Research and Practice, Vol. 182, 214-221

[83] Kim, N.; Takami, M.; Rho, J.; Josien, R. and Choi, Y. (2002), "A Novel Member of the Leukocyte Receptor Complex Regulates Osteoclast Differentiation", The Journal of Experimental Medicine, Vol. 195, 201-209

[84] Kim, K.; Kim, J. H.; Lee, J.; Jin, H.-M.; Lee, S.-H.; Fisher, D. E.; Kook, H.; Kim, K. K.; Choi, Y. and Kim, N. (2005), "Nuclear Factor of Activated T Cells c1 Induces Osteoclast-associated Receptor Gene Expression during Tumor Necrosis Factor-related Activation-induced Cytokine-mediated Osteoclastogenesis", Journal of Biological Chemistry, Vol. 280, 35209-35216

[85] Takayanagi, H.; Kim, S.; Koga, T.; Nishina, H.; Isshiki, M.; Yoshida, H.; Saiura, A.; Isobe, M.; Yokochi, T.; Inoue, J.-i.; Wagner, E. F.; Mak, T. W.; Kodama, T. and Taniguchi, T. (2002), "Induction and Activation of the Transcription Factor NFATc1 (NFAT2) Integrate RANKL Signaling in Terminal Differentiation of Osteoclasts", Developmental Cell, Vol. 3, 889-901

[86] Suzuki, H.; Nakamura, I.; Takahashi, N.; Ikuhara, T.; Matsuzaki, K.; Isogai, Y.; Hori, M. and Suda, T. (1996), "Calcitonin-induced changes in the cytoskeleton are mediated by a signal pathway associated with protein kinase A in osteoclasts", Endocrinology, Vol. 137, 4685-4690

[87] Chiu, Y.-H.; Mensah, K. A.; Schwarz, E. M.; Ju, Y.; Takahata, M.; Feng, C.; McMahon, L. A.; Hicks, D. G.; Panepento, B.; Keng, P. C. and Ritchlin, C. T. (2012), "Regulation of Human Osteoclast Development by Dendritic Cell-Specific Transmembrane Protein (DC-STAMP)", Journal of bone and mineral research : the official journal of the American Society for Bone and Mineral Research, Vol. 27, 79-92

[88] Zhang, C.; Dou, C.; Xu, J. and Dong, S. (2014), "DC-STAMP, the Key Fusion-Mediating Molecule in Osteoclastogenesis", Journal of Cellular Physiology, Vol. 229, 1330-1335

[89] Kukita, T.; Wada, N.; Kukita, A.; Kakimoto, T.; Sandra, F.; Toh, K.; Nagata, K.; Iijima, T.; Horiuchi, M.; Matsusaki, H.; Hieshima, K.; Yoshie, O. and Nomiyama, H. (2004), "RANKL-induced DC-STAMP Is Essential for Osteoclastogenesis", The Journal of Experimental Medicine, Vol. 200, 941-946

[90] Kim, M. S.; Day, C. J. and Morrison, N. A. (2005), "MCP-1 Is Induced by Receptor Activator of Nuclear Factor-κB Ligand, Promotes Human Osteoclast Fusion, and Rescues Granulocyte Macrophage Colony-stimulating Factor Suppression of Osteoclast Formation", Journal of Biological Chemistry, Vol. 280, 16163-16169

[91] Khan, U. A.; Hashimi, S. M.; Bakr, M. M.; Forwood, M. R. and Morrison, N. A. (2015), "CCL2 and CCR2 are Essential for the Formation of Osteoclasts and Foreign Body Giant Cells", Journal of Cellular Biochemistry, Vol. n/a-n/a

[92] Mizutani, K.; Sud, S.; McGregor, N. A.; Martinovski, G.; Rice, B. T.; Craig, M. J.; Varsos, Z. S.; Roca, H. and Pienta, K. J. (2009), "The Chemokine CCL2 Increases Prostate Tumor Growth and

Bone Metastasis through Macrophage and Osteoclast Recruitment", Neoplasia (New York, N.Y.), Vol. 11, 1235-1242

[93] Sul, O.-J.; Ke, K.; Kim, W.-K.; Kim, S.-H.; Lee, S.-C.; Kim, H.-J.; Kim, S.-Y.; Suh, J.-H. and Choi, H.-S. (2012), "Absence of MCP-1 leads to elevated bone mass via impaired actin ring formation", Journal of Cellular Physiology, Vol. 227, 1619-1627

[94] Kim, M. S.; Day, C. J.; Selinger, C. I.; Magno, C. L.; Stephens, S. R. J. and Morrison, N. A. (2006), "MCP-1-induced Human Osteoclast-like Cells Are Tartrate-resistant Acid Phosphatase, NFATc1, and Calcitonin Receptor-positive but Require Receptor Activator of NFκB Ligand for Bone Resorption", Journal of Biological Chemistry, Vol. 281, 1274-1285

[95] Miyamoto, K.; Ninomiya, K.; Sonoda, K.-H.; Miyauchi, Y.; Hoshi, H.; Iwasaki, R.; Miyamoto, H.; Yoshida, S.; Sato, Y.; Morioka, H.; Chiba, K.; Egashira, K.; Suda, T.; Toyama, Y. and Miyamoto, T. (2009), "MCP-1 expressed by osteoclasts stimulates osteoclastogenesis in an autocrine/paracrine manner", Biochemical and Biophysical Research Communications, Vol. 383, 373-377

[96] Burysek, L.; Syrovets, T. and Simmet, T. (2002), "The Serine Protease Plasmin Triggers Expression of MCP-1 and CD40 in Human Primary Monocytes via Activation of p38 MAPK and Janus Kinase (JAK)/STAT Signaling Pathways", Journal of Biological Chemistry, Vol. 277, 33509-33517

[97] Pheng, L. H.; Dumont, Y.; Fournier, A.; Chabot, J.-G.; Beaudet, A. and Quirion, R. (2003), "Agonist- and antagonist-induced sequestration/internalization of neuropeptide Y Y1 receptors in HEK293 cells", British Journal of Pharmacology, Vol. 139, 695-704

[98] Wieland, H. A.; Willim, K. D.; Entzeroth, M.; Wienen, W.; Rudolf, K.; Eberlein, W.; Engel, W. and Doods, H. N. (1995), "Subtype selectivity and antagonistic profile of the nonpeptide Y1 receptor antagonist BIBP 3226", Journal of Pharmacology and Experimental Therapeutics, Vol. 275, 143-9

[99] Gicquiaux, H.; Lecat, S.; Gaire, M.; Dieterlen, A.; Mély, Y.; Takeda, K.; Bucher, B. and Galzi, J.-L. (2002), "Rapid Internalization and Recycling of the Human Neuropeptide Y Y1 Receptor", Journal of Biological Chemistry, Vol. 277, 6645-6655

[100] Kogawa, M.; Findlay, D. M.; Anderson, P. H. and Atkins, G. J. (2013), "Modulation of osteoclastic migration by metabolism of 25(OH)-vitamin D3", The Journal of Steroid Biochemistry and Molecular Biology, Vol. 136, 59-61

[101] Van Liefde, I.; Vanderheyden, P. M. L.; De Backer, J. P.; Ebinger, G. and Vauquelin, G. (2001), "EFFECTS OF BIBP3226 AND BIBP3435 ON CYTOSOLIC CALCIUM IN NEUROPEPTIDE Y Y1 RECEPTOR-TRANSFECTED CHINESE HAMSTER OVARY CELLS AND WILD TYPE CHO-K1 CELLS", Journal of Receptors and Signal Transduction, Vol. 21, 11-23

[102] Vanderheyden, P. M. L.; Van Liefde, I.; DeBacker, J. P.; Ebinger, G. and Vauquelin, G. (1998), "Effect of BIBP3226 on inositol phosphate accumulation and cytosolic calcium level in control and NPY Y1 receptor expressing CHO-K1 cells", Regulatory Peptides, Vol. 75–76, 191-199

[103] Perez-Amodio, S.; Vogels, I. M. C.; Schoenmaker, T.; Jansen, D. C.; Alatalo, S. L.; Halleen, J. M.; Beertsen, W. and Everts, V. "Endogenous expression and endocytosis of tartrate-resistant acid phosphatase (TRACP) by osteoblast-like cells", Bone, Vol. 36, 1065-1077

[104] Gramoun, A.; Azizi, N.; Sodek, J.; Heersche, J. N. M.; Nakchbandi, I. and Manolson, M. F. (2010), "Fibronectin inhibits osteoclastogenesis while enhancing osteoclast activity via nitric oxide and interleukin-1β-mediated signaling pathways", Journal of Cellular Biochemistry, Vol. 111, 1020-1034

[105] Van 't Hof, R. J. and Ralston, S. H. (1997), "Cytokine-Induced Nitric Oxide Inhibits Bone Resorption by Inducing Apoptosis of Osteoclast Progenitors and Suppressing Osteoclast Activity", Journal of Bone and Mineral Research, Vol. 12, 1797-1804

[106] Cheng, J.; Liu, J.; Shi, Z.; Xu, D.; Luo, S.; Siegal, G. P.; Feng, X. and Wei, S. (2011), "Interleukin-4 Inhibits RANKL-Induced NFATc1 Expression Via STAT6: A Novel Mechanism Mediating its Blockade of Osteoclastogenesis", Journal of cellular biochemistry, Vol. 112, 3385-3392

[107] Yu, M.; Qi, X.; Moreno, J. L.; Farber, D. L. and Keegan, A. D. (2011), "NF-κB signaling participates in both Receptor Activator of NF-κB Ligand- (RANKL) and interleukin-4- (IL-4) induced macrophage fusion: Receptor cross-talk leads to alterations in NF-κB pathways", Journal of immunology (Baltimore, Md. : 1950), Vol. 187, 1797-1806

[108] Jules, J.; Zhang, P.; Ashley, J. W.; Wei, S.; Shi, Z.; Liu, J.; Michalek, S. M. and Feng, X. (2012), "Molecular Basis of Requirement of Receptor Activator of Nuclear Factor κB Signaling for Interleukin 1-mediated Osteoclastogenesis", The Journal of Biological Chemistry, Vol. 287, 15728-15738

[109] Girasole, G.; Passeri, G.; Jilka, R. L. and Manolagas, S. C. (1994), "Interleukin-11: a new cytokine critical for osteoclast development", Journal of Clinical Investigation, Vol. 93, 1516-1524

[110] Schulze, J.; Bickert, T.; Beil, F. T.; Zaiss, M. M.; Albers, J.; Wintges, K.; Streichert, T.; Klaetschke, K.; Keller, J.; Hissnauer, T.-N.; Spiro, A. S.; Gessner, A.; Schett, G.; Amling, M.; McKenzie, A. N. J.; Horst, A. K. and Schinke, T. (2011), "Interleukin-33 is expressed in differentiated osteoblasts and blocks osteoclast formation from bone marrow precursor cells", Journal of Bone and Mineral Research, Vol. 26, 704-717

[111] Udagawa, N.; Horwood, N. J.; Elliott, J.; Mackay, A.; Owens, J.; Okamura, H.; Kurimoto, M.; Chambers, T. J.; Martin, T. J. and Gillespie, M. T. (1997), "Interleukin-18 (Interferon-γ–inducing Factor) Is Produced by Osteoblasts and Acts Via Granulocyte/Macrophage Colony-stimulating Factor and Not Via Interferon-γ to Inhibit Osteoclast Formation", The Journal of Experimental Medicine, Vol. 185, 1005-1012

# Annex

**A**

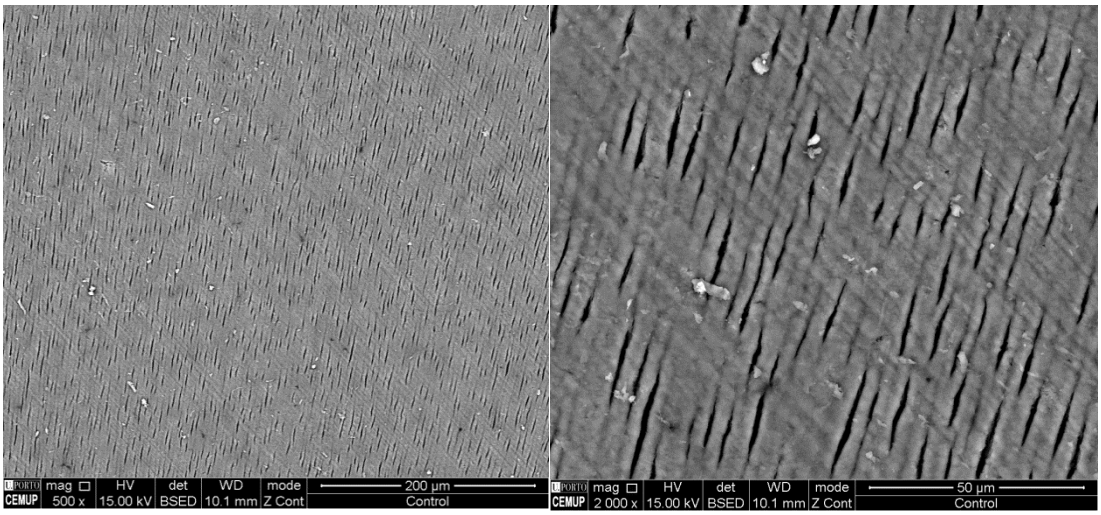


**B**

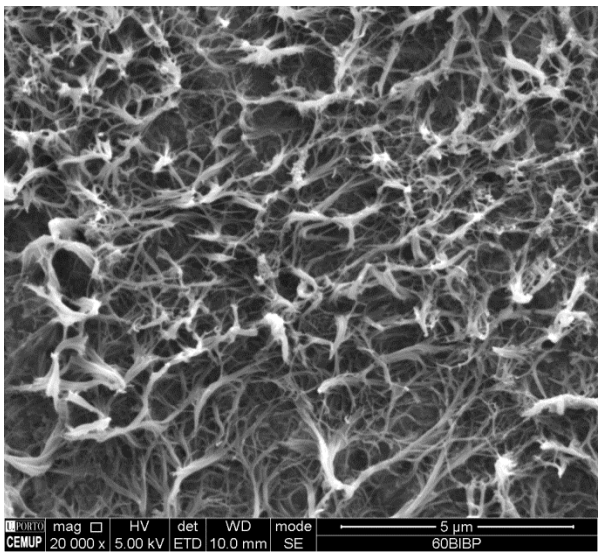


**Figure 32 – Dentine disc SEM images.** (A) Control samples without seeded cells at 500x and 2000x magnification. (B) Resorption pit at 20000x magnification. Collagen fibres are clearly visible.